Lesion Dynamics in Experimental Models of Endometriosis

Dissertation

zur Erlangung des akademischen Grades des

Doktors der Naturwissenschaften (Dr. rer. nat.)

eingereicht im Fachbereich Biologie, Chemie, Pharmazie

der Freien Universität Berlin, Deutschland

vorgelegt von

Masters of Science - Biology

Payman Harirchian

aus Teheran

November 2013

Meinen Eltern

For My Parents

Gutachter / Referees

1. Gutachter: **Priv. Doz. Dr. Thomas M. Zollner**

Bayer HealthCare, Berlin, Deutschland

Gynecological Therapies

2. Gutachter: **Prof. Dr. Rupert Mutzel**

Freie Universität Berlin, Berlin, Deutschland

Institut für Pflanzenphysiologie und Mikrobiologie

Disputation am: May 13, 2014

This work was performed at Bayer Healthcare, Global Drug Discovery, Transgenic and *in vivo* Pharmacology in Berlin, Germany. It is being presented with their permission.

Table of Contents

1 Introduction....1

1.1 Endometriosis....1

1.2 Pathogenic Mechanisms Implicated in the Development of the Chronic Disorder....8

1.2.1 Putative Role of Cellular Proliferation in Endometriosis....8

1.2.2 Putative Role of Apoptosis in Endometriosis....12

1.2.3 Putative Role of Immune Cells in Endometriosis....17

1.3 Lesion Kinetics in Endometriosis....27

1.4 Animal Models For the Study of Endometriosis....29

1.4.1 Mouse Model....30

1.4.2 Non-human Primate Model....31

1.5 Thesis Aim....32

2 Materials and Methods....33

2.1 Mouse Studies....33

2.1.1 Syngeneic Transplantation Endometriosis Mouse Model Using C57BL/6 Mice....35

2.1.2 Syngeneic Transplantation Endometriosis Mouse Model Using FVB/N Mice....37

2.1.3 Necropsy: Lesion Photography and Tissue Harvesting....38

2.2 Ex vivo Analysis of Mouse Samples....39

2.2.1 Gene Expression Analysis....39

2.2.2 Protein Expression Analyses....41

2.2.3 Immunohistochemistry....45

2.2.4 Flow Cytometry....49

2.3 Retrospective Analysis of Baboons with Induced Endometriosis Conducted at Michigan State University....54

2.3.1 Gene Expression Analysis of Baboon Lesions....56

2.4 Statistical Analysis....59

3 Results....60

3.1 Effects of Estradiol on Experimental Endometriosis....60

3.1.1 Impact of Hormones on Lesion Development in C57Bl/6 Mice..61

3.1.2 17β-estradiol's Effect on Lesion Size in FVB/N Mice....63

3.1.3 Proliferation Is Not the Main Driver of Estrogen Mediated Lesion Growth....67

3.1.4 Apoptosis Is Not the Main Driver of Estrogen Mediated Lesion Growth....79

3.1.5 Immune Cell Composition of Lesions Is Altered According to Time and Treatment....101

3.1.6 Measurement of Host Cells Infiltration Into the Implants Using a Novel Syngeneic Mouse Model....109

3.2 Lesion Kinetics in Non-human Primate Model of Endometriosis....112

3.2.1 Baboon Endometriotic Lesion Location and Morphology....113

3.2.2 Lesion Development in Baboons Inoculated with Menstrual Tissue....115

3.2.3 Recurrence of Excised/Ablated Lesions in Baboons Inoculated with Menstrual Tissue....120

3.2.4 Lesion Occurrence in Baboons Not Inoculated with Menstrual Tissue....123

3.2.5 Gene Expression Analysis of Baboon Lesions....124

4 Discussion....127

4.1 Effects of Estradiol on Experimental Endometriosis....127

4.1.1 Estradiol Impacted Size, But Not the Establishment of Mouse Endometriotic Lesions....128

4.1.2 Total Proliferation Was Unchanged in Mouse Endometriotic Lesions Regardless of E_2 Treatment....130

4.1.3 Total Apoptosis Was Unchanged in Mouse Endometriotic Lesions Regardless of E_2 Treatment....134

4.1.4 Alterations of Cell Composition and Apoptosis Frequency in Mouse Lesions According to Time and Treatment....140

4.1.5 Compromised Estrogen Receptor Signaling Decreased Mouse Endometriotic Lesion Inflammation....151

4.2 Lesion Kinetics in Non-human Primate Model of Endometriosis....156

4.2.1 Lesion Turnover in Baboons Inoculated With Menstrual Tissue....157

4.2.2 Recurrence of Excised/Ablated Lesions in Baboons Inoculated with Menstrual Tissue....161

4.2.3 Lesion Occurrence in Baboons Not Inoculated With Menstrual Tissue....162

5 Conclusions and Outlook....164

6 Summary/Zusammenfassung....166

7 References....170

8 Appendix....201

8.1 List of Publications....201

8.2 Abbreviations....202

8.3 Acknowledgements....204

1 Introduction

1.1 Endometriosis

Endometriosis is a chronic, endocrine dependent (Cramer and Missmer, 2002), gynecological disorder affecting 10% of women of reproductive age (Bernuit, et al., 2011), in particular 50 to 60% of women and teenage girls with pelvic pain, and up to 50% of women with infertility (Eskenazi and Warner, 1997). The disease is characterized by the presence of endometrial glands and stroma outside the uterus, predominantly in the pelvic peritoneum (Giudice and Kao, 2004). These endometriotic lesions or implants are frequently found in the pelvis minor, especially on fixed organs like the ovaries, on parietal peritoneum, in the pouch of Douglas, on fallopian tubes, and rectovaginal septum (Figure 1). The activity of endometriotic lesions formed by the misplaced endometrial tissue, and the development of subsequent adhesions, are the likely causes of the described disease symptoms, which include chronic pelvic pain, dyspareunia, dysmenorrhoea as well as sub- and infertility (Giudice, 2010).

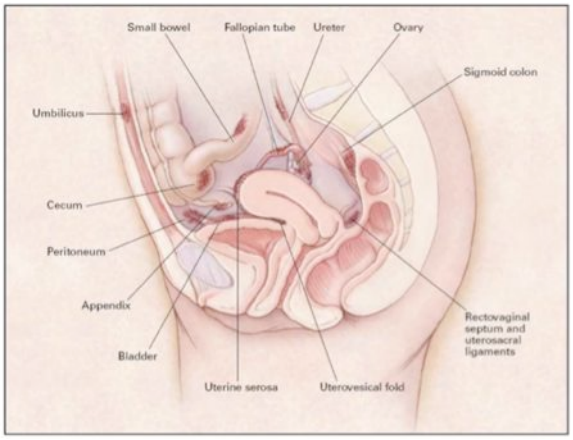

Figure 1: Locations of endometriotic lesions (indicated as dark red patches) within the peritoneal cavity

Common lesion locations are the ovaries, bladder, uterine serosa (perimetrium), rectovaginal septum and the pouch of Douglas (Olive and Pritts, 2001)

To facilitate coherent and faster diagnosis of pelvic endometriosis, the American Society for Reproductive Medicine (ASRM) has categorized the morphology of endometriotic lesions as red (including red, red-pink and clear lesions), white (including white, yellow-brown) and black (including black and blue lesions, Figure 2). Red lesions are highly vascularized; white lesions are supposed to be scar tissue remnants of regressed lesions and include fibrotic material; black and blue lesions often contain clotted blood and are high in hemosiderin (Van Langendonckt, et al., 2002). The lesion size ranges from pinhead up to large, egg-shaped cystic formations. Additionally, appearance of adhesions is common, which often impair several organs making difficult macroscopic visualization of lesions during diagnostic laparoscopies.

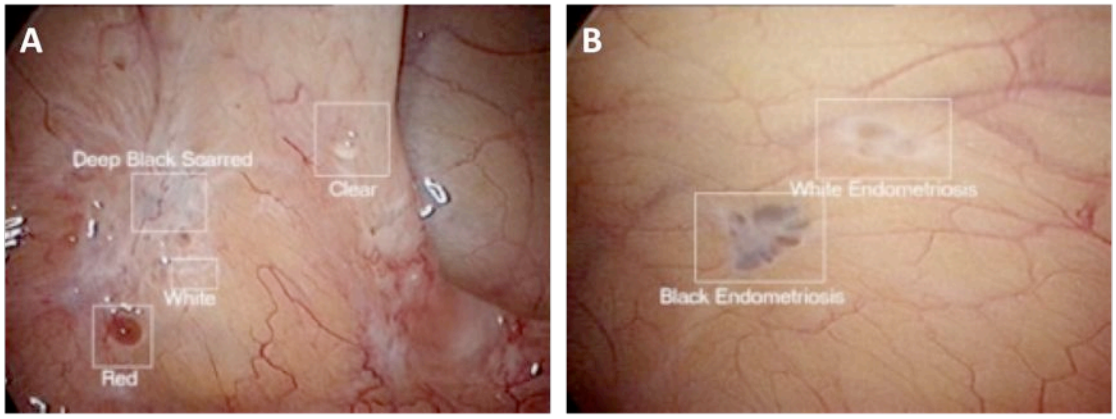

Figure 2: Varied appearance of endometriotic lesions in women with endometriosis

Laparoscopic photographs depict the inherent variation of endometriotic lesion appearance in women with endometriosis. **A:** Photograph from the left pelvic sidewall, under the ovary. **B:** Photograph from the right side of the pelvis beneath the right ovary (www.womenssurgerygroup.com).

ASRM (1997) has recommended staging of endometriosis as (I) minimal, (II) mild, (III) moderate, and (IV) severe endometriosis. This staging determination is based on a weighted point system in which superficial or deep endometriosis, severity of adhesions (filmy or dense), obliteration of the pouch of Douglas and enclosure of the ovaries are taken into consideration. It must be noted however that the severity of the symptoms of endometriosis does not always correlate with the anatomic severity of the disease (Abbott, et al., 2003, Candiani, et al., 1991, Garry, et al., 2000). Indeed, due to variations in symptomatology and disease progression women can suffer for 8–12 years before diagnosis (Hadfield, et al., 1996). The picture after diagnosis remains bleak since many physicians must resort to surgical removal of lesions after failed medical therapy, which often leads to recurrence.

The gold standard for diagnosis of pelvic disease is surgical assessment, via laparoscopy. To avoid this invasive procedure, women are often empirically treated for endometriosis based on clinical factors and less invasive testing, such as ultrasound and physical exam, to see if symptoms improve (Rodgers and Falcone, 2008). If symptoms persist, laparoscopy accompanied by excision/ablation of the detected endometriotic lesions is performed (Rice, 2002). However, this procedure is far from ideal due to short-lived relief of symptoms and high recurrence of lesions (Jacobson, et al., 2009, Yeung, et al., 2009). Medical therapy helps to prolong the remission period after surgery. Treatment options for medical therapy include androgenic agents, gonadotropin releasing hormone (GnRH) analogues, progestogens and oral contraceptives (Farquhar, 2007). All suppress ovarian activity, menses and at-

rophy of endometriotic implants, although the extent to which they achieve this varies.

Danazol was the first pharmaceutical agent approved for the treatment of endometriosis. It has androgenic agonist effects, inhibits enzymes in the steroidogenic pathway, and increases free testosterone concentrations resulting in anovulation with hypoestrogenism and hyperandrogenism, thus relieving pain symptoms (Olive and Pritts, 2001). Weight gain, acne, hirsutism, decreased breast size, hot flashes, and muscle cramps frequently occur in women treated danazol. GnRH analogues are another group of approved pharmaceuticals where the pathway involves blocking of ovarian steroids such as 17β-estradiol (E_2) and reducing their concentrations to postmenopausal levels. As with Danazol, GnRH analogues present adverse side effects such as dizziness, vaginal dryness, loss of libido plus increased risk of thrombosis and osteoporosis (Griesinger, et al., 2005). Due to their severe side effects, Danazol and GnRH analogues are often used for short-term relief of symptoms.

Recent addition to the field of approved medical therapies includes the progestogen Dienogest (marketed as Visanne by Bayer Healthcare), which inhibits ovulation and reduces menstrual flow. Due to fewer side effects and pain relief capabilities, progestogens such as Dienogest are often used as standard long-term treatment medication for endometriosis (Strowitzki, et al., 2010). “Off-label use” (drug use beyond indications and not reimbursed by insurance) of combined oral contraceptives (COCs) is another frequently applied therapy, leading to a pregnancy-pretending hormonal

state with decreased gonadotropin levels, ovulation inhibition, and reduced menstrual flow alleviating endometriosis symptoms (Rice, 2002). However, COC treatment requires additional pain relief agents such as non-steroidal anti-inflammatory drugs (NSAIDs) or opioids to yield similar results as Dienogest (Davis, et al., 2007).

There are no medical therapies proven effective for endometriosis related infertility although surgical removal of lesions followed by assisted reproductive technology (ART) will allow some women to achieve a stable pregnancy (Falcone and Hurd, 2007). New agents to treat endometriosis that target the hormonal metabolism (i.e. estrogen synthetase (aromatase) inhibitors) or try to modulate the immune system (i.e. c-Jun N-terminal kinase (jnk) inhibitors) are in the various stages of human clinical trials (www.clinicaltrials.gov). Currently there is no cure for endometriosis and better understanding of pathophysiological processes is needed to create additional therapeutic options to prevent or treat/cure endometriosis.

Endometriosis is an enigmatic disease because neither the etiology, nor the natural history, nor the precise mechanisms of the associated symptoms are completely understood. Various theories for pathogenesis exist including retrograde menstruation (Sampson, 1927), lymphatic and vascular metaplasia (Javert, 1949), coelomic metaplasia (Gardner, et al., 1953), deficient cellular immunity (Dmowski, et al., 1981), and transdifferentiation of the peritoneal mesothelium (Suginami, 1991). Most commonly accepted remains Sampson's retrograde menstruation transplantation theory, which states that endometrial fragments flow back through the fallopian

tubes, reach the peritoneal cavity, attach on the pelvic mesothelium, invade the peritoneum, acquire a blood supply, and develop into endometriotic lesions (Groothuis, et al., 2005). After endometrial tissue transplantation, the factors that regulate the attachment phase and thereafter initiate chronic ectopic growth are not entirely understood. The newly attached tissue is hypothesized to undergo proliferation and obtain a blood supply as well as metabolic degradation of heme and appearance of fibrosis leading to change in morphologic appearance over time (Figure 3).

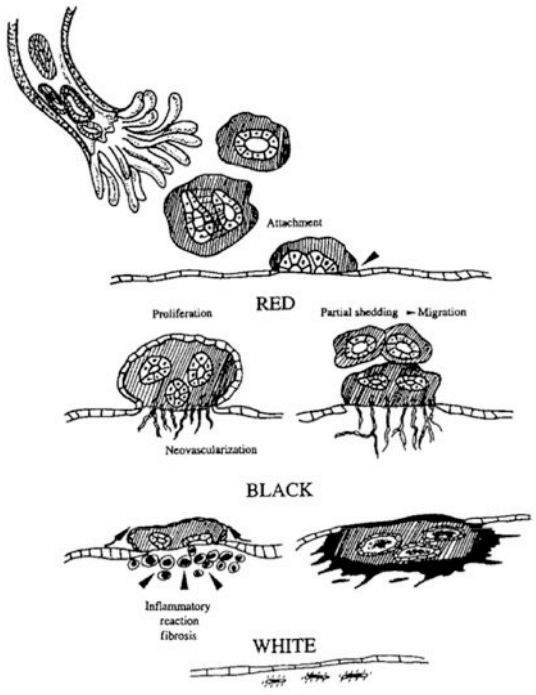

Figure 3: Hypothetical scheme of evolution for peritoneal endometriosis

Red lesions are newly attached endometrium and are highly vascularized; black and blue lesions evolve next and often contain clotted blood and are high in hemosiderin; white lesions are supposed to be scar tissue remnants of regressed lesions and include fibrotic material (Nisolle and Donnez, 1997)

Oddly enough, retrograde menstruation occurs in >90% of women of reproductive age (Halme, et al., 1984), but only one in 10 is diagnosed with endometriosis. Due to this disparity, other factors have been suggested to play a role in the pathogenesis of endometriosis: to permit and promote survival, implantation, and proliferation of the endometrial cells (Osuga, 2008). These factors include hormones, growth factors, cytokines and prostaglandins, as well as various cell types that are present in the endometriotic lesions and the peritoneum such as epithelial cells, stromal cells, and immune cells.

A constant feature of endometriosis is its occurrence during the reproductive period of life (Punnonen, et al., 1980), and thus its general dependence on estrogen stimulation. Indeed, inhibition of estrogen by GnRH analogues, progestins, and aromatase inhibitors reduced endometriotic lesions and clinical symptoms, including dysmenorrhea and pelvic pain (Olive and Pritts, 2001). It is postulated that estrogen enhances the survival or persistence of endometriotic tissue, whereas prostaglandins and cytokines mediate pain, inflammation, and infertility (Bruner, et al., 1997, Ryan and Taylor, 1997). However, even these latter pathways have been associated with the presence of estrogen. High concentrations of the active form of estrogen, 17ß-estradiol (E_2), as well its receptor, estrogen receptor 1 and 2 (ER1 and 2), have been consistently demonstrated in human endometriotic lesions (Matsuzaki, et al., 2001, Noble, et al., 1996). Furthermore, it has been proposed that local estrogen synthesis transpires in endometriotic lesions (Bulun, 2009, Delvoux, et al., 2009). This evi-

dence points to a pivotal role for estrogen in the development and persistence of the pelvic disorder.

In endometriosis, abnormal adhesion of endometrial fragments to ectopic sites could be due to abnormalities in proliferation and apoptosis properties of menstrual endometrium and/or anomalies in the target tissue microenvironment. In the following sections the pathogenic mechanisms implicated in the development and chronic manifestation of endometriosis are introduced.

1.2 Pathogenic Mechanisms Implicated in the Development of the Chronic Disorder

1.2.1 Putative Role of Cellular Proliferation in Endometriosis

Endometriosis is characterized by the presence and proliferation of viable endometrial glands and stroma outside the uterine cavity. Aberrations in the regulation of endometrial physiology may facilitate the pelvic disease. The endometrium, the inner membrane of the mammalian uterus, is divided into the basalis layer, which is permanent, and superficialis or functionalis layer, which undergoes cyclic remodeling in a highly regulated process that involves menstrual cycle dependent changes in cellular survival, proliferation, and differentiation. These changes occur via interaction of the sex hormones E_2 and progesterone (P_4) with the pituitary hormones follicle-stimulating hormone (FSH) and luteinizing hormone (LH).

The human female menstrual cycle is divided into three phases: the follicular phase, ovulatory phase, and luteal phase (Greenberg, et al., 2007). In the follicular phase, a decrease in the levels of E_2 and P_4 triggers tissue degeneration that involves a process of necrosis as well as apoptosis where the thickened functionalis layer of endometrium breaks down and is shed, resulting in bleeding (Hopwood and Levison, 1976). Concurrently, in the ovaries, levels of FSH increase slightly, stimulating the development of several oocyte-containing follicles. FSH levels subsequently decrease and only one or two follicles continue to develop. The developing follicles release E_2, and this initiates proliferation leading to thickening of the endometrium, something that continues throughout the rest of the menstrual cycle. During ovulation the levels of LH and FSH increase dramatically; levels of E_2 peaks at this time, and levels of P_4 begin to increase leading to the rupture of the follicle and release of the oocyte (Aitken, et al., 2008). During the luteal phase the levels of LH and FSH decrease and the ruptured follicle forms the corpus luteum, which produces large amounts of P_4 leading to modifications in the endometrium so that it is receptive to implantation of an embryo if fertilization has occurred. In the absence of fertilization, the corpus luteum degenerates and the loss of P_4 production, combined with decreased levels of E_2, initiates a new menstrual cycle (Figure 4).

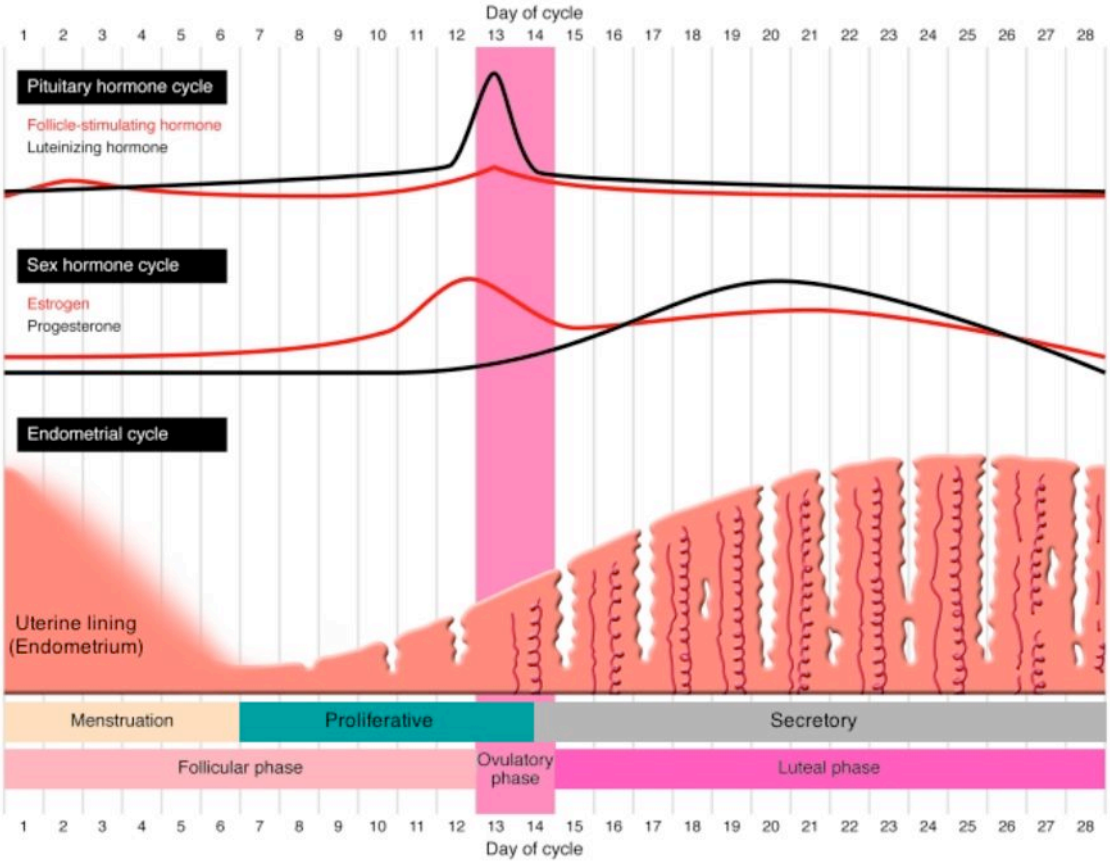

Figure 4: The human female menstrual cycle

The menstrual cycle is divided into three phases: follicular, ovulatory, and luteal, which vary in length among women and among cycles; average times are indicated. Normal endometrial growth is regulated by the menstrual cycle-dependent changes in cellular survival, proliferation, and differentiation induced via changes in levels of the sex hormones, estrogen and progesterone, along with the pituitary hormones, follicle-stimulating hormone and luteinizing hormone. The cyclical changes of the uterine lining induced by the menstrual cycle are divided into three phases: menstruation, proliferative and secretory (adapted from Aitken, et al., 2008).

Conflicting reports exist about anomalies in proliferation in the eutopic endometrium of women with endometriosis. Meresman et al. (2002), using immunohistochemistry (IHC), saw that endometrial tissue at the epithelial and stromal levels from women with endometriosis has significantly higher degree of cell proliferation

(Ki-67 staining) in comparison with women without endometriosis. Conversely, Scotti et al. (2000) did not see differences in Ki-67 staining between women with and without endometriosis. It is unclear whether these abnormal findings in the eutopic endometrium are primary in origin and significantly contribute to the development of the disease or secondary in nature to an established pelvic disease process.

Proliferation is restrained through control of the cell cycle. Cyclin B1/cyclin-dependent kinase 2 (cdc2) interaction along with Polo-like kinase 1 (Plk1) are the key components of the cell cycle machinery (Jackman, et al., 2003). Cyclin B1 binds to cdc2 at the beginning of the G2 phase, forming an activated cyclin B1–cdc2 complex (maturation-promoting factor) and then phosphorylates a number of important substrates to control the G2 to M transition (Jin, et al., 1998). Unscheduled modulation of these regulatory genes during the cell cycle can help cells override the death sentence, and lead to uncontrolled cell proliferation. Tang et al. (2009) noted that the expression levels of cyclin B1 and Plk1, but not cdc2, in ectopic endometrium were significantly higher than in eutopic endometrium. Furthermore, ectopic endometrial expression levels of cyclin B1 or Plk1 were positively correlated with serum E_2 levels. Cyclin B1 and Plk1 may play important roles in the pathogenesis of endometriosis by mediating ectopic endometrial cell proliferation under regulation of sex hormones.

In women with endometriosis, the peritoneal fluid (PF) has high concentrations of cytokines, growth factors, and angiogenic factors (Bedaiwy and Falcone, 2003), which may contribute to proliferation of endometriotic implants and neoangiogenesis. Transforming growth factor β1 (TGF-β1) is a multifunctional cytokine that regulates a number of biological processes including cell proliferation, extracellular matrix fomation, tissue remodeling, and inflammation (Massague, et al., 2000). Similar biological events occur during endometriotic lesion establishment. Interestingly, TGF-β1 level was elevated in PF, endometriotic lesions and serum of women with endometriosis (Pizzo, et al., 2002). In a humanized mouse model of endometriosis, using TGF-β1 knockout mice, there was a significant reduction in size and weight along with dramatic reduction in glandular epithelium within endometriotic xenografts in the absence of host derived TGF-β1 (Hull, et al., 2012). Proliferation alone may not suffice in the chronic manifestation of endometriosis. Indeed, other biological processes have been implicated.

1.2.2 Putative Role of Apoptosis in Endometriosis

Ectopic dissemination of endometrial cells may give rise to endometriotic lesions, but retrograde menstruation occurs in the majority of women. For reasons still not fully elucidated, misplaced endometrial cells in healthy women do not develop into endometriotic lesions. There may be abnormal resistance of endometriotic cells to apoptosis, which can be either intrinsic or brought about by environmental factors (Nasu, et al., 2011). Programmed cell death or apoptosis is essential in maintaining tissue homeostasis, shaping the immune repertoire, terminating immune responses,

and restricting the progress of infections (Steller, 1995). Unlike necrosis, the orderly progression of events during apoptosis leads to cell death without the leakage of protease enzymes and cellular content of dying cells, thereby reducing the likelihood of an immune or inflammatory response (Wyllie, et al., 1980). A group of cysteine proteases, termed caspases, form the core activation cascade in programmed cell death with upstream, or initiator caspases (8–10), and downstream, or effector caspases (3, 6 and 7). Apoptosis is highly regulated with two major initiation pathways: the intrinsic mitochondrial pathway and the extrinsic death-receptor signaling pathway (Chen and Wang, 2002).

The intrinsic pathway is activated by intracellular stress, such as DNA damage, hypoxia, and growth factor deprivation. Here, increasing permeability of the mitochondrial membrane releases Cytochrome c that triggers the caspase cascade and the formation of apoptosomes, which in turn results in the activation of caspase 9 and 3, leading to apoptosis. The extrinsic pathway is initiated by the death-receptors (Fas/CD95, TNF receptor, TRAIL receptor). The ensuing multiprotein complex then activates initiator caspases 8 and 10 that in turn activate the effector caspases 3 and 7. These two pathways are not distinct, and the activation of one usually involves the other (Nachmias, et al., 2004). A network of pro- and anti-apoptotic proteins closely regulates apoptosis (Figure 5). Some proteins such as p53 regulate the expression of death-receptors (Fridman and Lowe, 2003), while others like the B-cell lymphoma 2 (Bcl-2) family members act at the level of initiator caspases (Yin,

2000), and a third group of factors, the inhibitor of apoptosis (IAP) family, can regulate both initiator and effector caspases (Deveraux, et al., 1999).

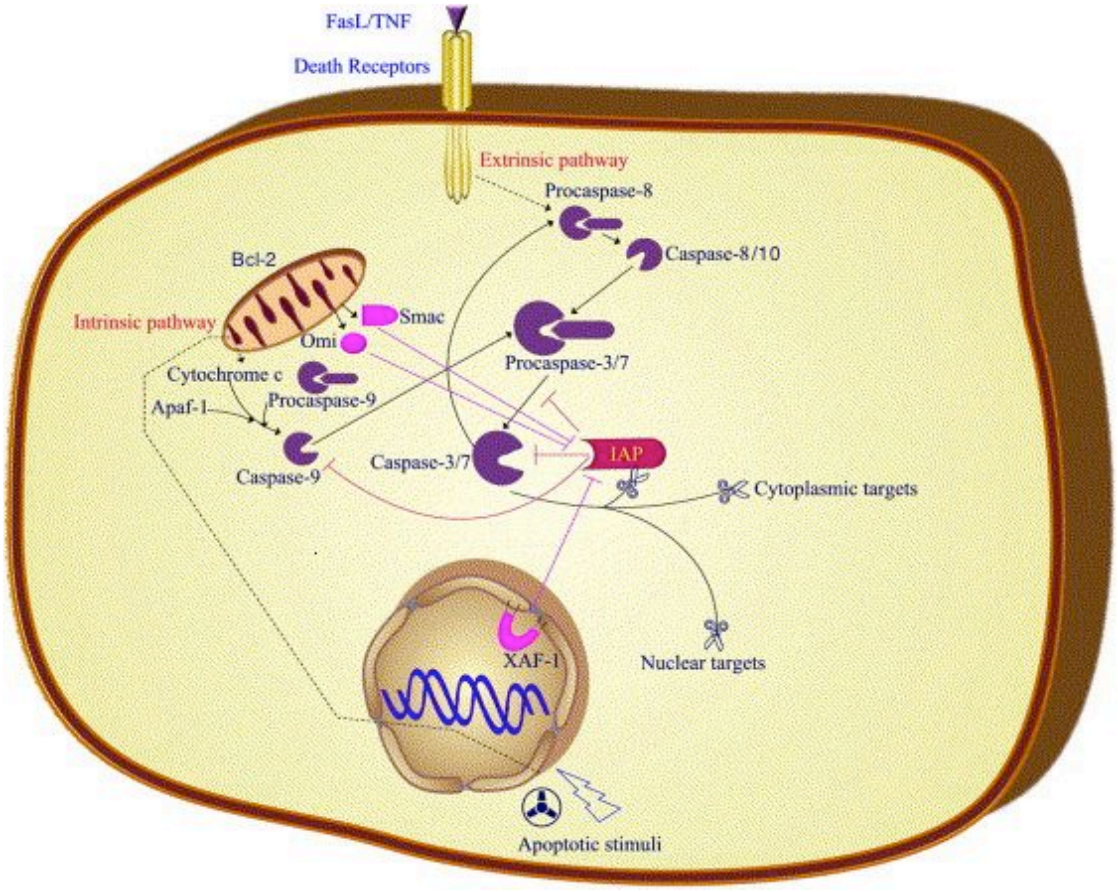

Figure 5: Apoptosis, programmed cell death

The intrinsic pathway, initiated by cellular stress, involves increasing permeability of mitochondrial membrane via regulation of Bcl-2 family proteins, leading to the release of Cytochrome c, recruitment of Apaf-1 plus Procaspase-9, formation of apoptosomes, and activation of caspase-9. The extrinsic pathway, initiated by the death-receptors, involves activation of caspase-8 and 10. From here, the intrinsic and the extrinsic pathways converge on the activation of executioner caspases-3 and 7, which cleave more than 200 cellular target proteins and lead to cell death. IAP family of proteins, regulated by proteins such as Smac, Omi, and XAF-1, can bind to active caspases and either directly inhibit their enzyme activities or subject them to ubiquitin-proteasome degradation (adapted from Nachmias, et al., 2004).

The Bcl-2 protein, founding member of the Bcl-2 family, blocks cell death by regulating mitochondrial membrane and is an integral part of the intrinsic pathway of apoptosis (Cory and Adams, 2002). Conflicting data exists regarding the difference in Bcl-2 expression between eutopic and ectopic endometrial tissue. Some investigators showed increased expression in lesions (Jones, et al., 1998) while others observed unchanged expression level between lesions and the eutopic endometrium from women with or without endometriosis (Meresman, et al., 2000). Furthermore, there exists variation in Bcl-2 expression depending on morphology (cyst and non-cyst) and location (ovarian and peritoneal) of endometriotic lesions (Nezhat, et al., 2002, Nezhat and Kalir, 2002). Additionally, Bcl2 is indirectly involved in the death-receptor pathway through caspase-8 and BH3 interacting-domain death agonist (Bid) in lymphocytes and macrophages (Strasser, et al., 1995).

Bid is inactive until cleavage by caspase-8 via signaling from the death-receptor pathway. In essence, Bid is a pro-apoptotic protein that connects the death-receptor pathway to the mitochondrial pathway by counteracting the anti-apoptotic protection of Bcl-2 at the mitochondrial membrane and inducing Cytochrome C and second mitochondria-derived activator of caspases (Smac) release (Gross, et al., 1999). Smac is a mitochondrial protein that promotes Cytochrome c dependent activation of apoptosis by eliminating the inhibition of caspases by IAPs such as baculoviral inhibitor of apoptosis repeat-containing (Birc) 1a, 4, and 5 (Vucic, et al., 2002).

The relationship of estrogen, its receptors, and apoptosis in the development of the chronic pelvic disorder remain unclear. Furthermore, conflicting reports show fluctuation of ER1 and 2 numbers in the endometrial tissue from women with and without endometriosis (Beliard, et al., 2004). Interestingly, in breast cancer cells, estrogen and ER1 and 2 have been shown to regulate expression of pro and anti-apoptotic molecules from Bcl-2 and IAP family of proteins (Martin and Dowsett, 2013). Cyclic expression pattern of Bcl-2 in eutopic endometrium was observed in women with and without endometriosis and histologically was correlated to changes in ER1 levels during the cycle (Otsuki, et al., 1994).

Endometriosis is an estrogen dependent disease; its relations with apoptosis may be an important link in the etiology of the disorder. In the uterus, apoptosis helps to maintain cellular homeostasis during the menstrual cycle (Figure 4), through the elimination of senescent cells from the functional layer of the uterine endometrium during the late secretory and menstrual phases of the cycle (Kokawa, et al., 1996). Abnormalities in programmed cell death signaling of eutopic tissue may attribute to the viability of loose endometrial tissue at ectopic sites. Two mechanisms may enhance survival of endometrial tissue at ectopic sites: decreased sensitivity to pro-apoptotic signaling via enhanced anti-apoptotic signaling (i.e. Bcl-2 and IAPs) in ectopic endometrial tissue and increased apoptosis via extrinsic death-receptor pathway in immune cells, which are introduced in the following section (Jiang and Wu, 2012).

1.2.3 Putative Role of Immune Cells in Endometriosis

The immune system participates in the homeostasis of the peritoneal cavity. Assuming retrograde menstruation as the potential source of endometriotic lesions, then there already exists a highly inflammatory peritoneal environment due the presence of the misplaced eutopic endometrium. In some women, refluxing endometrial cells are not destroyed, either because they are genetically programmed not to respond to endometrial antigens, or because the reflux is so abundant that the scavenging capacity of the peritoneal immune cells is overloaded. Refluxing cells could be protected due to an abnormal adherence to the mesothelium, which exceptionally expresses certain adhesive molecules such as intercellular adhesion molecule (ICAM) and vascular cellular adhesive molecule-1 (VCAM-1, (Vinatier, et al., 1996). Undestroyed, these endometrial cells would cause an inflammation with activation of the immune system and trigger pain and discomfort. Conversely, endometriotic implants constitute an autograft, a tissue or organ transferred into a new position in the body of the same person. Autografts generally accept transplantation with little to no local immune response. However, ectopic endometrium in some patients seems to elicits a significant inflammatory response with activated immune cells and aberrant cytokine expression in the PF, whereas in others, it elicits little reaction (Barrier, 2010). Indeed, ectopic endometrial tissues often express the same proinflammatory cytokines as the eutopic tissue, but in a dysregulated manner (Lebovic, et al., 2001, Wu and Ho, 2003).

As with the diversity in endometriosis symptomatology and progression, the diversity of immune response among patients is striking. For example in some women with endometriosis immunoreactivity is greater against interleukin-8 (IL-8) in endothelial cells and against both IL-8 and monocyte chemotactic protein-1 (MCP-1) in epithelial cells when compared with matched eutopic endometrium from patients with and without endometriosis (Ulukus, et al., 2009). These elevated levels can often be correlated with the severity of the symptoms (Gazvani, et al., 1998). IL-8 and MCP-1 increase angiogenic potential and promote the recruitment of inflammatory immune cells into the local microenvironment (Brenner, et al., 2002). Not withstanding these inherent differences in immune response, modifications in the immune system function have been implicated and must be taken into account when studying endometriosis and its consequences.

Immune cells have been noted to play crucial roles in either rejecting or accepting refluxed endometrial cells. In addition to their direct functions, immune cells may contribute to the disease development by secreting various cytokines that control cell inflammation, proliferation, migration and apoptosis (Wu and Ho, 2003). The cytokines released by these cells are multifunctional proteins and may play a key role in the endometriosis-associated inflammatory response, tissue repair, and maintenance of homeostasis. A variety of immune cells such as natural killer (NK) cells, B and T lymphocytes, monocytes (macrophages and dendritic cells) and granulocytes are present in endometriotic lesions and the PF, indicating their potential roles in the disease. These cells all originate from hematopoietic stem cells (HSC) in

the bone marrow and are generated via a process called hematopoiesis (Figure 6). Here, immune cells that may be involved in the pathogenesis of endometriosis are presented according to their lineage.

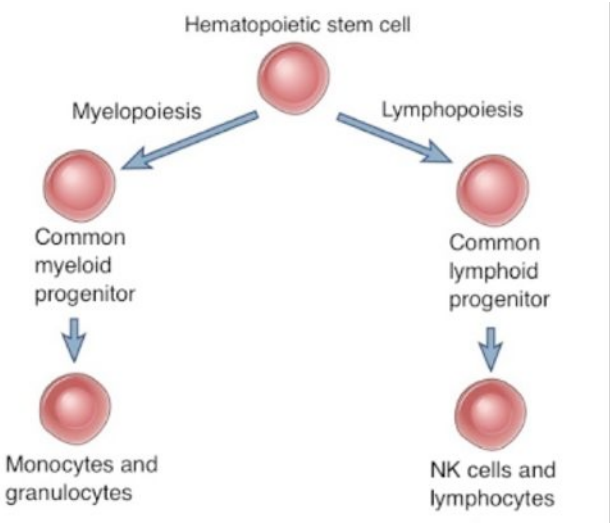

Figure 6: Hematopoiesis

Immune cells arise from hematopoietic stem cell (HSC) via a process called hematopoiesis. HSCs give rise to two kinds of multipotent cells, the common lymphoid and common myeloid progenitors (CLP and CMP). CLPs are the source of precursors for NK cells, B and T lymphocytes. CMPs give rise to monocytes, which differentiate into macrophages or dendritic cells and granulocytes (adapted from Abbas, et al., 2012).

Natural Killer Cells and Lymphocytes in Endometriosis

Common lymphoid progenitors (CLP) give rise to lymphocytes that are comprised of NK cells, B and T lymphocytes. These cells might play essential roles in determining either accept or reject survival, implantation, and proliferation of endometrial and endometriotic cells (Osuga, et al., 2011).

B Lymphocytes

B cells are lymphocytes that play a large role in the humoral immune response (as opposed to the cell-mediated immune response). The principal functions of B cells are to make antibodies against antigens, perform the role of antigen-presenting cells (APCs) and eventually develop into memory B cells after activation by antigen interaction. B cells are an essential component of the adaptive immune system (Kindt, et al., 2007). An increase in B cell reactivity in women with endometriosis has been observed (Startseva, 1980) suggesting an autoimmune response including local activation and consumption of complementary factors by the antigen-antibody complex (Weed and Arquembourg, 1980). B lymphocytes may be responsible for specific and non-specific autoantibody production in the endometrium and thus in turn may contribute to the pathogenesis of endometriosis by increasing immunoinflammation at the ectopic site (Osuga, et al., 2011).

Natural Killer Cells

NK cells are cytotoxic and destroy target cells by releasing small cytoplasmic granules of proteins that induce apoptosis (Oldham, 1983) and can efficiently destroy endometrial cells (Oosterlynck, et al., 1991). However, several studies have shown that in women with endometriosis the cytotoxic ability of NK cells against autologous and heterologous endometrium is diminished when compared with women without endometriosis (Garzetti, et al., 1993) and the reduction correlated with the increase in disease stage (Oosterlynck, et al., 1992). This diminished cytoxicity may

lead to the ineffectiveness of NK cells in destroying refluxed eutopic endometrium allowing transplantation and lesion formation.

A specific subset of NK cells can only be found in the uterus and are called decidual or uterine NK (uNK) cells. These cells inherently have lower cytotoxic activity than that of peripheral blood NK cells and may play an important role in initiation of menstruation, maintenance of decidua, embryo implantation and endometrial angiogenesis (Moffett-King, 2002). In some women with endometriosis related infertility, an increase in the frequency of this cell population is observed (Kusakabe, et al., 2007). Danazol, which decreases NK cell frequency in the uterus (Fukui, et al., 1999), can successfully be used to treat infertility in the patients who have undergone unsuccessful ART, implicating aberrant expression of NK cells in the uterus as a culprit in endometriosis induced infertility.

T Lymphocytes

T lymphocytes, as determined by IHC, are a major immune cell subpopulation in endometriotic tissue (Oosterlynck, et al., 1993). They play a central role in cell-mediated immunity and are classified into cytotoxic T cells and T helper cells. Cytotoxic T cells are capable of destroying a specific target by cytotoxic mechanism, and T helper cells transmit signals from antigen-presenting cells and enhance further immune response (Kindt, et al., 2007).

Cytotoxic T Cells

A decrease in cytotoxic T cell proliferative response to autologous endometrial cells has been observed in women with endometriosis (Helvacioglu, et al., 1997). Furthermore, it has been shown that the cytotoxicity of T lymphocytes that manage to reach autologous endometrial cells is hampered in women with endometriosis (Steele, et al., 1984). This defect in cytotoxicity can be corrected by stimulating peripheral blood lymphocytes with recombinant IL-2. Indeed, IL-2 treatment decreased the size of endometriotic lesions in the rat model of endometriosis (Velasco, et al., 2007) implying a therapeutic potential of IL-2 for endometriosis.

The presence of cytotoxic T cells is not always enough as it has been postulated that endometriotic cells are able to escape from immune surveillance of cytotoxic T lymphocyte by expressing Fas ligand (FasL). FasL induces apoptosis by binding to the Fas receptor expressed on the surface of lymphocytes. Interestingly, FasL expression in endometrial stromal cells can be induced by cytokines and chemokines (Agic, et al., 2008, Akoum, et al., 1996, Ohata, et al., 2008). Similarly, the level of endogenous FasL was higher in PF of women with the pelvic disease (Garcia-Velasco, et al., 2002). A decrease in activation of cytotoxic T cells has been shown in PF of women with endometriosis (Gallinelli, et al., 2004). Hence, the decrease in proliferation, cytotoxicity and activation along with increase of apoptosis inducing signals may lead to ineffectiveness of cytotoxic T cells in battling endometrial and endometriotic cells.

T Helper Cells

In contrast to Cytotoxic T Cells, CD4+ helper T cells have no cytotoxic activity. Rather, they help the immune response by activating and directing other immune cells (Kindt, et al., 2007). Activation of helper T cells is essential for their role in directing further immune response. Although there are high number of helper T cells found in PF of women with endometriosis (Hill, et al., 1988), the number of activated helper T cells is suppressed as compared with women without endometriosis (Gallinelli, et al., 2004). This may lead to an environment where eutopic endometrium can survive and induce endometriosis.

Monocytes in Endometriosis

Monocytes evolve from common myeloid progenitor (CMP, Figure 7) and are primarily involved in the innate immune system. Their role in the immune response includes replenishing resident macrophages and dendritic cells (DCs) under normal states, and in response to inflammation signals, monocytes can move quickly to sites of infection in the tissues and divide/differentiate into macrophages and DCs to elicit an immune response (Swirski, et al., 2009).

Figure 7: Common myeloid progenitors give rise to monocytes and granulocytes

The common myeloid progenitors (CMP) give rise to granulocytic, and monocytic lineages, which give rise, respectively, to granulocytes (neutrophils, eosinophils, basophils), monocytes (differentiate into macrophages in tissue) and dendritic cells (adapted from Abbas, et al., 2012).

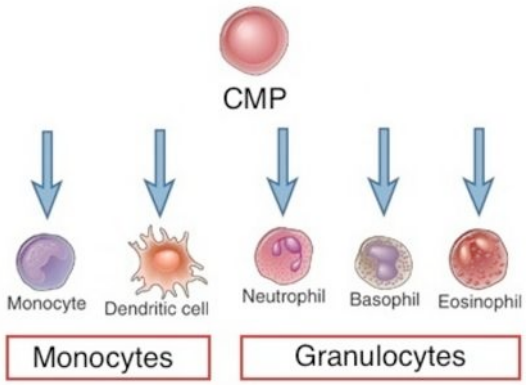

Macrophages

Upon entry into the peripheral tissue, monocytes mature into macrophages. Macrophages are the major resident cells in the peritoneal cavity as determined by IHC (Oosterlynck, et al., 1993). They kill cells, such as retrograde endometrial tissues, and their presence is commonly associated with an inflammatory process. Peritoneal fluid and intact tissues derived from women with endometriosis have been shown to contain higher numbers of activated macrophages than women without endometriosis (Hever, et al., 2007).

Activated macrophages in patients with endometriosis are believed to mediate and exacerbate inflammation and sustain the disease (Taylor, et al., 2002). Activation of macrophages, along with their increased secretion and synthesis of different pro-inflammatory mediators has been observed at ectopic sites in patients with endometriosis compared with peritoneum or PF of women without endometriosis (Taylor, et al., 1997). Interactions between the endometriotic cells and macrophages are mediated by growth factors, cytokines, and chemokines, leading to the paradoxi-

cal survival of implants rather than their demise (Lebovic, et al., 2001). Therefore, activation of macrophages within the peritoneal cavity and endometriosis implants may contribute to inflammation and associated with endometriotic lesions. Classically activated M1 macrophages are essential for host defense and tumor cell killing (Ding, et al., 1988). Conversely, alternatively activated M2 macrophages promote angiogenesis and matrix remodeling while suppressing destructive immunity (Sica, et al., 2006). The M2 macrophage phenotype might be more pertinent to endometriosis because they may be involved in allowing ectopic transplantation of endometrial cells leading to endometriotic lesions.

Dendritic Cells

Dendritic cells (DCs) are a heterogeneous population of antigen presenting cells that are mainly involved in the initiation and modulation of the immune response (Abbas, et al., 2012). DCs function in T cell stimulation through the capture, transport, processing and presentation of antigens to naive T cells, and are also involved in the maintenance of self-tolerance (Schulke, et al., 2009). In the human uterus, DCs may act as local mediators of endometrial transformation during the menstrual cycle, leading up to implantation or in the absence of pregnancy, menstruation (Bengtsson, et al., 2004). In lieu of these functions, alterations in DC populations may lead to dysregulation of other types of leukocytes and disruption of the normal endometrial cytokine profile, which may contribute to the development of endometriosis or endometriosis associated infertility. Immature DCs are primarily involved

in immune surveillance and antigen capture in peripheral tissues while mature DCs are APCs that are highly involved in modulation of immune response.

Granulocytes in Endometriosis

Although many of the studies on the immunology of endometriosis focus on the aforementioned immune cells, there has been little attention paid to granulocytes. Granulocytes are classified as neutrophils, eosinophils, and basophils; they arise from CMPs (Figure 7). The first two are motile phagocytes that can migrate from the blood into the tissue space while the latter is nonphagositic and functions by releasing pharmacologically active substances from their granules (Kindt, et al., 2007). Low concentrations of neutrophiles have been found in the PF of patients with endometriosis (Tariverdian, et al., 2009). Indeed, neutrophile concentration increased by 10-fold in direct correlation with increase in severity of the endometriosis when compared with women without endometriosis (Milewski, et al., 2011). Interestingly, other major leukocyte populations (T cells and macrophages) were unchanged, thus suggesting that severe endometriosis is associated with the specific accumulation of neutrophils in the pelvic cavity.

1.3 Lesion Kinetics in Endometriosis

The severity of the symptoms of endometriosis has not always correlated with the anatomic severity of the disease (Abbott, et al., 2003, Crosignani, et al., 1996, Garry, et al., 2000). This lack of correlation may be due, in part, to variations in the activity

of the endometriotic lesions present at different episodes of the disease. Furthermore, indirect and distant effects of established lesions might be a major precondition for new lesion development and disease progression. Therefore, understanding the macroscopic appearance of lesions may afford additional assistance in the prognosis of the disease and determining the appropriate treatment method.

Observational studies suggest that endometriosis is a dynamic disorder. Follow-up studies of women with endometriosis showed that 17 to 29% of the lesions resolved spontaneously, 24 to 64% progressed and 9 to 59% were stable over a 12-month period (Sutton, et al., 1997). Another study following 14 women 6 months after initial laparoscopy demonstrated dynamic progression and regression of disease burden as assigned by the revised ASRM (formerly known as the American Fertility Society) guidelines (1985), independent of endocrine treatment (Telimaa, et al., 1987). Therefore, using quantitative scoring system as a metric, the literature suggests that endometriosis has a variable, if not largely progressive, clinical course (Koninckx, et al., 1991).

Lesion turnover is difficult to study in women with endometriosis since there are significant delays in diagnosis as well as numerous variations in symptomatology and disease progression (see next section). Thus the olive baboon (Papio anubis) has been developed as an appropriate model to better examine the establishment and progression of endometriotic lesions. Dynamic progression and regression of lesions has been demonstrated in this induced endometriosis model (Hastings and

Fazleabas, 2006, Jones, et al., 2006). Furthermore, baboons are menstruating primates and can develop endometriosis spontaneously (Merrill, 1968). There is evidence of lesion turnover in baboons with spontaneous endometriosis. In a 32-month kinetic analysis, there was oscillation of the total number as well as remodelling and transformation of lesions in animals with spontaneous endometriosis (D'Hooghe, et al., 1992, D'Hooghe, et al., 1996a).

Lesion dynamics describe spontaneous lesion progression and regression, the development of new lesions, and changes in lesion appearance over time. Lesion turnover is a consequence of these dynamics, which are likely induced by hormonal and inflammatory fluctuations. Hormonal fluctuation has been implicated in a study by Koninckx et al., (1996) where palpation during menstruation increased the detection rate of endometriosis by fivefold versus routine examination not timed to menstruation. Studying lesion turnover may provide clues regarding the biological activity of the endometrial implants, increase our understanding of the natural history of endometriosis and possibly reveal new insights into its clinical management and prognosis. Here we examine lesion kinetics in a non-human primate model of endometriosis with the goal of providing a better understanding of lesion dynamics, which may lead to new opportunities for targeted therapies to prevent and/or treat endometriosis.

1.4 Animal Models For the Study of Endometriosis

Controlled investigation of endometriotic lesions in humans is limited by ethical concerns since it is difficult to justify repeated laparoscopies for no medical benefits. Furthermore, in most patients, the time from the onset of disease to diagnosis is between 8–11 years (Hadfield, et al., 1996), eliminating the possibility to characterize factors involved at the beginning and throughout disease progression. Thus, investigating the pathophysiology of endometriosis and consequently developing new therapeutic approaches requires a robust animal model system.

The most commonly used models for endometriosis research have been established using either different inbred mouse strains or non-human primates (NHPs). The only animals known to develop endometriosis are NHPs such as baboons and macaques (Fanton and Hubbard, 1983, Merrill, 1968) making them the best candidate for studying endometriosis. However, the long duration of endometriosis occurrence and the rare incidence of spontaneous endometriosis hinder systematic evaluation of NHPs with spontaneous pelvic disease. Artificial induction of endometriotic lesions in difference animal species represents an alternative model. In the current study mouse and baboon experimental models were used to gain a better understanding of the dynamic of endometrial tissue at ectopic sites.

1.4.1 Mouse Model

The first model of endometriosis was performed in rabbits where autologous endometrial fragments from one uterus horn were transplanted onto the peritoneum (Schenken and Asch, 1980). Vernon and Wilson (1985) adapted this model to rats while Cummings and Metcalf (1995) published the first transplantation model in mice where they sutured autologous uterus biopsies onto the mesentery vessels of the small intestine. Biopsies were additionally sutured onto the peritoneum to mimic peritoneal lesions (Becker, et al., 2005).

In contrast to humans and some NHPs, mice do not shed their endometrial tissue and therefore do not develop endometriosis. Furthermore, mice and humans differ in their levels of sex hormones as well as the duration of their cycles. For example the murine cycle lasts about 4-5 days while human cycle lasts 28 days with varying hormonal levels (Byers, et al., 2012). Nevertheless, transplanting endometrial tissue at ectopic sites in mice can induce lesions with histological characteristics comparable to the human disease. The murine models are classified into two types: heterologous and homologous. Heterologous (humanized) models utilize human endometrial fragments, which are transferred either intraperitoneally (i.p.) or subcutaneously (s.c.) to immunodeficient mice, whereas in homologous models there is surgical transplantation of endometrium from either autologous, when transplantation involves only one animal, and is from, for example, the uterus to the peritoneal cavity (Fainaru et al., 2008), or syngeneic, when using a donor and recipient animal of identical genotype (Bacci, et al., 2009).

For the purposes of this study, a homologous model called the syngeneic transplantation model was utilized. Here, uterus horn from syngeneic mice was excised, cut into small biopsies, and sutured onto the peritonea of genetically identical recipient mice. The advantage of this model is the high take rate and the easy recovery. The limitations of this model include the lack of menstruation and subsequent spontaneous endometriosis. Additionally, use of the entire uterus, including myometrium, does not completely mimic the situation in human endometriotic lesions. Nevertheless, the opportunity to examine large groups of identical animals as well as long-term studies, low costs, and a well-characterized murine genome are important advantages of this model (Grummer, 2006).

The growth of the ectopic endometrial tissue in mice is estrogen dependent (Fang, et al., 2004) making the species useful for studying the effects of the sex hormone in the establishment and persistence of endometriotic lesions. Furthermore, to counteract variations in biological estrogen levels between individual mice, the ovaries, major source of estrogen (Bulun, et al., 2005), are often removed (ovariectomized, ovx) at least one-week prior to the transplantation surgery to allow control over the concentration of the sex hormone during the experiments.

1.4.2 Primate models

Women with endometriosis should ideally be compared to women with normal pelvis (negative controls) as well as women with disorders that result in similar symptomatology (positive controls). Furthermore, endometriosis progression can only be

confirmed by repetitive laparoscopic examinations. However, ethical issues hinder such studies in humans and have prompted the design of different strategies to induce endometriosis-like lesions in non-human primates, with the aim of establishing models that allow the identification and elucidation of the mechanisms by which endometrial cells adhere and persist at ectopic sites.

Spontaneous development of endometriosis has been detected in 11 different NHPs (Story and Kennedy, 2004) and offers an ideal situation to examine the influence of ectopic implants on eutopic endometrium and the differences between the two tissues as well as cause and effect of the disease development (Grummer, 2006). However, major limitation is the low frequency, which necessitates large experimental groups (ethical consideration), long periods to disease manifestation, and high costs of care. Hence, artificial induction of endometriosis has been established with various methods like repositioning of the cervix (Te Linde and Scott, 1950), suturing of endometrial fragments at ectopic sites (Fazleabas, et al., 2002) or injection of endometrium (D'Hooghe, et al., 1995). For the current study of lesion kinetics introduced in section 1.3, the well-established baboon model with i.p. inoculation of autologous menstrual endometrium was utilized (Braundmeier and Fazleabas, 2009).

1.5 Thesis Aims

The aim of this study was to analyze hormone induced lesion dynamics and morphological lesion dynamics in experimental models of endometriosis. Hormonal dy-

namics were analyzed using a mouse syngeneic transplantation model routinely utilized in endometriosis research. Changes in endometriotic lesion size, morphology, and progression over time in a controlled estrous cycle environment were determined. Furthermore, estradiol's affect on lesion size promotion was analyzed by looking at proliferation, apoptosis, and cell composition of the lesions. Additionally, the origin of the cells residing in the mouse lesions was measured using a clever syngeneic transplantation luminescence mouse model that allowed noninvasive monitoring of lesions over time.

Macroscopic appearance and kinetic of endometriotic lesions was analyzed in a non-human primate model of endometriosis with the goal of providing a better understanding of lesion dynamics. Here, a retrospective analysis of baboon video and surgical notes was conducted to accumulate data in regards to lesion morphological progression and regression over time. Furthermore, the affect of lesion excision/ablation on recurrence of lesions was determined. Additionally possible promotion in spontaneous development of endometriosis due surgical trauma in control baboons was investigated.

2 Materials and Methods

2.1 Mouse Studies

All protocols involving animals were performed in accordance with institutional, state, and federal guidelines. The mice were housed under controlled temperature (24°C) and lighting (12:12 hrs light-dark cycle) conditions with free access to food (normal chow) and water.

All animals (donors and acceptors) underwent ovariectomy (ovx) at least one-week prior to the transplantation surgery. Briefly, the animals were anaesthetized via intraperitoneal (i.p.) injection with 1:1 ketamine hydrochloride (Ketavet; Pfizer, Karlsruhe, Germany) and xylazine hydrochloride (Rompun; Bayer, Leverkusen, Germany), diluted 1:10 in sterile distilled water. A dorsal midline excision was made to the posterior border of the ribs. Using a blunt dissection forceps, the muscle of the posterior abdominal wall was separated in order to enter the abdominal cavity. The ovary was located in a fat patch just beneath the muscle, was grasped and using electrocautery the vessels in and around it was burned to avoid excessive bleeding. Using scissors, the ovary was excised from the uterus horn. The uterine horn was returned to the abdomen and the process was repeated for the other side. The skin was glued together by placing one drop of histoacryle blue adhesive (Aesculap, Tüttlingen, Germany) on one side and placing the other side thereupon. The animals were supplemented subcutaneously (s.c.) with daily dose of 1 μg/kg 17β-estradiol (E_2, Sigma-Aldrich, Munich, Germany) dissolved in 5% ethanol plus 95% peanut oil (vehicle) starting four days prior to the transplantation surgery.

2.1.1 Syngeneic Transplantation Endometriosis Mouse Model Using C57BL/6 Mice

Eight to 10 weeks old female syngeneic C57BL/6 mice were obtained from Janvier (Le Genest Saint Isle, France). Both donor and acceptor mice were anaesthetized as described previously.

The fur was disinfected with 70% ethanol; using scissors, the skin and abdomen were opened longitudinally. For the donor animals, the uterus horns and cervix were exposed and ligated. In a Petri dish filled with sterile 37°C Dulbecco's modified eagle medium (DMEM without phenol red; Invitrogen, Karlsruhe, Germany), each horn was longitudinally opened and 2 mm in diameter (3.14 mm^2 area) uterus biopsies were taken using a steel biopsy punch (Fine Science Tools, Heidelberg, Germany). Seven punch tissue fragments were transplanted into each acceptor with the endometrial side to the recipient's peritonea using needles with suture (Prolene 6.0, Ethicon Johnson & Johnson, Norderstedt, Germany). The positioning of the biopsies in the peritonea is demonstrated in Figure 8A. Uterus fragments were fixed with simple nodes at about 1 cm distance to the laparotomic incision. The temperature of the surrounding organs was maintained by suspending 1 mL of 37°C physiological saline into the peritoneal cavity. A continuous 5.0 Prolene (Ethicon Johnson & Johnson) suture was used to close the peritoneal incision. The abdominal skin was glued together by placing one drop of histoacryle blue adhesive (Aesculap) on one side and placing the other side thereupon. The mice were allowed to awaken on a warm

plate, and their recovery was monitored for at least 4 hours post surgery. Operated animals received daily s.c. application of either vehicle or 1 μg/kg E_2.

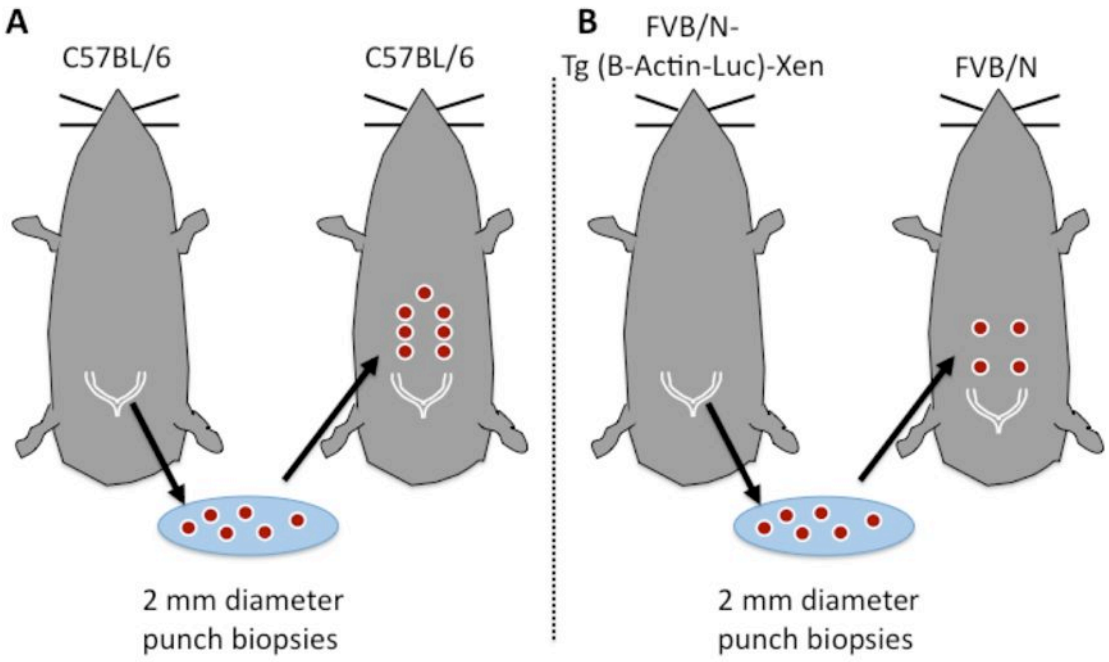

Figure 8: Positions of uterus punch biopsies transplanted onto the acceptor mouse

A: For the C57BL/6 experiment, the same syngeneic donor and acceptor were used.
B: For the FVB/N experiment, syngeneic FVB/N-Tg (B-Actin-Luc)-Xen was used as donor and syngeneic wild type FVB/N mice was used as acceptor.

2.1.2 Syngeneic Transplantation Endometriosis Mouse Model Using FVB/N Mice

In order to determine host cell infiltration in the lesions, eight to 10 weeks old wild type female syngeneic FVB/N mice were transplanted with uterus punch biopsies from syngeneic FVB/N-Tg (B-Actin-Luc)-Xen (Taconic, Ry, Denmark). The latter expresses firefly luciferase, which luminesces when supplemented with D-Luciferin (Greer and Szalay, 2002). This can be quantified via ex vivo imaging of the animals. Four punch biopsies were transplanted onto each animal as previously described (Figure 8B). Animals received daily s.c. application of either vehicle or 1 µg/kg E2. Luminescence was measured at days 2, 4, 7, 13, and 27 after transplantation surgery. Briefly, animals were injected intraperitoneally (i.p.) with 100 mg/kg D-Luciferin (Sigma-Aldrich) dissolved in physiological saline. The animals were anesthetized using 2.5% isoflurane (Abbot, Wiesbaden-Delkenheim, Germany); the fur was removed chemically using Nair hair removal lotion (Church & Dwight Canada Corp., Mississauga, ON, Canada) from the abdomen to prevent interference. Luminescence was measured using the NightOWL instrument (Berthold, Hamburg, Germany). Exposure time for luminescence was set to 1 min (Figure 9). For analysis, WinLight32 (Berthold) software was used and the optimal threshold level of 1000 was determined and kept constant for every animal. Mean grey area per mouse was calculated and plotted.

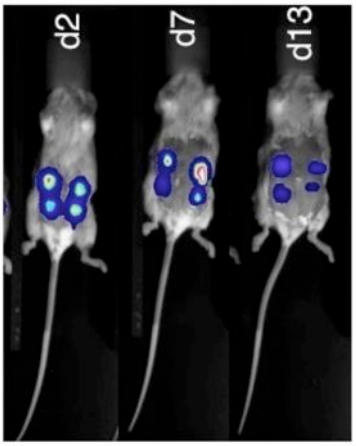

Figure 9: Ex vivo imaging of endometriotic lesion luminescence in FVB/N mice

Luminescence was measured at two, four, seven, 13, and 27 days after transplantation. Animals received 100 mg/kg D-Luciferin via i.p. injection. Luminescence was measured using the NightOWL instrument approximately 10 min after injection. Exposure time for luminescence was set to 1 min.

2.1.3 Necropsy: Lesion Photography and Tissue Harvesting

There were four treatment periods of four, seven, 14, and 28 days (Figure 10). Each group contained n ≥ 10 animals. On the respective days of necropsy, mice were anesthetized as described previously. Abdominal skin was incised using a scissor and cut longitudinally to the flanks. The skin was pulled cranially to overview the peritoneum. By cutting the peritonea proximal to the thorax, direct top viewing of the endometriotic lesions was accomplished. After photographing the lesions using a Canon Power Shot A640 (Tokyo, Japan), the area was measured from the photographs using the AxioVision Software (Zeiss, Jena, Germany). Accurate area determination in mm^2 was performed after calibration of the measuring unit via photography of a 10x10 mm graph paper. The lesions and uterus were excised. Samples were snap frozen for protein and mRNA analysis. Tissue for flow cytometry was transferred to 2% Fetal Calf Serum (FCS; Invitrogen) PBS solution and analyzed on the same day. To fix tissues for histology, a formalin solution containing 100 mL formaldehyde (Sigma-Aldrich, Munich, Germany), 4g NaH2PO4.H2O, 7.96g

Na2HPO4.H20 (Merk KGaA, Darmstadt, Germany) diluted in 1L volume using Milli-Q water, was utilized.

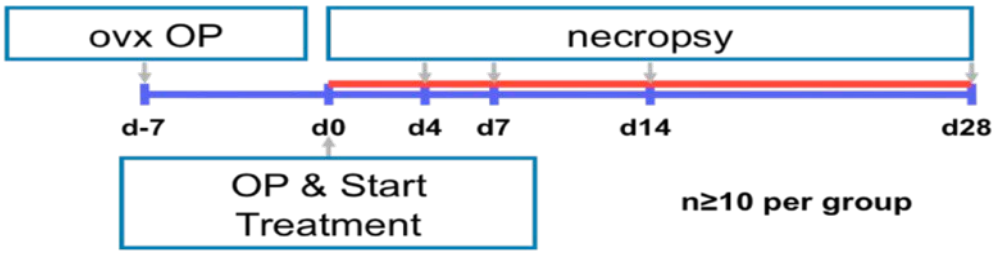

Figure 10: Experimental design and time line for the mouse studies

All animals underwent ovariectomy (ovx) at least one-week prior to the transplantation operation (OP). They were then pretreated with 1 μg/kg E_2 for four days prior to OP. Treatment with vehicle or 1μg/kg E_2 started immediately on the day of the transplantation. Each treatment group contained n ≥ 10 mice.

2.2 *Ex vivo* Analysis of Mouse Samples

2.2.1 Gene Expression Analysis

At necropsy, endometriotic lesions were snap frozen in ceramic sphere Lysing Matrix tubes (MP Biomedicals, Illkirch, France) and stored at -80°C. For RNA extraction, 550 mL TRK lysis buffer was added and samples were homogenized for 30 seconds using the FastPrep 24 instrument (MP Biomedicals). RNA was extracted using the HiBind RNA columns from the E.Z.N.A Kit (Omega Bio-Tek, Norcross, GA, USA) with incorporated DNase digestion according to the manufacturer's protocol. Total RNA was eluted in 30 mL diethylenepyrocabonate (DEPC) treated water. The concentration was measured using optical density at 260 nm with Nanodrop 3300 (Thermo Scientific, Waltham, MA, USA) in ng/mL. RNA was stored at -80°C for further applications.

250 ng of RNA was used in the reverse transcription reaction using High-Capacity cDNA Reverse Transcription Kit including RNase inhibitor (Applied Biosystems, Carlsbad, CA, USA). RNA samples were diluted with ultra pure distilled water (Invitrogen). The reaction was conducted using a 9800 Fast Thermal Cycler (Applied Biosystems) that included an initial incubation at 25°C for 10 min followed by reverse transcription at 48°C for 30 min and enzyme deactivation at 96°C for 5 min. The resulting cDNA (complementary deoxyribonucleic acid) was stored at -20°C for further applications.

Real Time-Polymerase Chain Reaction (RT-PCR) entails the use of two unlabeled primers that are complementary to a defined sequence on each of the two strands of the DNA along with a probe complimentary to a sequence located in between the two primers. The probe contains a reporter dye at 5' end and a quencher dye at the 3' end. During PCR, the probe anneals specifically to the complementary sequence between the forward and reverse primer sites. When the probe is intact, the proximity of the reporter dye to the quencher dye results in suppression of the reporter fluorescence. The DNA polymerase cleaves only probes that are hybridized to the target. Cleavage separates the reporter dye from the quencher dye resulting in increased fluorescence by the reporter. The increase in fluorescence signal occurs only if the target sequence is complementary to the probe and is amplified during PCR (Higuchi, et al., 1993). By using the housekeeping gene Hprt1 as reference, we can normalize quantification of a cDNA target for differences in the amount of cDNA added to each reaction.

Each RT-PCR reaction was carried out on a 7900 HT Sequence Detection System (Applied Biosystems) with 20 ng of cDNA under the following thermal conditions: 10 min 95°C, 40 cycles, 15 sec 95°C and 1 min 60°C. Eurogentec Universal PCR Master Mix without UNG (Liege, Belgium) was used for the reaction. In 384-well plates, 5.7 μL cDNA and 6.8 μL Master Mix containing forward and reverse primers along with the fluorescent dye tracer agent 6-Carboxyfluorescein (FAM)-phosphoramidit labeled probe for each gene of interest (Sigma-Aldrich) were mixed and quantified. The primers used were exon spanning and are listed in Table 1. All reactions were performed in triplicates. The expressions for genes of interest were quantified as Ct-values of Hprt1 using n-fold gene expression by ΔΔCt-method (Bubner, et al., 2004).

Gene	Forward Primer 5'-3' (bp)	Reverse Primer 5'-3' (bp)	FAM-probe 5'-3' (bp)
Hprt1	TGTTGTTGGATATGCCCTTG (20)	ATTTGGCTTTTCCAGTTTCACT (22)	TCAGGGATTTGAATCACGTTTGTGTCA (27)
Ccnb1	ATGGTGCATTTTGCTCCTTC (20)	TCCATTCACCGTTGTCAAGA (20)	AATTGCAGCTGGGGCTTTCTGCTTA (25)
Tgfb1	CCCTGGATACCAACTATTGC (20)	CTTCCAACCCAGGTCCTT (18)	TGTGCGGCAGCTGTACATTGACTTT (25)
Bcl2	AGTACCTGAACCGGCATCTG (20)	CATGCTGGGGCCATATAGTT (20)	ATAACGGAGGCTGGGATGCCTTTGT (25)
Bid	TTCATGAATGGCAGCCTGT (19)	GCTGTCTTCACCTCATCAAGG (21)	AAAGGAACTGCCTGGCCAAAGC (22)
Birc1a	CATGGAGTCTGACCTCTCCAA (21)	CGAAAGGAAATCACATTTCAGA (22)	CAGAACTCTCCAAATCTCCATGTTTTCCA (29)
Smac	TCAGAGATGGCTGCTGAGG (19)	GGATGTGATTCCTGGCAGTT (20)	TCAAACTGGAGCAGATCAGGCCTCC (25)

Table 1: Forward and reverse primers plus labeled probes for gene quantification using RT-PCR

2.2.2 Protein Expression Analyses

At necropsy, endometrial lesions were snap frozen in microfuge tubes (Eppendorf, Hamburg, Germany) and stored at -80°C. To extract the protein, 200 μL lysis buffer (Table 2A) containing freshly dissolved protease and phosphatase inhibitor tablets (Roche, Basel, Switzerland) were added. Samples were then homogenized using an

Ultra Turrax T10 (IKA, Staufen, Germany) and were centrifuged at 3000g at 4°C for 10 min. The supernatant was collected, and the total protein concentration was determined using a bicinchoninic acid (BCA) protein assay kit (Pierce, Rockford, MA, USA). A standard curve was used consisting of 1000, 750, 500, 250, 125, 62.5 and 0 mg/mL bovine serum albumin (BSA), diluted in lysis buffer. The protein lysates were diluted 1:20 in lysis buffer. 5 µL/well of each diluent was added in triplicates to a 96 well plate. 5 µL/well of the BSA standard was added in duplicates. 100 µL/well of the BCA working reagent was prepared according to the manufacturer's suggested protocol and was added to each well. The plate was incubated at 37°C for 30 min. The color formation with BCA is dependent upon: the macromolecular structure of the protein, the number of peptide bonds, and the presence of four particular amino acids cysteine, cystine, tryptophan and tyrosine (Stich, 1990). The absorbance was measured at 562 nm using a spectramax plate reader (Molecular Devices, Ismaning, Germany). Sample protein concentrations were extrapolated from the linear part of the BSA standard curve.

A: Lysis Buffer		B: Running Buffer (1L Water)		C: Blotting Buffer (2L, Water 8:2 Methanol)	
Reagent	**Vendor**	**Reagent**	**Vendor**	**Reagent**	**Vendor**
50 mM Tris pH 7.5	Sigma-Aldrich	12.1 g Tris Base	Sigma-Aldrich	11.7 g Tris	Sigma-Aldrich
150 mM NaCl	Sigma-Aldrich	23.8 g HEPES	Sigma-Aldrich	5.8 g Glycine	Sigma-Aldrich
2 mM EGTA	EMD Millipore	1 g SDS	Sigma-Aldrich	0.76 g SDS	Sigma-Aldrich
1 mM NaF	Sigma-Aldrich				
1% Triton-x-100	Sigma-Aldrich				

Table 2: Protein expression analysis buffers

A: Lysis buffer **B:** Running buffer dissolved in 1L total water **C:** Blotting buffer dissolved in 2L volume containing 8 parts water and 2 parts methanol (Sigma-Aldrich)

Sodium dodecyl sulfate polyacrylamide gel electrophoresis (SDS-PAGE) was used to detect the expression of a specific protein in tissue homogenates after size separation by gel electrophoresis. The protein homogenate was dissolved in a buffer containing SDS, which acted as an anionic detergent that binds quantitatively to proteins, giving them linearity and uniform charge, so that they can be separated solely on the basis of their size. Dithiothreitol (DTT; Sigma-Aldrich) was added in the buffer to reduce any disulphide bonds within the protein. Detection of the protein of interest was conducted after electroblotting the separated proteins onto a nitrocellulose membrane and by using high-quality primary antibodies directed against the desired protein (Towbin, et al., 1979). The detection reaction was accomplished with horseradish peroxidase-conjugated (HRP) secondary antibodies and chemiluminescence.

Precast 10% polyacrylamide gel (Pierce) was used. Approximately 10 µg of each protein sample was mixed with 5 µL sample reducing buffer containing DTT and 0.1% bromophenol blue (BPB). The samples were mixed and denatured at 96°C for 5 min. 6 µl of pre-stained broad range protein marker (12-225 kDa) ladder (Amersham, Buckinghamshire, UK) was added to the first well while samples were added to the other wells. The gel was run using running buffer (Table 2B) at 100 V for 60 minutes using a BioRad PowerPac 300 (BioRad, Munich, Germany) power supply.

Nitrocellulose membrane (BioRad), sponges, and filter paper were soaked in blotting buffer (Table 2C). The order of layers in the transfer cassette were arranged as follows: black cassette, sponge, filter paper, gel, nitrocellulose membrane, filter paper, sponge, and red cassette. This blot sandwich was slotted into the blotting apparatus (BioRad) with the black cassette facing the back. Blotting buffer was poured into the electrophoresis rig (BioRad) and proteins were transferred at 40 V for 90 min.

Membranes were blocked with 5% milk powder in PBS/0.1%Tween-20 (PBST) (Sigma-Aldrich) for 1 hour at room temperature. Membranes were incubated at 4°C overnight in either rabbit anti-BCL-2 or rabbit anti-a-Tubulin (Cell Signaling) at 1:500 and 1:5000 respectively in 10 mL 5% milk PBST. After being washed twice in 10 mL PBST for 15 minutes, the membranes were incubated in horseradish peroxidase-conjugated anti-rabbit antibody (Cell Signaling) at 1:5000 in 10 mL 5% milk PBS/Tween-20. Enhanced chemiluminescent (ECL; Millipore, Schwalbach, Ger-

many) reagent was used for 1 minute for visualization. In a dark room, 1 piece of x-ray film (Fujifilm, Düsseldorf, Germany) was placed on top of the membrane and the cassette was closed. The film was exposed to the membrane for 30 seconds to 5 min. The film was then developed using a CURIX 60 tabletop processor (Agfa Healthcare NV, Mortsel, Belgium). It was scanned to obtain a digital image and the band density of BCL-2 was determined and normalized to a-Tubulin using Image J software (National Institutes of Health, Bethesda, MD, USA).

2.2.3 Immunohistochemistry

Immunohistochemistry (IHC) is a process utilizing specific antibody to bind and detect antigens (e.g. proteins or nucleotides) in cells of a tissue section. Once antigen–antibody binding occurs, it can be demonstrated with a colored histochemical reaction visible by light microscopy or fluorochromes with ultraviolet light (Ramos-Vara, 2005).

The tissue samples were fixed for 24-48 hrs using formalin. After which, the formalin was rinsed off by submerging samples into a water bath with constant flow for 2 hrs. Leica ASP200 S (Wetzlar, Germany) was used for the paraffinization of samples. After paraffinization, a Modular Paraffin Embedding System (Medax, Neumünster, Germany) was used to embed tissue into cassettes. Using a Leica RM2155 Microtome, 4 μm sections were cut and placed onto SuperFrost Ultra Plus Slides (Thermo Scientific, Waltham, MA, USA).

To deparaffinize, the slides were incubated at 60 degrees for 20 min and then were immersed twice in xylene (Merk KGaA) for 10 min. The same procedure was repeated with isopropanol (Merk KGaA) and 96% ethanol (Sigma-Aldrich), but for 2 min each. Next, the samples were incubated in 80% and 70% ethanol and then Milli-Q water (Milli-Q Water Purification System; Millipore) for 2 min each.

Ki-67 Measurement of Proliferation

The Ki-67 antigen is a nuclear protein expressed during all active phases of the cell cycle, except in resting cells (G0). Therefore, antibodies against the Ki-67 antigen can be utilized for the monitoring of the proliferating fraction of a pool of cells (Scholzen and Gerdes, 2000).

The deparaffinized sections were incubated for 20 min in the pre-heated (in a vegetable steamer) target retrieval solution (Citrate buffer pH 6; Dako Cytomation, Glostrup, Denmark). They were allowed to cool for 10-20 min while still immersed. The slides incubated in a container filled with room temperature (RT) Milli-Q water for 10 min. The slides were transferred into the Dako Autostainer instrument. The specimens underwent peroxidase blocking for 5 min after which they were rinsed with Milli-Q water. The samples were blocked with 3% normal goat serum in Dako wash buffer (0.05 mol/L Tris/HCl, 0.15 mol/L NaCl, 0.05% Tween 20, pH 7.6) for 5 min and then the liquid was blown off (not rinsed off). The sections were then incubated for 60 min in the Dako mouse Ki67 TEC3 antibody (1:25 dilution in wash

buffer). The antibody was rinsed off with wash buffer, and the sections were incubated for 15 min with the Goat Anti Rat IgG Secondary antibody (1:100 dilution in wash buffer; BD Biosciences, Heidelberg, Germany). The sections were rinsed with wash buffer, and then incubated for 10 min with Streptavidin. The Streptavidin was washed off using Milli-Q water. The AEC (3-amino-9-ethylcarbazole) Substrate-Chromogen solution was added, and the slides were incubated for 20 min. The AEC was rinsed off using wash buffer. The samples were counterstained for 1 min with Hematoxylin (1:8 dilution in Milli-Q water). Slides were rinsed with wash buffer and incubated for 10 min in tap water. They were then removed from the autostainer and covered using glass cover slides with aqueous mounting medium (Dako). The slides were dried over night before imaging. For imaging Pannoramic MIDI (3DHISTECH, Budapest, Hungary) automatic digital slide scanner was utilized.

The images were analyzed semi-quantitatively by using a scoring system. Negative Ki-67 staining was assigned 0, some Ki-67 positive was assigned 1, middle Ki-67 positive was assigned 2, and highly Ki-67 positive was assigned 3. Mouse spleen was used as positive control since it contains many proliferating cells.

TUNEL Measurement of Apoptosis

Terminal deoxynucleotidyl transferase dUTP nick end labeling (TUNEL) is a method for detecting DNA fragmentation, which results from the apoptotic signaling cascade, by labeling the terminal end of nucleic acids (Gavrieli, et al., 1992). Since there

were three cuts of the same tissue on each slide, they were separated using a wax-dispensing pen from Dako Cytomation. The sample tissues were permeabilized by pretreatment with 20 mg/mL Proteinase K (Dako Cytomation) for 15 min at room temperature. They were then washed with two changes of Milli-Q water. As positive control, mouse testes pretreated with 100 mg/mL DNase I in PBS for 20 min at 37°C were utilized. ApopTag Peroxidase *In Situ* Apoptosis Detection Kit (Chemicon International, Schwalbach, Germany) was used to label fragmented DNA following the manufacturers suggested protocol. To develop the peroxidase color, the samples were incubated with DAB (3,3'-Diaminobenzidine; Dako Cytomation) for 2 min. They were washed with Milli-Q water and counterstained with 0.5% methyl green (Sigma-Aldrich) for 5 min. They were rinsed with Milli-Q water and submerged into N-butanol (Sigma-Aldrich) for 2 min with agitation. For dehydration, the slides were incubated through three jars of Xylene for 2 min. They were mounted under glass cover slip using a non-aqueous mounting medium (Dako Cytomation) and dried overnight.

For imaging, Pannoramic MIDI automatic digital slide scanner was utilized. For counting, since there were three cuts of each specimen per slide, all the cells in one cut were counted. This number was set as the total number of cells in each cut, then the positive cells were counted in all three cuts and the percent of positive cells was calculated.

2.2.4 Flow Cytometry

Flow cytometry was used for counting and separating specific cells, by suspending them in a stream of fluid and passing them by an electronic detection apparatus. A wide range of fluorophores can be used as labels in flow cytometry. They are typically attached to an antibody that recognizes a target feature on or in the cell; they may also be attached to a chemical entity with affinity for the cell membrane or another cellular structure (Ormerod MG. 2000). Here we utilized Becton, Dickinson, and Company FACSCanto II flow cytometer (Heidelberg, Germany) for cellular composition measurement of uterus and lesion tissue from mouse.

Tissue Digestion for Flow Cytometry

In order to free the cells from the extracellular matrix, the uterus and lesions were cut into smaller pieces. They were transferred into 15 mL Falcon tubes (BD Biosciences) containing 2 mL DMEM with 100 mg/mL DNase I (Sigma-Aldrich) and 100 mg/mL Liberase Blendzyme (Roche). Liberase Blendzyme contains a mixture of collagenase and neutral protease enzymes. They were incubated at 37°C with agitation for 60 min. Immediately after incubation, 4 mL of ice cold 2% FCS PBS was added to stop the collagenase activity. The samples were passed through a cell strainer (BD Biosciences). The remaining tissue was discarded. The samples were spun down at 1200 rpm for 6 min. The supernatant was discarded and the pellet was resuspended in 300 mL 2% FCS PBS. The cells were split into two 96-well plates.

BrdU Measurement of Proliferation

Bromodeoxyuridine (BrdU) is a synthetic nucleoside that is commonly used in the detection of proliferating cells. BrdU can be incorporated into newly synthesized DNA when cells enter the S phase (DNA synthesis phase) of the cell cycle (Miltenburger H.G. et al. 1987). 1 g/L of BrdU (Sigma-Aldrich) was added to the drinking water of animals starting 4 days prior to necropsy.

BrdU Flow kit (BD Biosciences) was used to measure BrdU in uterus and lesions. The first of the two 96-well plates (from above) was centrifuged at 1200 rpm for 2 min. The supernatant was tapped off, and the samples were allowed to incubate at room temperature (RT) for 20 min in 50 mL of BD Cytofix/Cytoperm Buffer. The plate was washed twice, using 200 mL/well 1X BD Perm/Wash Buffer, centrifuging at 1200 rpm for 2 min and discarding the supernatant each time. 50 mL of BD Cytoperm Plus Buffer was added and the plate was incubated for 10 min on ice. The plates were washed as before and the cells were resuspended in 50 mL volume of 300 mg/mL DNase I (Sigma-Aldrich). The plate was incubated at 37°C for 60 min. The samples were again washed as before and resuspended in 50 mL of the antibody cocktail in 1X BD Perm/Wash Buffer (Figure 11A). They were incubated in the dark at RT for 20 min. After the incubation with the antibodies, the samples were washed as before and were resuspended in 50 mL 1:100 Anti Rabbit IgG FITC (BD Biosciences) and incubated in the dark at RT for another 20 min. The plates were washed as before and resuspended in 200 mL 2%FCS PBS. They were transferred to

the BD FACSCanto II and analyzed. BD FACS Diva software was used to analyze the results. The gating strategy is depicted in Figure 11B.

A: List of Antibodies

Antibody	Target	Dilution	Vendor
Cytokeratin	epithelial cells	1:100	BD Biosciences
BrdU APC	BrdU, proliferation	1:200	BD Biosciences
CD45 APC-Cy7	hematopoietic cells	1:400	BD Biosciences

B: Gating Strategy

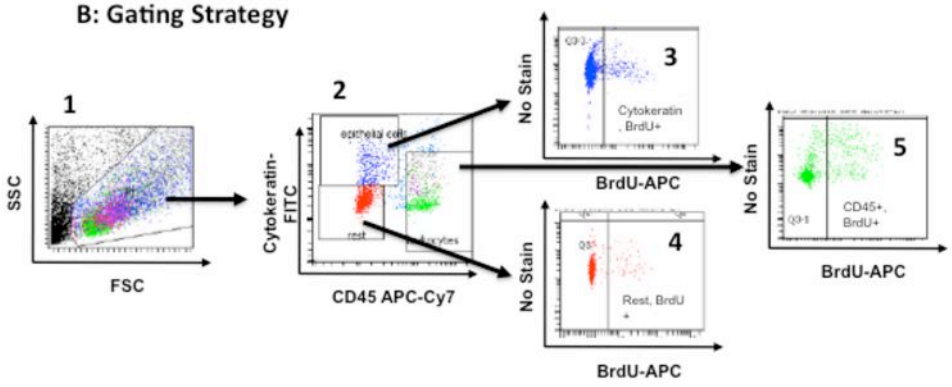

Figure 11: BrdU measurement of proliferation

A: The list of antibodies used **B1:** Cells were sorted based on size and granularity **B2:** Cells were sorted using Cytokeratin and CD45 **B3-5:** The BrdU positive cells were sorted

Cell Composition and Annexin V Measurement of Apoptosis

The second 96-well plate from the tissue digestion was used to measure immune cell composition of the uterus and the lesions. The samples were split into two

groups and were stained for small cells: T cells, B cells, and natural killer cells (NK cells); and large cells: macrophages, dendritic cells (DCs), and granulocytes (Figure 12A-B). 4',6-diamidino-2-phenylindole (DAPI) was used to exclude dead cells. The antibodies were diluted using 2% FCS PBS. The gating strategy for small and large cells is depicted in Figure 12C-D. All antibodies were acquired from BD Biosciences.

A: Antibodies Targeting Small Cells

Antibody	Target	Dilution
CD4 APC	T helper cells	1:200
CD45 APC-Cy7	hematopoietic cells	1:400
CD5 PE	cytotoxic T cells	1:200
B220 Pacific Blue	B cells	1:200
CD69 FITC	T cell activation	1:200
NK11 PE-Cy7	natural killer cells	1:400
Annexin V APC	Annexin V	1:30
DAPI	live cells	1:5000

B: Antibodies Targeting Large Cells

Antibody	Target	Dilution
F4/80 PE	macrophages, dendritic cells (DC)	1:200
CD45 APC-Cy7	hematopoietic cells	1:400
Gr1 PerCP	granulocytes	1:400
CD206 APC	macrophage & DC activation	1:200
Cd11c PE-Cy7	dendritic cells	1:400
MHC II FITC	macrophage & DC activation	1:400
Annexin V FITC	Annexin V	1:30
DAPI	live cells	1:5000

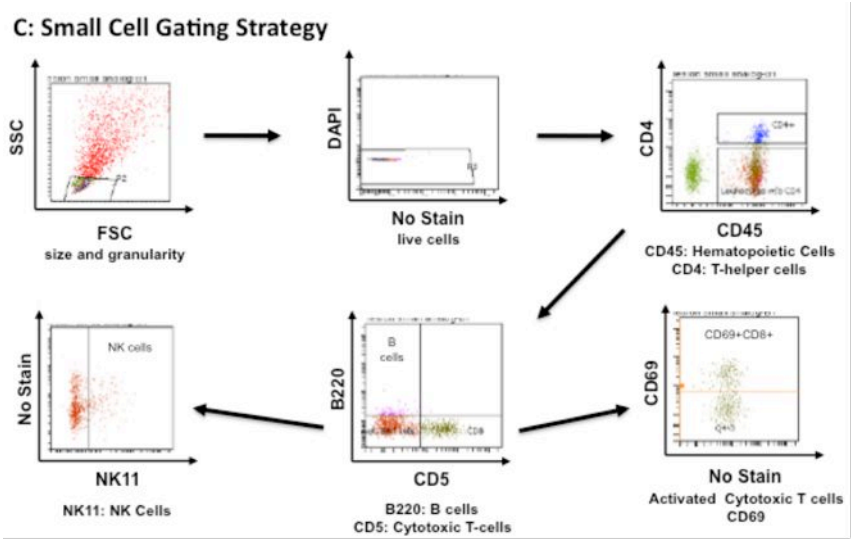

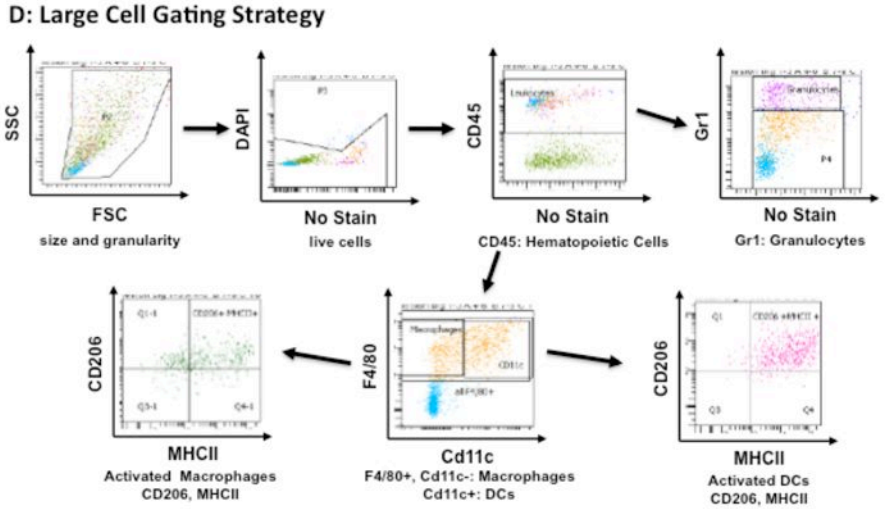

Figure 12 continued: A: The list of antibodies targeting small cells. **B:** The list of antibodies targeting large cells. For the Annexin V experiment, MHC II FITC antibody was omitted. **C:** Small cells were sorted by size; live cells were sorted using DAPI; T helper cells were separated from the rest of CD45 cells; B cells, cytotoxic T cells, and NK cells were separated using B220, CD5 and NK1.1 respectively; activated T cells were separated using CD69 marker. **D:** Large cells were sorted by size and granularity; live cells were sorted using DAPI, CD45 cells were separated from the rest, granulocytes (neutophils) were separated using Gr-1 (Ly-6G); macrophages and DCs were separated using F4/80 and Cd11c; activated macrophages and DCs were separated using CD206 and MHC II.

Annexin V was used as a probe to detect cells that have expressed phosphatidylserine (PS) on the cell surface, a feature found in dying cells (Vermes I. et al. 1995). APC conjugated Annexin V was used for the small cell staining and FITC conjugated Annexin V was used for large cell staining. The interaction of Annexin V and PS is calcium dependent (Raynal P. et al. 1994). Therefore, Annexin V staining was performed using Annexin V binding buffer (BD Biosciences) containing optimal concentration of calcium for PS binding. Samples treated with 2mM Staurosporine (Sigma-Aldrich) for 60 min at 37°C were used as a positive control. Staurosporine acts as an apoptosis-inducing agent through its activation of the caspase-3 pathway (Chae HJ. et al. 2000). As shown in Figure 13A-B, upon Staurosporine treatment, the frequency of Annexin V positive CD45- and CD45+ cells increased when compared to the same sample without the treatment. Tissue without the addition of Annevin V antibody was used as the negative control (Figure 13C).

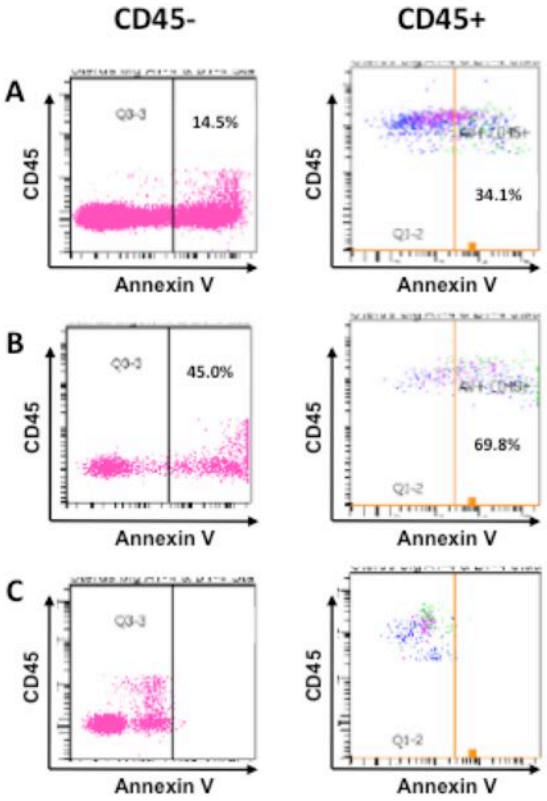

Figure 13: Annexin V staining controls
A: Uterus tissue stained with Annexin V
B: Uterus tissue treated with the apoptosis-inducing agent Staurosporine. There was an increase in the frequency of positive cells observed when comparing with A.
C: Uterus tissue not stained with Annexin V was used as negative control

2.3 Retrospective Analysis of Baboons with Induced Endometriosis

A retrospective analysis of video and surgery documentation from baboons with induced endometriosis was conducted and the location of endometriotic lesions as well as their morphology was recorded.

All protocols involving animals were performed in accordance with institutional, state, and federal guidelines. Endometriosis was experimentally induced in 9 female adult *Papio anubis* baboons with documented regular menstrual cycles by intraperitoneal inoculation of autologous menstrual endometrium on day 2 of visible menses

on two consecutive menstrual cycles. Diagnostic laparoscopies were performed at day 8-12 post ovulation at 1, 3, 6, 9, 12, and 15 months following the 2nd inoculation (Figure 14 A-C). The inoculations and subsequent laparoscopies were performed according to techniques previously described (Hastings JM. & Fazleabas AT. 2006). In two animals, lesions were excised at 6 months and recurrence was recorded. Furthermore, 5 animals did not undergo inoculation but had diagnostic laparoscopies conducted to detect spontaneous endometriosis.

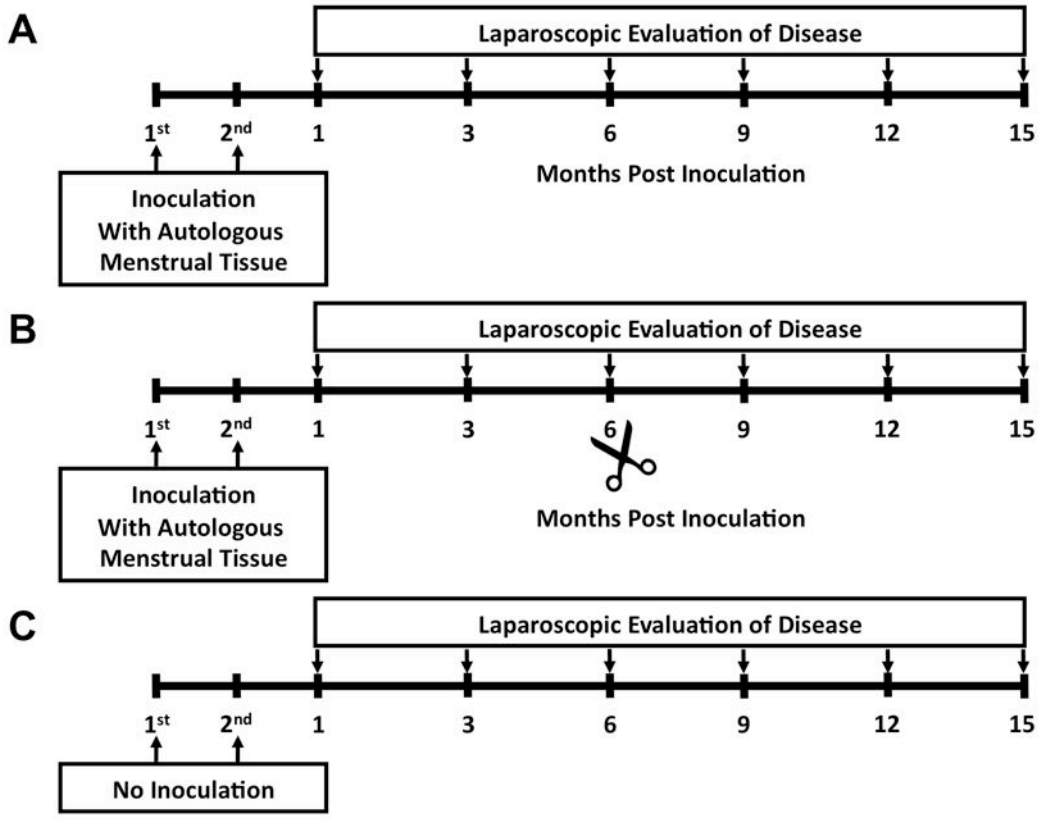

Figure 14: Experimental design and timeline for the baboon study

A: Nine baboons were inoculated with autologous menstrual tissue at two consecutive menses **B:** Two baboons with induced endometriosis had all lesions removed at 6 months laparoscopy **C:** Five animals did not undergo inoculation. All animals had diagnostic laparoscopies conducted at day 8-12 days post ovulation at 1, 3, 6, 9, 12, and 15 months following the 2nd inoculation.

2.3.1 Gene Expression Analysis of Baboon Lesions

RNA Extraction and cDNA Synthesis

Baboon lesions with different morphology (color) from 3 months and 15 months post inoculation were available for analysis. The samples were formalin fixed and paraffin embedded, therefore, using a Leica RM2155 Microtome, 8X20 mm sections were cut and placed onto microfuge tubes. To deparaffinize, 1 mL Xylene (Sigma-Aldrich) was added. Samples were briefly vortexed and incubated at 50°C for 3 min. RNA was extracted using the RecoverAll Total Nucleic Acid Isolation Kit (Ambion, Austin, TX, USA) with incorporated DNase digestion according to the manufacturer's protocol. Total RNA was eluted in 60 µL diethylenepyrocabonate (DEPC) treated water. The concentration was measured using optical density at 260 nm with Nano-drop 2000 (Thermo Scientific) in ng/mL. RNA was stored at -80°C for further applications. cDNA was synthesized using High-Capacity cDNA Reverse Transcription Kit including RNase inhibitor (Applied Biosystems) as previously described.

RT-PCR of Select Genes

RT-PCR reaction was carried out on a StepOnePlus Real-Time PCR System (Applied Biosystems) with 2.5 ng of cDNA under the following thermal conditions: 2 min 50°C of UNG (uracil-DNA glycosylase) incubation, 20 sec at 90°C for polymerase activation, 40 cycles of 1 sec at 95°C to denature and 20 sec at 60°C to anneal/extend. TaqMan Fast Advanced Master Mix (Applied Biosystems) was used for the reaction. In 96-well plates that were custom plated with the genes of interest in triplicates

(Table 3), 10 µL of cDNA diluted 1/50 with Master Mix was added and quantified. The expressions for genes of interest were quantified as Ct-values of 18S using n-fold gene expression by DDCt-method (Bubner et al. 2004). Genes expressed in four or more lesions were analyzed.

Indication	Gene	AB Assay ID	Indication	Gene	AB Assay ID
	IL-23p19	Hs00372324_m1		MKi67	Hs01032443_m1
	TGFß3	Hs01086000_m1		ENG (CD105)	Hs00923996_m1
Cytokines	CYR61	Hs00155479_m1		Bid	Hs00609632_m1
	CXCL12 (SDF-1a/b)	Hs00171022_m1	**Proliferation/**	XIAP	Hs01597783_m1
	CD2	Hs00233515_m1	**Apoptosis**	Naip1	Hs03037952_m1
Immune Cells	CD209 (DC-Sign)	Hs01588349_m1		Diablo (Smac)	Hs00219876_m1
	CD14	Hs00169122_g1		XAF1	Hs00213882_m1
	MX1	Hs00895608_m1			
	NOS2 (iNOS)	Hs01075529_m1			
Inflammation	MMP2	Hs01548727_m1			
	MMP9	Hs00234579_m1		KRT8	Hs01630795_s1
			Tissue	CD31 (PECAM-1)	Hs00169777_m1
			Composition	Vim	Hs00185584_m1
	AKR1C3	Hs00366267_m1		IGF1	Hs01547656_m1
	11ßHSD-1	Hs01547870_m1		IGF2	Hs00171254_m1
Endocrine	11ßHSD-2	Hs00388669_m1			
	Aromatase	Hs00903413_m1			
	PGR	Hs01556702_m1			
	ESR1	Hs00174860_m1	**internal**	18S	Hs99999901_s1
	ESR2	Hs01100353_m1	**controls**	RPS17	Hs00734303_g1

Table 3: List of select genes and their Applied Biosystems assay IDs

The primers were custom plated by Applied Biosystems in 96-well plates. RPS17 and 18S were present on every plate and were used as housekeeping control genes. All reactions were performed in triplicates.

Taqman Array Micro Fluidic Cards

TaqMan Array Micro Fluidic Cards (Applied Biosystems) are 384-well cards pre-loaded with TaqMan Gene Expression Assays. 24 baboon lesions, 12 from 3 months and 12 from 15 months post inoculation, were analyzed in Applied Biosystems Human Protein Kinase Array (containing 68 kinases and 26 non-kinase genes) and Human Immune Array (containing 94 immune related genes). RT-PCR reaction was

carried out on a ViiA 7 Real-Time PCR System (Applied Biosystems) with 1 ng of cDNA under the following thermal conditions: 20 sec at 90°C for polymerase activation, 40 cycles of 1 sec at 95°C to denature and 20 sec at 60°C to anneal/extend. In microfuge tubes, 16 µL cDNA was mixed with 184 µL water. To this mixture, 200 mL of the Taqman Universal Master Mix II without UNG (Applied Biosystems) was added. The expressions for the genes of interest were quantified as Ct-values of 18S using n-fold gene expression by DDCt-method (Bubner et al. 2004). Genes expressed in four or more lesions were analyzed.

2.4 Statistical Analysis

When applicable the results were presented as mean ± standard deviation. The standard deviation (SD) was calculated in order to demonstrate the scatter existing due to biological variation. Statistical analysis was conducted using GraphPad Prism 5.0 software (La Jolla, CA, USA). Statistical significance was evaluated using unpaired Student's t-test for comparisons between two means. The one-way Analysis of Variance along with Tukey's Multiple Comparison Post Hoc Test was utilized for the comparison of three or more unpaired groups. For Ki-67 staining scores served as a parameter and thus did not follow a Gaussian distribution. Accordingly, the nonparametric Two-tailed Mann-Whitney test (Fay and Proschan, 2010) was utilized to determine statistical significance. p value ≤ 0.05 was considered as significant.

3 Results

3.1 Effects of Estradiol on Experimental Endometriosis

Examining endometriosis evokes the need of an animal model. As previously mentioned (Introduction 1.4), the most adequate model is the menstruating non-human primate such as baboons. However, high cost and difficulty of handling limits the use of the baboon model. In order to study the effects of 17β-estradiol (E_2) on the establishment, development, and persistence of endometriotic lesions, a syngeneic transplantation endometriosis mouse model was utilized. Initially, to determine the appropriate mouse strain, a syngeneic transplantation experiment involving several strains of normal cycling (intact ovaries) mice were performed within the Transgenic and *in vivo* Pharmacology (TASIP) department at Bayer Healthcare. Here, FVB/N showed a significantly higher (t-test, $p \leq 0.05$) lesion area (7.14 ± 2.07 mm^2) as measured two-dimensionally when compared with C57BL/6 strain (5.10 ± 0.93 mm^2) twenty-eight days after transplantation (Figure 7). Accordingly, C57BL/6 was chosen as the mouse strain exhibiting small lesions while FVB/N was chosen as the strain exhibiting large lesions and were used in further experiments.

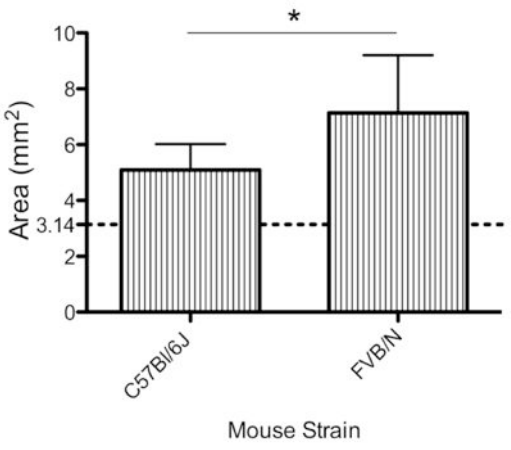

Figure 7: Comparison of lesion area in normal cycling C57BL/6 and FVB/N mouse strains 28 days post-transplantation

The y-axis shows lesion area as measured two-dimensionally in mm^2. The x-axis shows the two mouse strains. The initial area of the transplanted uterus fragments was approximately 3.14 mm^2 (dashed line). The lesion area in the FVB/N *(n=10)* mice was significantly higher than the C57BL/6 *(n=11)* mice (t-test, $*p \leq 0.05$). Error bars depict standard deviation.

3.1.1 Impact of Hormones on Lesion Development in C57BL/6 Mice

The ovaries, major source of E_2, were removed (ovariectomized, ovx) at least one-week prior to the transplantation surgery to allow control over the concentration of E_2 during the experiments. Corresponding syngeneic uterus donor and transplantation acceptor mice were used. All animals were supplemented subcutaneously (s.c.) with daily dose of 1 µg/kg E_2 starting four days prior to transplantation surgery. Seven 3.14 mm^2 punch uterus biopsies from syngeneic ovx C57BL/6 donor mice were transplanted onto the peritonea of identical acceptor mice using needle and suture. Operated animals received daily s.c. application of either vehicle or 1 µg/kg E_2 or 1 µg/kg E_2 plus 1 mg/kg progesterone (P_4). There were four treatment periods of 4 *(n=10)*, 7 *(n=10)*, 14 *(n=31)*, and 28 *(n=34)* days.

In the vehicle group, there was a small increase in mean lesion area at day 4 (d4, 3.38 ± 0.57 mm^2) followed by a decrease at d7 (2.70 ± 0.75 mm^2) as compared to the 3.14 mm^2 starting value. In the absence of E_2, the mean lesion area at d14 (1.71 ± 0.62 mm^2) and d28 (1.32 ± 0.63 mm^2) were significantly (t-test, $p \leq 0.05$) lower when compared with the d4 mice. In the E_2 treatment group, no significant difference in the mean lesion area between d4 (3.51 ± 0.75 mm^2), d7 (3.14 ± 0.61 mm^2), d14 (3.04 ± 0.67 mm^2), and d28 (4.12 ± 1.65 mm^2) animals was observed. Supplementing animals with E_2 plus 1 mg/kg P_4 resulted in no statistically significant difference in lesion area than E_2 only group (Figure 8A). Furthermore, the mean lesion area of E_2 only and E_2 + P_4 animals at d14 and d28 were significantly higher (t-test) than the vehicle treated animals from the corresponding time points. Accordingly, all further studies focused on the sole supplementation with E_2 as the main driver of lesion growth/persistence in this experimental model for endometriosis. Visual analysis of d4 lesions showed the presence of mostly red lesions that had already adhered to the adjacent peritonea with blood vessels being directed towards them. The lesions from d7 onwards often had a cyst-like appearance and displayed a smooth, white to transparent homogenous surface. There were no obvious visual differences between lesions from d7, d14, and d28 groups (Figure 8B).

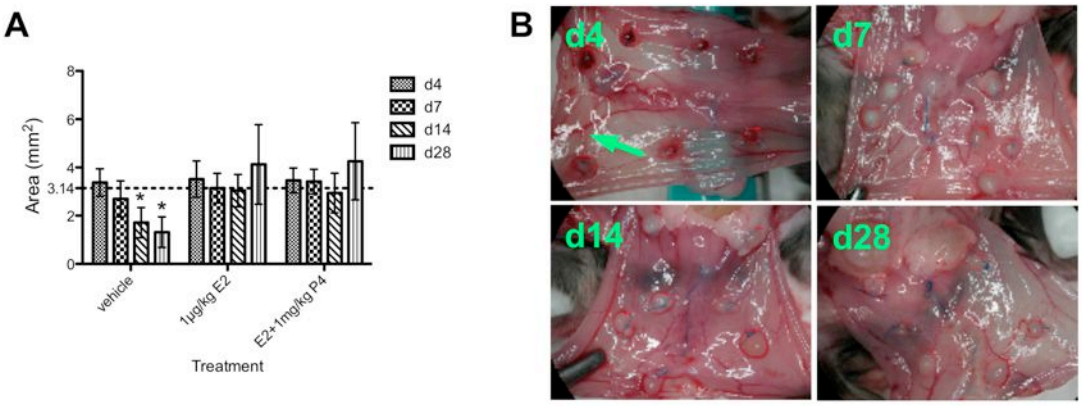

Figure 8: Microscopic evaluation of lesion area for the C57BL/6 mouse strain

A: The y-axis shows mean lesion area as measured two-dimensionally in mm^2. The x-axis depicts the different treatment groups. The error bars show standard deviation of the mean. There were four treatment periods of 4, 7, 14, and 28 days. The initial area of the transplanted uterus fragments was approximately 3.14 mm^2 (dashed line). In the vehicle treated mice, there was a significant decrease in lesion size over time when compared with the E_2 and the E_2 + P_4 treated groups (t-test, $*p \leq 0.05$). There was no significant difference in lesion area between E_2 only and the E_2 + P_4 groups. **B:** Photographs of lesions from the E_2 treated animals. At d4 lesions looked red and were already adhered with blood vessels directed towards them (arrow). From d7 onwards seemingly more established fluid filled cysts replaced the red lesions. There was no obvious visual difference between lesions from d7, d14, and d28 groups.

3.1.2 17β-estradiol's Effect on Lesion Size in FVB/N Mice

Four 3.14 mm^2 punch uterus biopsies from syngeneic ovx FVB/N-Tg (B-Actin-Luc)-Xen donor mice were transplanted onto the peritonea of syngeneic wild type ovx FVB/N mice using needle and suture. Operated animals received daily s.c. application of vehicle or 1 µg/kg E_2. There were two treatment periods of 14 *(n=9)* and 28 *(n=10)* days.

In the vehicle treated mice, the mean lesion area at d14 and 28 were 3.15 mm^2 (± 2.15) and 4.95 mm^2 (± 3.21) respectively. The difference between d14 and d28 vehicle treatment group, as with the C57BL/6 strain, was not statistically significant. However, in contrast to the reduction observed in mean lesion area over time in the vehicle treated C57BL/6 mice, the mean lesion area for the vehicle treated FVB/N mice increased between d14 and 28. In the E_2 treatment group, similar to C57BL/6 strain, no statistically significant difference in the mean lesion area between d14 (6.17 ± 3.21 mm^2) and d28 (8.57 ± 2.56 mm^2) animals was observed even though the mean area increased (Figure 9A). Similarly, the mean lesion areas from the E_2 treated FVB/N mice were significantly higher (t-test, $p \leq 0.05$) than the vehicle treated animals from the corresponding time points. Visually, the lesions from both treatment groups and time points manifested a cyst-like appearance and displayed a smooth, white to transparent homogenous surface (Figure 9B).

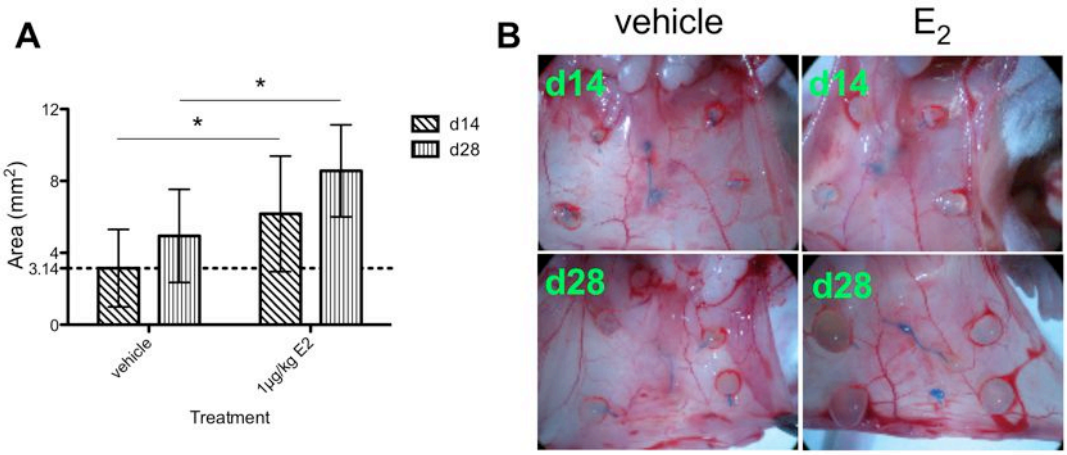

Figure 9: Microscopic evaluation of lesion area for the FVB/N mouse strain

A: The y-axis shows the mean lesion area as measured two-dimensionally in mm^2. The x-axis depicts the different treatment groups. The error bars depict standard deviation of the mean. There were two treatment periods of 14 *(n=9)* and 28 *(n=10)* days. The initial area of the transplanted uterus fragments was approximately 3.14 mm^2 (dashed line). In the vehicle treated mice, the mean area remained unchanged at d14 and increased at d28 in comparison to the initial value. When comparing the E_2 treated group with the vehicle, there was a significant increase in lesion area upon E_2 treatment group at both time points (t-test, $*p \leq 0.05$). **B:** Photographs of lesions from the d14 and 28 time points showed the presence of fluid filled cysts. In contrast to the vehicle group, the amount of fluid inside the lesions seems to increase over time in the E_2 treated group.

For further evaluation, the lesions were excised and examined histologically using hematoxylin and eosin (HE) staining. Figure 10 shows four typical mouse endometriotic lesions exhibiting hallmark histological characteristic of human lesions like the presence of glands (GL) and stromal (ST) structures. The glands, cyst-like formation, had a wide lumen, filled with non-specifically stained liquid and were lined with epithelial cells (EP). In some of the lesions, the remnants of the blue suture (S) used initially to hold the lesion in place were visible. In order to recognize the proper orientation of the lesions, when collecting lesions for immunohistochem-

istry (IHC) at necropsy, a small section of the attached peritonea were included. This peritonea tissue mainly contained muscle tissue (MT).

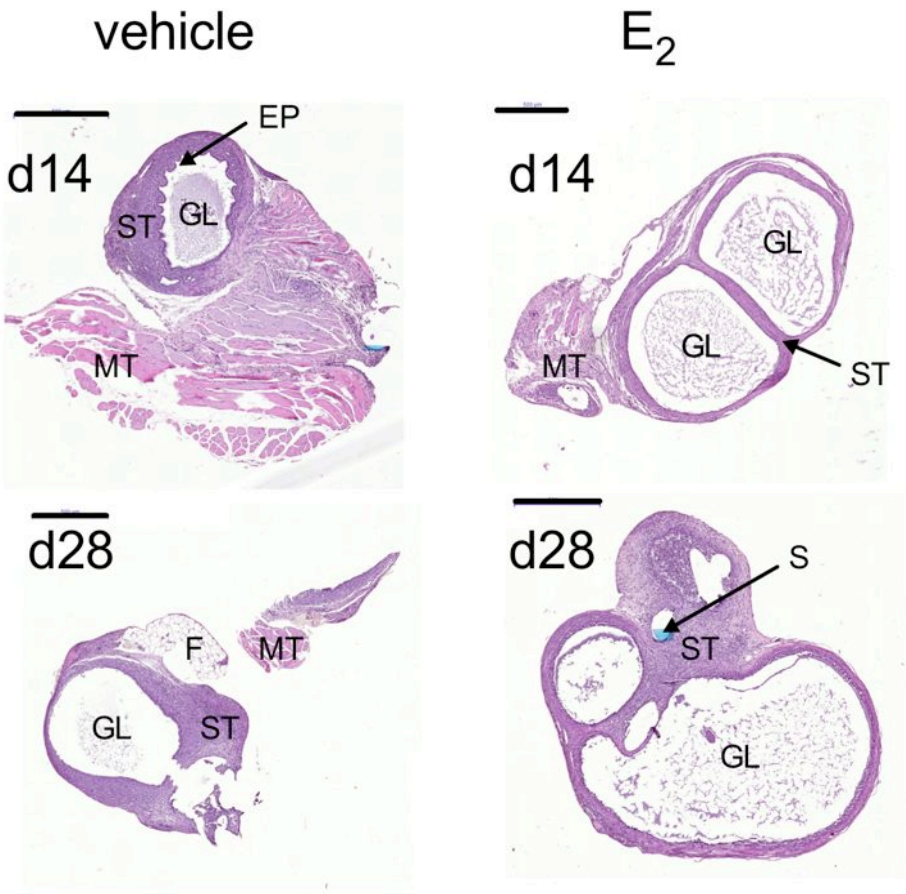

Figure 9: Hematoxylin and eosin (HE) staining of FVB/N mouse lesions

The mouse lesions showed typical histological characteristic of endometriotic lesions like the presence of glands (GL) and stromal (ST) structures. The glands had a wide lumen filled with non-specifically stained liquid and were lined with epithelial cells (EP). In some of the lesions, the remnants of the blue suture (S) used initially to hold the uterus biopsy in place were visible. Fat (F) was visible in some lesions. For orientation purposes, a small section of the attached adjacent peritonea were included in each staining and mainly contained muscle tissue (MT). Scale bar: 500 μm

3.1.3 Proliferation Is Not the Main Driver of Estrogen Mediated Lesion Growth

Endometriosis is characterized by the proliferation of endometrial glands and stroma outside the uterine cavity. Accordingly, the bigger lesion areas observed in the E_2 treated mice may be attributed to an increase in proliferation. To this extent, several techniques were utilized to measure E_2 mediated cellular proliferation of the endometriotic lesions from the C57BL/6 mouse syngeneic transplantation model of endometriosis.

BrdU Measurement of Proliferation

Bromodeoxyuridine (BrdU) is a synthetic nucleoside that can be incorporated into newly synthesized DNA during cellular proliferation. Approximately 1 g/L of BrdU was added to the drinking water of animals starting 4 days prior to necropsy. Using flow cytometry the frequency of BrdU+ cells in the lesions and the uterus were determined as percentage of total cells. When looking at all cells and regardless of treatment or time point in the mouse endometriotic lesions there was no statistically significant difference in the frequency of BrdU+ cells (Figure 10, white bars). In the uterus, there was a significant (t-test, $p \leq 0.05$) increase in the frequency of BrdU+ cells at d4 between vehicle treated mice (2.93% ± 1.15) and E_2 treated mice (5.71% ± 0.92; Figure 10, black bars).

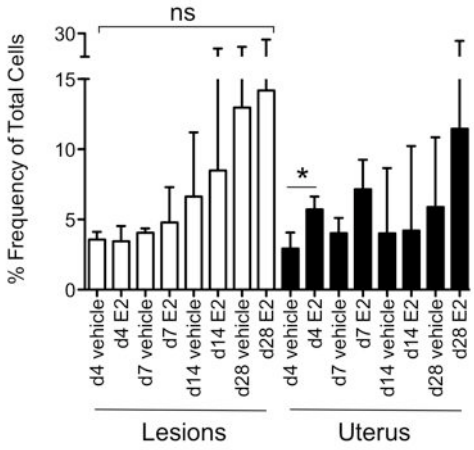

Figure 10: Frequency of BrdU+ cells in the lesions and uterus of C57BL/6 mice

The y-axis shows the frequency of BrdU+ cells as percentage of total cells. The x-axis shows the different treatment groups (vehicle and E_2) and the four treatment periods of 4 *(n=10)*, 7 *(n=10)*, 14 *(n=31)*, and 28 *(n=34)* days. In the lesions (white bars) there was no significant difference in BrdU+ cells between different treatments and time points. In the uterus (black bars) there was a significant difference in the frequency of BrdU positive cells at d4 between vehicle treated and E_2 treated mice. Error bars depict standard deviation. Significance: $*p \leq 0.05$, ns: not significant (one-way ANOVA Tukey's Multiple Comparison Post Hoc Test).

There are two distinct subpopulations of cells in the lesions and uterus: leukocytes (immune cells, CD45+) and non-leukocytes (CD45-), which include epithelial cells (CD45-, cytokeratin+). In order to determine the frequency of leukocytes, they were distinguished in C57BL/6 mouse endometriotic lesions and uterus using CD45 antibody, commonly used to differentiate leukocytes (Kishimoto, 1998). Interestingly, there was significantly higher percentage of leukocytes in the lesions (87.3% ± 7.58) in contrast to the uterus (24.3% ± 10.7; Figure 11A, white vs. black bars). However, there was no difference in the frequencies of BrdU+ leukocytes in the lesions (9.23% ± 9.85) and uterus (7.88% ± 6.36; Figure 11B, white vs. black bars). In the lesions,

regardless of treatment and time, there was no significant difference in the leukocyte frequency (Figure 11A, white bars) as well as BrdU+ leukocyte frequency (Figure 11B, white bars). In the uterus there was a significant increase in leukocyte frequency between d4 vehicle (17.5% ± 5.17) and d7 vehicle (35.4% ± 5.18) treated mice. The uterus from d7 vehicle group also had significantly higher frequency of leukocyte in comparison to the d7 E_2 treated animals (18.5% ± 3.21; Figure 11A, black bars). The uterus samples showed no significant difference in the BrdU+ leukocyte frequency regardless of treatment and time (Figure 11B, black bars).

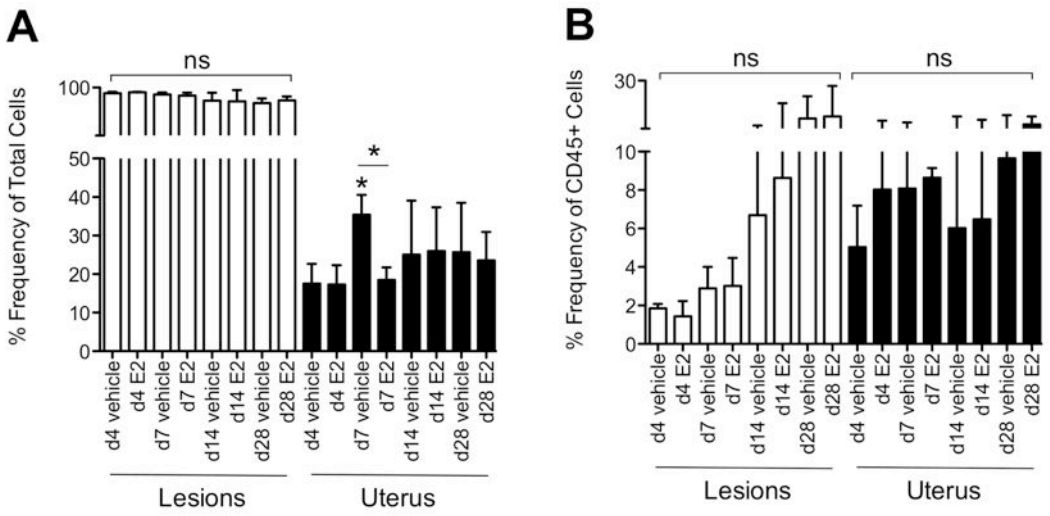

Figure 11: Frequency of leukocytes and BrdU+ leukocytes in the lesions and uterus of C57BL/6 mice

There were two treatments (vehicle and E_2) and four treatment periods of 4 *(n=10)*, 7 *(n=10)*, 14 *(n=31)*, and 28 *(n=34)* days. **A:** The y-axis shows the frequency of leukocytes (CD45+) as percentage of total cells. The x-axis shows the different treatment groups and the four time points. In the lesions (white bars) there was no significant difference in the leukocyte frequency between different treatment groups and time points. In the uterus (black bars) there was significantly higher percentage of leukocytes in the d7 vehicle treated mice when compared with d4 vehicle and d7 E_2 treated animals. **B:** The y-axis shows the frequency of BrdU+ leukocytes as percentage of total leukocytes. The x-axis is the same as A. No significant difference in the frequency of BrdU+ leukocytes was seen in both the lesions and uterus regardless of treatment or time point. Error bars depict standard deviation. Significant: $*p \leq 0.05$, ns: not significant (one-way ANOVA Tukey's Multiple Comparison Post Hoc Test).

Higher percentage of CD45- cells (non-leukocytes) was present in the uterus (74.8% ± 10.6) as compared to the lesions (12.7% ± 7.58; Figure 12A, black vs. white bars). There were similar frequencies of BrdU+ CD45- cells in the lesions (12.0% ± 12.2) and uterus (4.76% ± 7.90; Figure 12B, white vs. black bars). In the absence of E_2, the lesions had a significantly higher frequency of CD45- cells at d28 than d4 with 16.2% (± 4.83) and 5.95% (± 1.55) respectively. Furthermore, application of E_2 for

28 days yielded a significantly higher frequency of CD45- cells (13.4% ± 4.17) when compared to the d4 E_2 treated animals (4.96% ± 0.40; Figure 12A, white bars). There was significantly higher percentage of BrdU+ CD45- cells in the vehicle treated lesions from d4 (32.2% ± 11.1) when compared with d14 (6.7% ± 5.62) and 28 (5.83% ± 4.64) time points. Upon E_2 treatment, d4 lesions (42.0% ± 4.13) exhibited significantly higher frequency of BrdU+ CD45- cells in comparison to d7 (22.4% ± 8.78), 14 (7.44% ± 9.60) and 28 (9.24% ± 7.07) treatment time points (Figure 12B, white bars). The uterus for the d7 vehicle group contained 64.6% (± 5.18) CD45- cells, which was significantly lower than the d4 vehicle treated animals (82.5% ± 5.17; Figure 12A, black bars). There was a significantly higher frequency of BrdU+ CD45- cells in the uterus of E_2 treated animals at d7 in comparison to the vehicle group from the same time point with 6.89% (± 2.56) and 2.06% (± 0.47) respectively (Figure 12B, black bars).

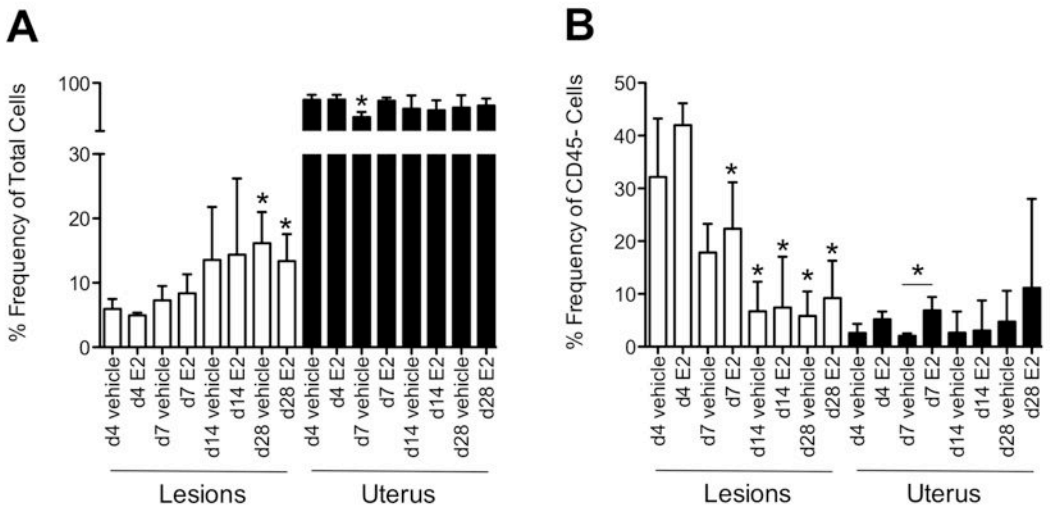

Figure 12: Frequency of non-leukocyte and BrdU+ non-leukocytes cells in the lesions and uterus of C57BL/6 mice

There were two treatments (vehicle and E_2) and four treatment periods of 4 *(n=10)*, 7 *(n=10)*, 14 *(n=31)*, and 28 *(n=34)* days. **A:** The y-axis shows the frequency of CD45- cells (non-leukocytes) as percentage of total cells. The x-axis shows the different treatment groups and the four time points. In the vehicle group the lesions (white bars) had a significantly higher frequency of CD45- cells at d28 in comparison to d4. In the E_2 treatment group there was a significantly higher frequency of CD45- cells at d28 when compared to the d4. The uterus (black bars) for the d7 vehicle group contained significantly lower frequency of CD45- cells than the d4 vehicle treated animals. **B:** The y-axis shows the frequency of BrdU+ CD45- cells as percentage of total CD45- cells. The x-axis is the same as A. There were a significantly higher percentage of BrdU+ CD45- cells in the vehicle treated lesions from d4 when compared with d14 and 28. Upon E_2 treatment, d4 lesions exhibited significantly higher frequency of BrdU+ CD45- cells in comparison to d7, 14 and 28. There was a significantly higher frequency of BrdU+ CD45- cells in the uterus of E_2 treated animals at d7 in comparison to the vehicle group from the same time point. Error bars depict standard deviation. Significant: $*p \leq 0.05$

The average frequency of epithelial cells (CD45- cytokeratin+) in the lesions (3.80% ± 5.39) was lower than the uterus (17.2% ± 15.4; Figure 13A, white vs. black bars) while the average frequency of BrdU+ epithelial cells in the lesions (40.2% ± 42.4) was higher than the uterus (9.93% ± 9.70; Figure 13B, white vs. black bars). The le-

sions showed no significant difference in the epithelial cell frequency regardless of treatment and time (Figure 13A, white bars). There was significantly higher percentage of BrdU+ epithelial cells in the lesions of vehicle treated mice from d4 (54.1% ± 0.623) when compared with d14 (9.48% ± 6.03) and 28 (11.3% ± 8.37) time points. Upon E_2 treatment, d4 lesions (61.9% ± 0.180) exhibited significantly higher frequency of BrdU+ epithelial cells in comparison to d7 (34.0% ± 2.19), 14 (15.2% ± 5.12) and 28 (17.2% ± 3.23) time points (Figure 13B, white bars). There was a significantly higher frequency of epithelial cells in the uterus of E_2 treated animals at d4 (23.6% ± 3.07) and 7 (41.2% ± 3.43) in comparison to the vehicle group from the same time points (d4, 9.39% ± 0.428 and d7, 16.8% ± 2.11; Figure 13A, black bars). The uterus from d7 E_2 (12.1% ± 4.30) animals possessed a significantly higher frequency of BrdU+ epithelial cells when compared with the d7 vehicle (6.69% ± 0.540) treated animals. Furthermore, the latter group had significantly lower BrdU+ epithelial cells than the d4 vehicle treated animals (12.6% ± 3.74; Figure 13B, black bars).

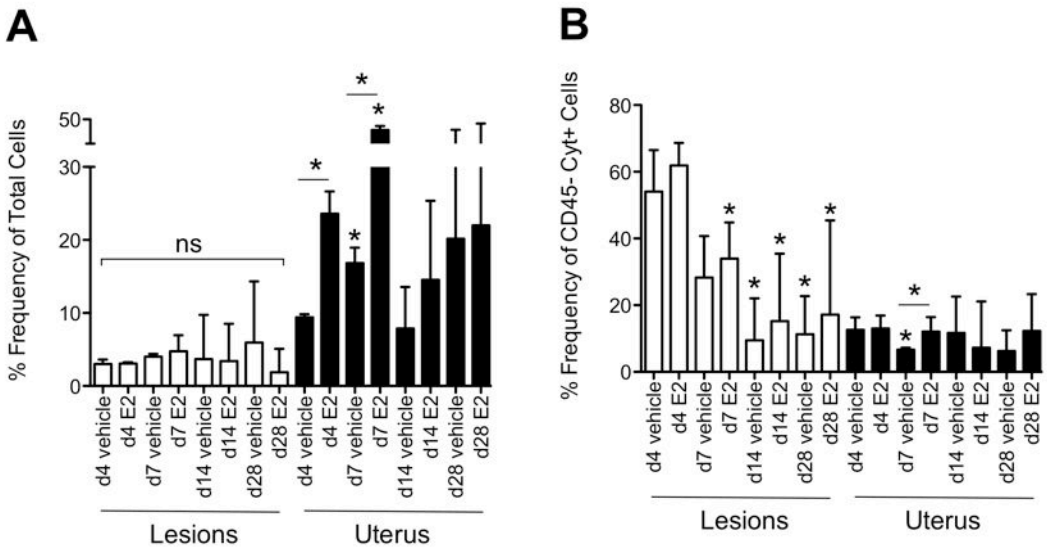

Figure 13: Frequency of epithelial cells and BrdU+ epithelial cells in the lesions and uterus of C57BL/6 mice

There were two treatments (vehicle and E_2) and four treatment periods of 4 *(n=10)*, 7 *(n=10)*, 14 *(n=31)*, and 28 *(n=34)* days. **A:** The y-axis shows the frequency of epithelial cells (CD45- cytokeratin+) as percentage of total cells. The x-axis shows the different treatment groups and the four time points. In the lesions (white bars) there was no significant difference in epithelial cell frequency regardless of treatment and time. In the uterus (black bars) there was significantly higher frequency of epithelial cells in the E_2 treated animals at d4 and 7 in comparison to the vehicle treated animals from the same time points. **B:** The y-axis shows the frequency of BrdU+ epithelial cells as percentage of total epithelial cells. The x-axis is the same as A. In the lesions there was significantly higher percentage of BrdU+ epithelial cells in vehicle treated mice from d4 when compared with d14 and 28. In the E_2 treated mice, d4 lesions had significantly higher frequency of BrdU+ epithelial cells in comparison to d7, 14 and 28. The uterus from d7 E_2 animals had a significantly higher frequency of BrdU+ epithelial cells when compared with the d7 vehicle treated animals. Furthermore, the latter group had significantly lower BrdU+ epithelial cells than the d4 vehicle treated mice. Error bars depict standard deviation. Significant: $*p \leq 0.05$, ns: not significant (one-way ANOVA Tukey's Multiple Comparison Post Hoc Test).

Gene Expression Analysis for Proliferation

RNA was extracted from the mouse endometriotic lesions and real time-PCR (RT-PCR) was performed to check the expression of pro-proliferation genes. Proliferation is restrained through control of the cell cycle machinery with a major regulator being cyclin B1. In the absence of E_2, significantly higher expression of cyclin B1 was observed in the d7 lesions in comparison to d4 lesions. Following a similar trend, in the presence of E_2, significantly higher cyclin B1 expression was seen at d7 and 14 as compared with d4 lesions. No difference in cyclin B1 expression was observed between the vehicle treated animals and the E_2 treated animals regardless of treatment period (Figure 14A). Transforming growth factor β1 (TGF-β1) is a cytokine, which among other biological processes regulates cellular proliferation. There was a significant increase in TGF-β1 expression when comparing the d4 vehicle and E_2 groups with the d7 vehicle and E_2 groups respectively. No difference in TGF-β1 expression was observed between the vehicle treated animals and the E_2 treated animals regardless of the length of treatment (Figure 14B).

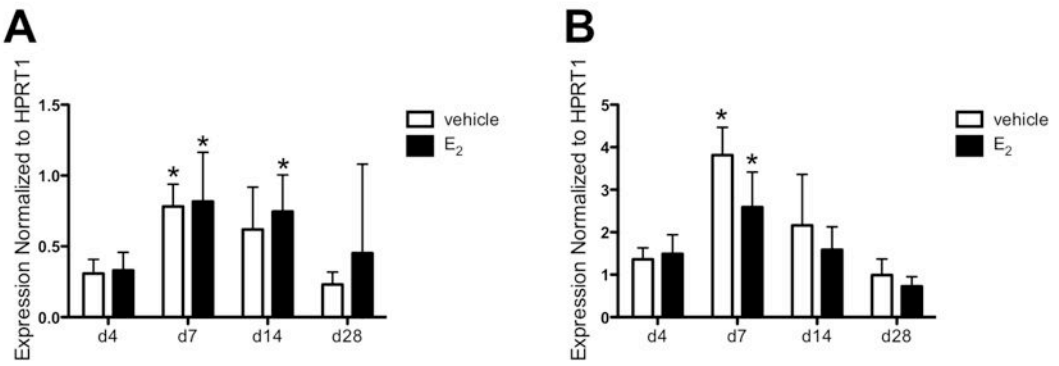

Figure 14: Gene expression analysis of cycling B1 and TGF-β1 in the lesions of C57BL/6 mice

There were two treatment groups of vehicle (white bars) and E_2 (black bars). The y-axis shows fold expression of RNA as normalized to the internal control HPRT1. The x-axis shows the four treatment periods of 4 *(n=10)*, 7 *(n=10)*, 14 *(n=31)*, and 28 *(n=34)* days. **A:** There was significantly higher expression of cyclin B1 in the d7 vehicle treated lesions in comparison to d4 vehicle treated lesions. Similarly, there was significantly higher cyclin B1 expression in the d7 and 14 E_2 treated mice than d4 E_2 mice. **B:** There was a significant increase in TGF-β1 expression between the lesions from d4 vehicle and E_2 treated groups with the d7 vehicle and E_2 groups respectively. Error bars depict standard deviation. Significant: $*p \leq 0.05$

Ki-67 Measurement of Proliferation

Staining for the proliferation marker Ki-67 in mouse lesions from C57BL/6 and FVB/N mice revealed cell proliferation within the epithelium and surrounding stromal cells, as illustrated by red nuclei (Figure 15A-B, arrows). Mouse spleen was used as positive control (Figure 15C).

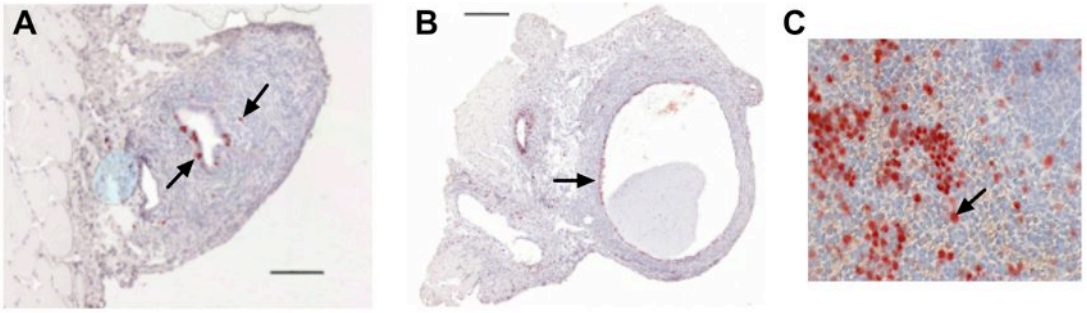

Figure 15: Ki-67 staining for proliferation in lesions from C57BL/6 mice

Proliferating cells positive for Ki-67 in lesion epithelium, stroma and in lesion lumen content are indicated by red stained nuclei (black arrows). **A:** Lesion from vehicle treated animal at d28 post transplantation, scale bar 100 μm. **B:** Lesion from E_2 treated animal at d28 post transplantion, scale bar 500 μm. **C:** Mouse spleen was used as staining control.

The lesions were analyzed semi-quantitatively by using a scoring system where negative Ki-67 staining was assigned 0, some Ki-67 positive was assigned 1, middle Ki-67 positive was assigned 2 and highly Ki-67 positive was assigned 3. In the C57BL/6 strain no significant (Mann-Whitney test) difference in Ki-67+ staining was seen in between the vehicle and E_2 treatments in the four treatment time points of 4, 7, 14, and 28 days (Figure 16A). Similarly, there was no significant difference in Ki-67+ staining of the FVB/N mice regardless of treatment in the two treatment periods of 14 and 28 days (Figure 16B). A combined analysis of d14 and 28 animals from the two strains showed that lesions of FVB/N mice (0.562 ± 0.512) have significantly lower mean Ki-67+ stain than the C57BL/6 mice (1.31 ± 0.704; Figure 16C).

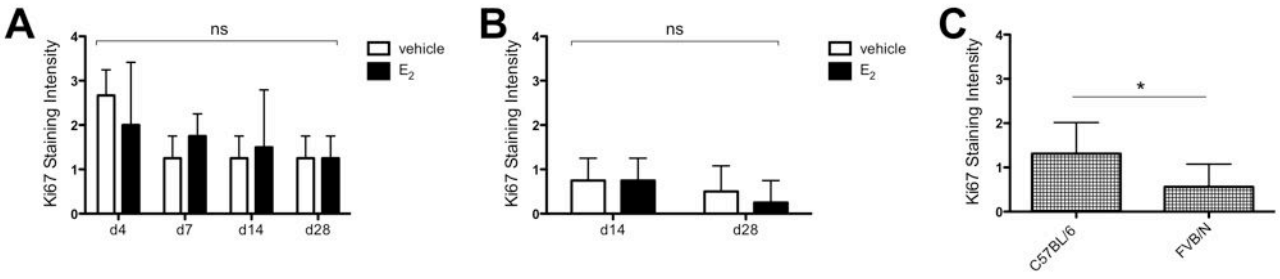

Figure 16: Analysis of Ki-67 staining intensity in the lesions of C57BL/6 and FVB/N mice

The Ki-67 staining intensity in the lesions was analyzed semi-quantitatively by using a scoring system as described in Materials and Methods. There were two treatment groups of vehicle (white bars) and E_2 (black bars). The y-axis shows Ki-67 staining intensity. **A:** The x-axis shows the four treatment periods of 4 *(n=4)*, 7 *(n=4)*, 14 *(n=8)*, and 28 *(n=8)* days. In the C57BL/6 mice no significant difference in Ki-67 staining intensity was observed. **B:** The x-axis shows the two treatment periods of 14 *(n=5)*, and 28 *(n=5)* days. In the FVB/N mice no significant difference in Ki-67 staining intensity was observed. **C:** A combined analysis of d14 and 28 animals from the two strains showed that FVB/N lesions have significantly lower mean Ki-67+ stain than C57BL/6 lesions. Error bars depict standard deviation. Significant: $*p \leq 0.05$, ns: not significant (Mann-Whitney test).

In the three methods utilized to measure proliferation, no difference between the vehicle and E_2 treated lesions was observed. Taken together, E_2 mediated proliferation does not contribute to lesion growth in this syngeneic transplantation mouse model of endometriosis.

3.1.4 Apoptosis Is Not the Main Driver of Estrogen Mediated Lesion Growth

Anomalies in programmed cell death may contribute to the larger lesion areas observed in the E_2 treated mice. Different methods were utilized to measure the impact of E_2 on modulation of apoptosis in endometriotic lesions from mouse syngeneic transplantation model of endometriosis.

Annexin V Measurement of Apoptosis

Annexin V (AV) is commonly used as probe for cells undergoing apoptosis. Using flow cytometry the frequency of AV+ cells in the lesions and the uterus of C57BL/6 and FVB/N mice were determined as percentage of total live cells. 4',6-diamidino-2-phenylindole (DAPI) was used to distinguish live cells. The C57BL/6 (Figure 17A) and FVB/N (Figure 17B) endometriotic lesions (white bars) and uterus (black bars) showed no significant difference in the frequency of AV+ cells regardless of treatment or time point. The combined analysis of d14 and 28 C57BL/6 mice showed that the mean frequency of AV+ cells in the uterus (16.7% ± 6.25) was significantly higher than the lesions (7.89% ± 2.42). Furthermore, the combined analysis of d14 and 28 animals from the two strains showed that uterus from C57BL/6 mice have significantly lower mean AV+ cell frequency than the FVBN uterus (9.47% ± 3.41). Additionally, no difference in mean lesion AV+ cell frequency was observed between the two mouse strains (Figure 17C).

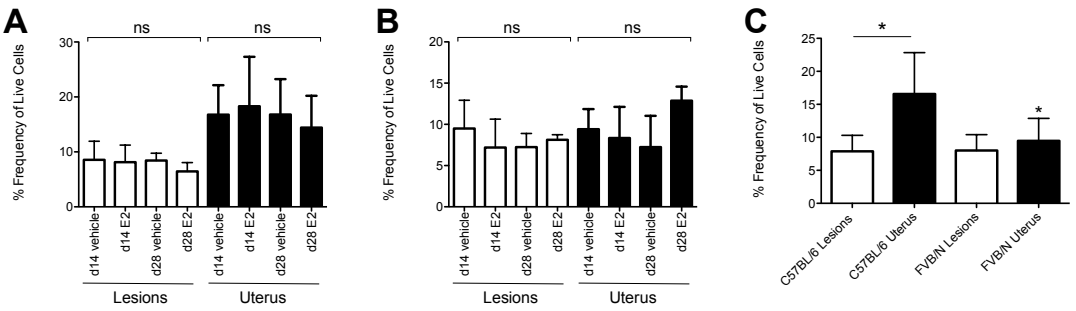

Figure 17: Frequency of Annexin V + cells in the lesions and uterus of C57BL/6 and FVB/N mice

The y-axis shows the frequency of Annexin V+ (AV+) cells as percentage of total live cells. DAPI was used to exclude dead cells as described in Materials and Methods. **A:** The x-axis shows the different treatment groups (vehicle and E_2) and the treatment periods of 14 *(n=10)* and 28 *(n=10)* days for C57BL/6 mice. In the lesions (white bars) and uterus (black bars) there was no significant difference in AV+ cell frequency regardless of treatment and time. **B:** The x-axis shows the different treatment groups (vehicle and E_2) and the treatment periods of 14 *(n=10)* and 28 *(n=10)* days for FVB/N mice. In the lesions (white bars) and uterus (black bars) there was no significant difference in AV+ cell frequency regardless of treatment and time. **C:** The x-axis shows the sum of C57BL/6 and FVB/N lesions and uterus. The uterus from C57BL/6 mice had significantly (t-test, $*p \leq 0.05$) higher frequency of AV+ cells than the lesions from C57BL/6 mice. Furthermore, the uterus from C57BL/6 mice has significantly lower mean AV+ cell frequency than the FVB/N uterus (9.47% ± 3.41). No difference in mean lesion AV+ cell frequency was observed between the two mouse strains. Error bars depict standard deviation. Significant: $*p \leq 0.05$, ns: not significant (one-way ANOVA Tukey's Multiple Comparison Post Hoc Test).

One of the major subpopulations of cells in the lesions and uterus are non-leukocytes (CD45-) that include the epithelial cells. The frequency of CD45- cells along with AV+ CD45- cells were analyzed in the lesions and uterus of C57BL/6 mice. There was lower percentage of CD45- cells in the lesions (79.5% ± 12.2) in contrast to the uterus (95.7% ± 1.55; Figure 18A, white vs. black bars). However, there was no difference in the frequencies of AV+ CD45- between the lesions (10.6% ± 9.53) and uterus (15.8% ± 6.29; Figure 18B, white vs. black bars). The lesions from

d28 vehicle (87.0% ± 3.94) and E_2 (91.1% ± 1.62) treated animals possessed a significantly higher frequency of CD45- cells when compared with the d14 vehicle (70.6% ± 8.99) and E_2 treated animals (69.2% ± 12.1) respectively (Figure 18A, white bars). The lesions from d14 E_2 (22.9% ± 12.7) mice possessed a significantly higher frequency of AV+ CD45- cells when compared with the d14 vehicle (8.77% ± 3.50) treated mice and d28 E_2 treated mice (4.68% ± 1.24; Figure 18B, white bars). The uterus samples showed no significant difference in the CD45- and AV+ CD45- cell frequency regardless of treatment and time (black bars).

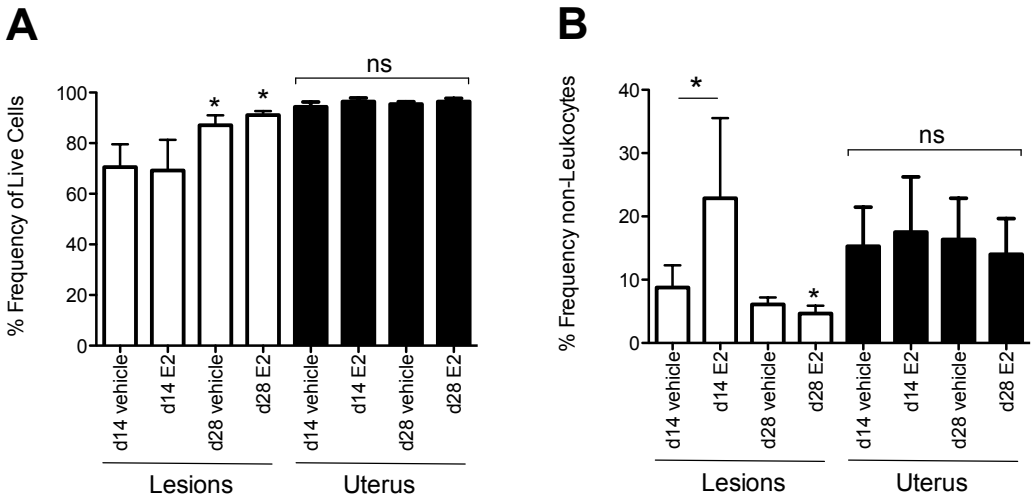

Figure 18: Frequency of non-leukocytes and Annexin V+ non-leukocytes in the lesions and uterus of C57BL/6 mice

There were two treatments (vehicle and E_2) and two treatment periods of 14 *(n=10)* and 28 *(n=10)* days. **A:** The y-axis shows the frequency of CD45- cells (non-leukocytes) as percentage of total live cells. The x-axis shows the different treatment groups and treatment periods. The lesions (white bars) from d28 vehicle and E_2 animals had a significantly higher frequency of CD45- cells when compared with the d14 vehicle and E_2 animals respectively. There was no difference in the uterus (black bars) CD45- cell frequency regardless of treatment or time point. **B:** The y-axis shows the frequency of Annexin V+ (AV+) CD45- cells as percentage of total

Figure 18 continued: CD45- cells. The x-axis is the same as A. The lesions from d14 E_2 animals had a significantly higher frequency of AV+ CD45- cells when compared with the d14 vehicle treated animals and the d28 E_2 treated animals. There was no difference in the uterus AV+ CD45- cell frequency regardless of treatment or time point. Error bars depict standard deviation. Significant: $*p \leq 0.05$, ns: not significant (one-way ANOVA Tukey's Multiple Comparison Post Hoc Test).

There was significantly higher percentage of leukocytes (CD45+) in the lesions (20.5% ± 12.2) in contrast to the uterus (4.3% ± 1.55; Figure 19A, white vs. black bars). However, there was no difference in the frequencies of AV+ leukocytes between the lesions (37.7% ± 13.9) and uterus (35.8% ± 12.9; Figure 19B, white vs. black bars). The lesions from d28 vehicle (13.0% ± 3.94) and E_2 (8.90% ± 1.62) animals had lower frequency of AV+ leukocytes when compared with the d14 vehicle (29.4% ± 8.99) and E_2 animals (30.8% ± 12.1) respectively (Figure 19A, white bars). Furthermore, the lesions from d28 vehicle (25.8% ± 3.99) and E_2 (25.1% ± 4.82) animals possessed a significantly higher frequency of AV+ leukocytes when compared with the d14 vehicle (45.0% ± 5.28) and E_2 animals (54.8% ± 5.82) respectively (Figure 19B, white bars). The uterus samples showed no significant difference in the leukocyte and AV+ leukocyte frequency regardless of treatment and time (black bars).

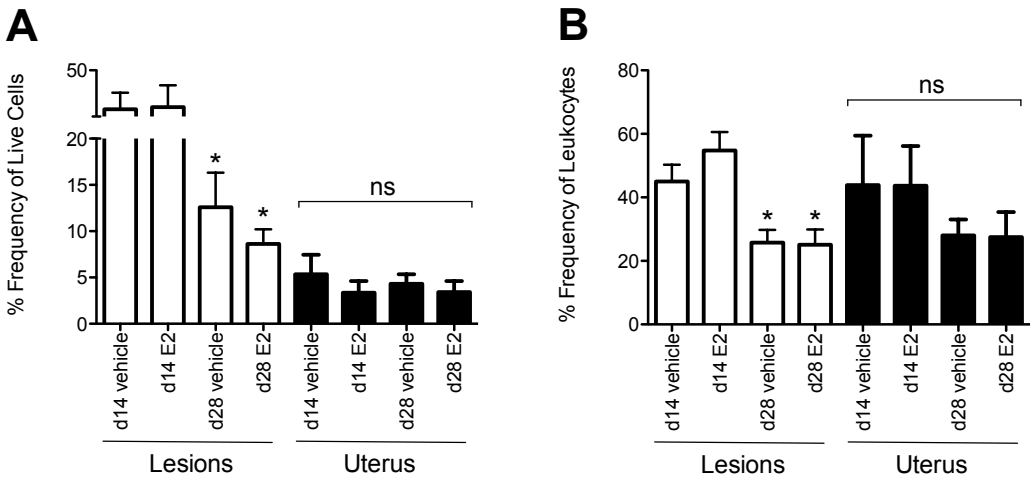

Figure 19: Frequency of leukocytes and Annexin V+ leukocytes in the lesions and uterus of C57BL/6 mice

There were two treatments (vehicle and E_2) and two treatment periods of 14 *(n=10)* and 28 *(n=10)* days. **A:** The y-axis shows the frequency of leukocytes as percentage of total live cells. The x-axis shows the different treatment groups and treatment periods. The lesions (white bars) from d28 vehicle and E_2 animals had a significantly higher frequency of leukocytes when compared with the d14 vehicle and E_2 animals. There was no difference in the uterus (black bars) leukocyte percentage regardless of treatment or time point. **B:** The y-axis shows the frequency of Annexin V+ (AV+) leukocytes as percentage of total leukocytes. The x-axis is the same as A. The lesions from d28 vehicle and E_2 animals had a significantly higher frequency of leukocytes when compared with the d14 vehicle and E_2 animals. There was no difference in the uterus AV+ leukocyte frequency regardless of treatment or time point. Error bars depict standard deviation. Significant: $*p \leq 0.05$, ns: not significant (one-way ANOVA Tukey's Multiple Comparison Post Hoc Test).

Using flow cytometry, leukocytes were sorted into natural killer (NK) cells, B cells, T cells, macrophages and dendritic cells (DCs) as described in the Materials and Methods. The lesions from d28 vehicle (1.31% ± 0.486) and E_2 (0.789% ± 0.090) mice had significantly lower frequency of NK cells than d14 vehicle (3.08% ± 1.28) and E_2 (4.12% ± 1.86) mice respectively (Figure 20A, white bars). Similar pattern was seen when looking at AV+ NK cells where lesions from d28 vehicle (14.4% ± 6.39) and E_2

(7.30% ± 3.34) mice had significantly lower percentage of AV+ NK cells than d14 vehicle (26.7% ± 7.45) and E_2 (27.0% ± 4.90) mice respectively (Figure 20B, white bars). In the uterus no difference was seen in the frequency of NK cells regardless of treatment or time (Figure 20A, black bars). At d14 there was a higher uterus AV+ NK cells frequency in the E_2 treatment group (39.2% ± 2.30) versus vehicle treatment group (28.0% ± 5.66). Conversely, at d28 there was a lower uterus AV+ NK cells frequency in the vehicle treated animals (20.6% ± 6.82) than the E_2 treated animals (39.2% ± 2.30). Additionally, upon E_2 treatment, there was significantly higher percentage of uterus AV+ NK cells at d14 than d28 treatment periods (Figure 20B, black bars).

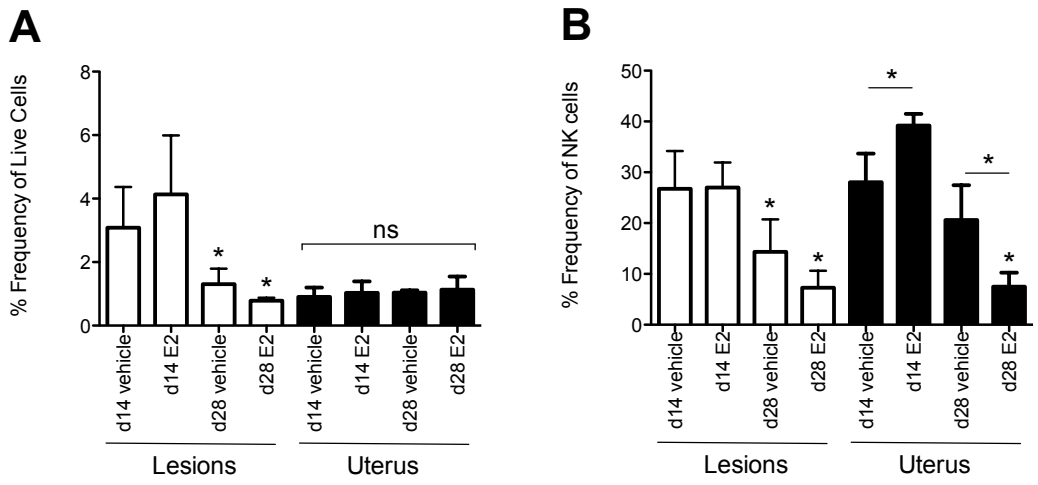

Figure 20: Frequency of NK cells and Annexin V+ NK cells in the lesions and uterus of C57BL/6 mice

There were two treatments (vehicle and E_2) and two treatment periods of 14 *(n=10)* and 28 *(n=10)* days. **A:** The y-axis shows the frequency of natural killer (NK) cells as percentage of total live cells. The x-axis shows the different treatment groups and treatment periods. The lesions (white bars) from d28 vehicle and E_2 groups had significantly lower frequency of NK cells than d14 vehicle and E_2 groups respectively. In the uterus (black bars) no difference was seen in the frequency of NK cells regardless of treatment or time. **B:** The y-axis shows the frequency of Annexin V+ (AV+) NK cells as percentage of total NK cells. The x-axis is the same as A. The lesions from d28 vehicle and E_2 groups had significantly lower frequency of AV+ NK cells than d14 vehicle and E_2 groups respectively. In the uterus at d14 there was a higher frequency of AV+ NK cells in the E_2 treated mice than the vehicle treated mice. At d28 there was a lower uterus AV+ NK cells frequency in the vehicle treated animals than the E_2 treated animals. Furthermore, upon E_2 treatment, there was significantly higher percentage of uterus AV+ NK cells at d14 than d28 treatment period. Error bars depict standard deviation. Significant: $*p \leq 0.05$, ns: not significant (one-way ANOVA Tukey's Multiple Comparison Post Hoc Test).

In the lesions there was a higher frequency of B cells in the d28 vehicle treated animals (0.255% ± 0.057) as compared with d28 E_2 treated animals (0.17% ± 0.014). The latter group had a significantly lower frequency of B cells than the d14 E_2 treated animals (0.783% ± 0.309; Figure 21A, white bars). Similarly, there was a higher frequency of lesion AV+ B cells in the d28 vehicle treated mice (56.0% ±

13.0) as compared with d28 E_2 treated animals (28.9% ± 10.4). The d28 E_2 treated animals had a significantly lower frequency of lesion AV+ B cells than the d14 E_2 treated mice (57.8% ± 5.49; Figure 21B, white bars). No significant difference in B cell frequency was seen in the uterus regardless of treatment and treatment period (Figure 21A, black bars). There was a lower frequency of uterus AV+ B cells in the d28 E_2 treatment group (34.7% ± 7.88) than d28 vehicle treatment group (86.3% ± 6.05). The uterus from d28 vehicle and E_2 treated animals possessed a significantly higher frequency of AV+ B cells when compared with the d14 vehicle (64.9% ± 25.1) and E_2 treated animals (77.5% ± 16.2) respectively (Figure 21B, black bars).

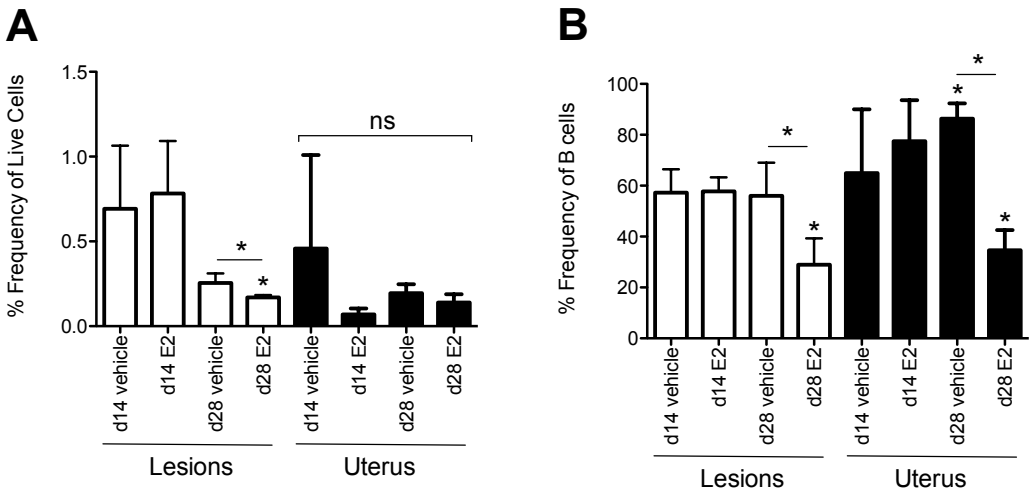

Figure 21: Frequency of B cells and Annexin V+ B cells in the lesions and uterus of C57BL/6 mice

There were two treatments (vehicle and E_2) and two treatment periods of 14 *(n=10)* and 28 *(n=10)* days. **A:** The y-axis shows the frequency of B cells as percentage of total live cells. The x-axis shows the different treatment groups and treatment periods. In the lesions (white bars) there was a higher frequency of B cells in the d28 vehicle treated animals than d28 E_2 treated animals. The d28 E_2 treated mice had a significantly lower frequency of B cells than the d14 E_2 treated mice. In the uterus (black bars) no difference was seen in the frequency of NK cells regardless of treatment or time. **B:** The y-axis shows the frequency of Annexin V+ (AV+) B cells as percentage of total B cells. The x-axis is the same as A. In the lesions there was a higher frequency of AV+ B cells in the d28 vehicle treated mice than d28 E_2 treated animals. The d28 E_2 treated animals had a significantly lower frequency of AV+ B cells than the d14 E_2 treated mice. In the uterus there was a significant differnce in the frequency of AV+ B cells between the d28 E_2 and vehicle treatment groups. The uterus from d28 vehicle and E_2 treated animals possessed a significantly higher frequency of AV+ B cells when compared with the d14 vehicle and E_2 treated animals respectively. Error bars depict standard deviation. Significant: $*p \leq 0.05$, ns: not significant (one-way ANOVA Tukey's Multiple Comparison Post Hoc Test).

There are two major subtypes of T cells: cytotoxic T cells and helper T cells. Cytotoxic T cells are capable of destroying a specific target by cytotoxic mechanism while helper T cells transmit signals from antigen-presenting cells and enhance further immune response. There was higher percentage of helper T cells present in the le-

sions (2.21% ± 1.12) in contrast to the uterus (0.561% ± 0.326; Figure 22A, white vs. black bars). However, there was a lower frequency of AV+ helper T cells in the lesions (26.2% ± 12.4) than the uterus (54.3% ± 16.1; Figure 22B, white vs. black bars). In the lesions there was a significant decrease in helper T cell frequency between d14 vehicle (3.25% ± 0.489) and d28 vehicle (1.96% ± 0.655) treated mice. The d28 vehicle treated mice had significantly higher frequency of helper T cells in comparison to the d28 E_2 treated mice (1.01% ± 0.120; Figure 22A, white bars). The d28 E_2 treatment lesions had significantly lower frequency of AV+ helper T cells when compared with d14 E_2 treatment lesions with 12.0% (± 8.22) and 32.9 (± 3.29) respectively (Figure 22B, white bars). In the uterus there was a higher percentage of helper T cells in the d28 vehicle treated animals (0.760% ± 0.220) as compared with d28 E_2 treated animals (0.328% ± 0.176; Figure 22A, black bars). The uterus from the E2 treated animals had a higher frequency of AV+ helper T cells at d14 (61.6% ± 3.99) than d28 (43.9% ± 6.06) treatment time point. Furthermore, the latter group had significantly lower frequency of AV+ helper T cell in comparison to the d28 vehicle treated animals (64.5% ± 6.40; Figure 22B, black bars).

The central event in the generation of humoral and cell mediated immune response is activation of T cells. One of the earliest cell surface antigens expressed by activated T cells is the CD69 antigen (Ziegler, et al., 1994). In the lesions (white bars) there was no significant difference in the frequencies of activated (CD69+) helper T cells (Figure 22C) and AV+ activated helper T cells regardless of treatment or time (Figure 22D). In the uterus, upon E_2 treatment, there was an increase in activated

helper T cell frequency at d14 (74.9% ± 2.53) and d28 (82.6% ± 6.17) when compared with the d14 (44.3% ± 23.1) and 28 (70.5% ± 7.54) vehicle treated animals (Figure 22C, black bars). When looking at AV+ activated helper T cells in the uterus there was a decrease observed between d28 vehicle treated and E_2 treated animals with 81.8% (± 4.95) and 49.7 (± 8.50) respectively (Figure 22D, black bars).

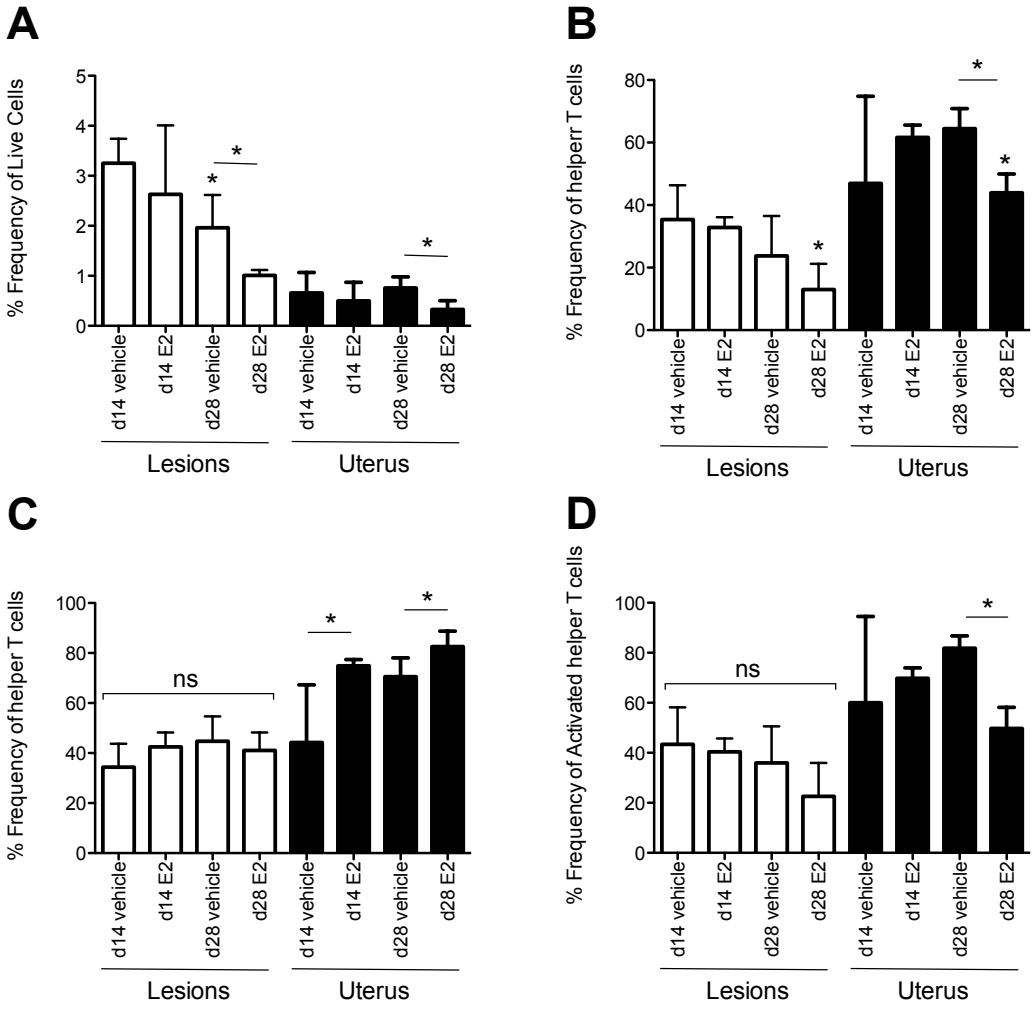

Figure 22: Frequency of helper T cells and Annexin V+ helper T cells in the lesions and uterus of C57BL/6 mice

Figure 22 continued: There were two treatments (vehicle and E_2) and two treatment periods of 14 *(n=10)* and 28 *(n=10)* days. **A:** The y-axis shows the frequency of helper T cells as percentage of total live cells. The x-axis shows the different treatment groups and treatment periods. In the lesions (white bars) there was a significant decrease in helper T cell frequency between d14 and 28 vehicle treated animals. The lesions from d28 vehicle treated mice had significantly higher frequency of helper T cells in comparison to the d28 E_2 treated mice. In the uterus (black bars) there was higher percentage of helper T cells in the d28 vehicle than d28 E_2 treated animals. **B:** The y-axis shows the frequency of Annexin V+ (AV+) helper T cells as percentage of total helper T cells. The x-axis is the same as A. The lesions from d28 E_2 treated animals had significantly lower frequency of AV+ helper T cells than d14 E_2 treated animals. In the uterus, upon E_2 treatment, there was an increase in activated helper T cell frequency at d14 and 28 as compared with d14 and 28 vehicle treated animals respectively. **C:** The y-axis shows the frequency of CD69+ (activated) helper T cells as percentage of total helper T cells. The x-axis is the same as A. In the lesions there was no difference in the frequency of CD69+ helper T cells regardless of treatment or treatment period. In the uterus there was an increase in CD69+ helper T cell frequency at d14 and 28 E_2 treated animals when compared with the d14 and 28 vehicle treated animals respectively. **D:** The y-axis shows the frequency of AV+ CD69+ helper T cells as percentage of CD69+ helper T cells. The x-axis is the same as A. In the lesions there was no difference in the frequency of AV+ CD69+ helper T cells regardless of treatment or treatment period. In the uterus there was a decrease in frequency of AV+ CD69+ helper T cells between d28 vehicle and E_2 treated animals. Error bars depict standard deviation. Significant: $*p \leq 0.05$, ns: not significant (one-way ANOVA Tukey's Multiple Comparison Post Hoc Test).

There was lower percentage of cytotoxic T cells in the lesions (1.29% ± 0.641) in contrast to the uterus (0.343% ± 0.206; Figure 23A, white vs. black bars). However, there was no difference in the frequencies of AV+ cytotoxic T cells between the lesions (16.2% ± 13.3) and uterus (23.4% ± 16.5; Figure 23B, white vs. black bars). In the absence of E_2 there was a significant decrease in lesion cytoctoxic T cell frequency between d14 (1.99% ± 0.603) and d28 (1.09% ± 0.390) treated mice (Figure 23A, white bars). The lesions from d28 vehicle (4.71% ± 2.92) and E_2 (2.52% ± 2.49) mice had significantly lower frequency of AV+ cytotoxic T cells than d14 vehicle (27.6% ± 2.71) and E_2 (30.1% ± 2.32) mice respectively (Figure 23B, white bars).

The uterus from d28 E_2 (0.175% ± 0.058) mice possessed a significantly lower frequency of cytotoxic T cells when compared with the d28 vehicle treated mice (0.515% ± 0.107; Figure 23A, black bars). Similar to the lesions from the same time points, the uterus from d28 vehicle (11.9% ± 5.48) and E_2 (5.50% ± 2.26) mice had significantly lower frequency of AV+ cytotoxic T cells than d14 vehicle (34.2% ± 5.84) and E_2 (42.1% ± 8.37) mice respectively (Figure 23B, black bars).

The lesions from d14 E_2 (21.3% ± 3.62) mice possessed a significantly lower frequency of activated cytotoxic T cells when compared with the d14 vehicle treated mice (28.3% ± 3.78; Figure 23C, white bars). The lesions from d28 vehicle (3.22% ± 2.43) and E_2 (1.84% ± 1.22) mice had significantly lower frequency of AV+ activated cytotoxic T cells than d14 vehicle (30.0% ± 13.2) and E_2 (37.0% ± 13.7) mice respectively (Figure 23D, white bars). There was a significantly higher frequency of activated T cells in the uterus of E_2 treated animals at d14 (67.1% ± 4.54) and 28 (59.1% ± 7.49) in comparison to the vehicle group from the same time points (d14, 41.4% ± 5.66 and d28, 31.7% ± 2.61; Figure 23C, black bars). The uterus from d14 vehicle treated mice (26.1% ± 3.36) had significantly higher frequency of AV+ activated cytotoxic T cells in comparison to the d14 E_2 treated mice (46.4% ± 13.0; Figure 23D, black bars).

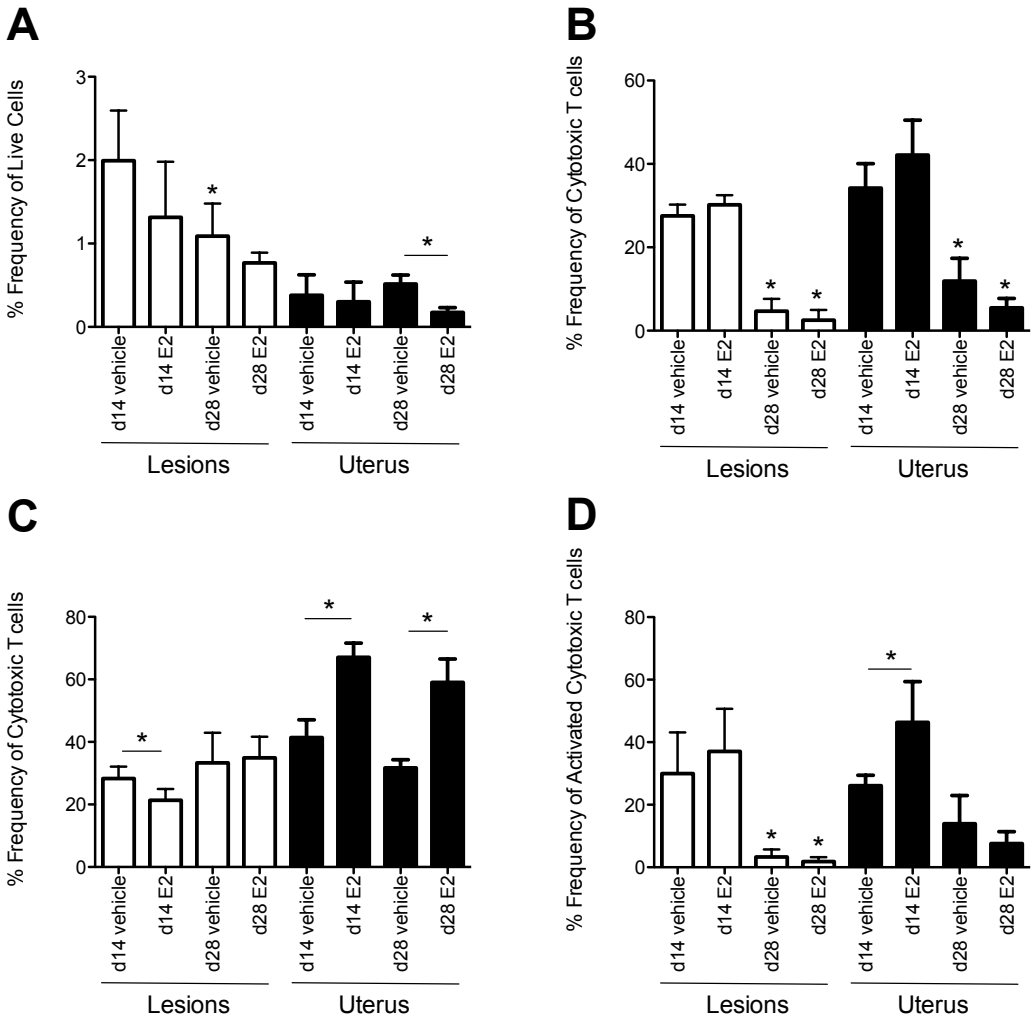

Figure 23: Frequency of cytotoxic T cells and Annexin V+ cytotoxic T cells in the lesions and uterus of C57BL/6 mice

There were two treatments (vehicle and E_2) and two treatment periods of 14 *(n=10)* and 28 *(n=10)* days. **A:** The y-axis shows the frequency of cytotoxic T cells as percentage of total live cells. The x-axis shows the different treatment groups and treatment periods. In the absence of E_2 there was a significant decrease in lesion (white bars) cytoctoxic T cell frequency between d14 and d28 treated mice. The uterus (black bars) from d28 E_2 mice had a significantly lower frequency of cytotoxic T cells when compared with the d28 vehicle treated mice. **B:** The y-axis shows the frequency of Annexin V+ (AV+) cytotoxic T cells as percentage of total cytotoxic T cells. The x-axis is the same as A. Both lesions and uterus from d28 vehicle and E_2 mice had significantly lower frequency of AV+ cytotoxic T cells than d14 vehicle and E_2 mice respectively. **C:** The y-axis shows the frequency of CD69+ (activated) cytotoxic T cells as percentage of total cytotoxic T cells. The x-axis is the same as A. The lesions from d14 E_2 mice possessed a significantly lower frequency of CD69+ cytotoxic T cells when compared with the d14 vehicle treated mice. In the uterus there

Figure 23 continued: was a significantly higher frequency of activated T cells in E_2 treated animals at d14 and 28 in comparison to the vehicle group from the same time points. **D:** The y-axis shows the frequency of AV+ CD69+ cytotoxic T cells as percentage of CD69+ cytotoxic T cells. The x-axis is the same as A. The lesions from d28 vehicle and E_2 mice had significantly lower frequency of AV+ CD69+ cytotoxic T cells than d14 vehicle and E_2 mice respectively. The uterus from d14 vehicle treated mice had significantly higher frequency of AV+ CD69+ cytotoxic T cells in comparison to the d14 E_2 treated mice. Error bars depict standard deviation. Significant: $*p \leq 0.05$ (one-way ANOVA Tukey's Multiple Comparison Post Hoc Test).

The lesions from d28 vehicle (1.04% ± 0.447) and E_2 (0.865% ± 0.177) mice had significantly lower frequency of macrophages than d14 vehicle (3.38% ± 1.97) and E_2 (3.55% ± 1.56) mice respectively (Figure 24A, white bars). There was an increase in the lesion AV+ macrophage frequency at d14 between the vehicle treated animals (46.4% ± 6.78) and the E_2 treated animals (62.3% ± 9.77). Furthermore, the d14 E_2 treatment group had significantly higher lesion AV+ macrophage percentage than animals from d28 E_2 treatment group (36.5% ± 9.55; Figure 24B, white bars). No significant difference in the uterus macrophage frequency was observed regardless of treatment or time (Figure 24A, black bars). There was a higher frequency of uterus AV+ macrophages in the d14 E_2 treated mice (50.1% ± 18.2) than d28 E_2 treated mice (23.3% ± 7.66; Figure 24B, black bars).

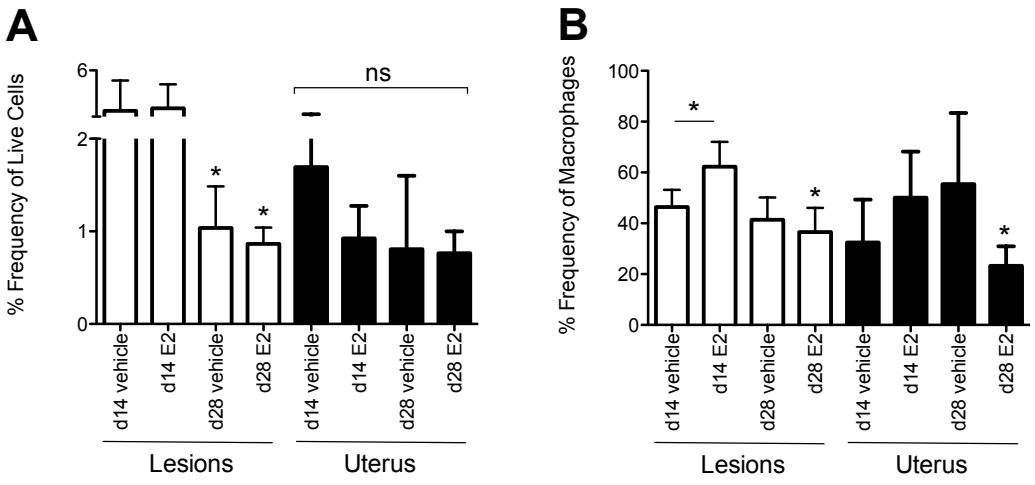

Figure 24: Frequency of macrophages and Annexin V+ macrophages in the lesions and uterus of C57BL/6 mice

There were two treatments (vehicle and E_2) and two treatment periods of 14 *(n=10)* and 28 *(n=10)* days. **A:** The y-axis shows the frequency of macrophages as percentage of total live cells. The x-axis shows the different treatment groups and treatment periods. The lesions (white bars) from d28 vehicle and E_2 mice had significantly lower frequency of macrophages than d14 vehicle and E_2 mice. No significant difference in the uterus (black bars) macrophage frequency was observed regardless of treatment or treatment period. **B:** The y-axis shows the frequency of Annexin V+ (AV+) macrophages as percentage of total macrophages. The x-axis is the same as A. In the lesions there was an increase in the AV+ macrophage frequency at d14 between the vehicle and E_2 treated animals. The d14 E_2 treatment group had significantly higher lesion AV+ macrophage percentage than animals from d28 E_2 treatment group. In the uterus there was a higher frequency of AV+ macrophages in the d14 E_2 treated mice than d28 E_2 treated mice. Error bars depict standard deviation. Significant: $*p \leq 0.05$, ns: not significant (one-way ANOVA Tukey's Multiple Comparison Post Hoc Test).

The lesions from d28 vehicle (0.513% ± 0.173) and E_2 (0.464% ± 0.074) mice had significantly lower frequency of dendritic cells (DCs) than d14 vehicle (3.03% ± 1.11) and E_2 (3.12% ± 2.10) mice respectively (Figure 25A, white bars). Similarly, The lesions from d28 vehicle (76.6% ± 5.24) and E_2 (66.7% ± 5.84) mice had significantly lower frequency of AV+ DCs than d14 vehicle (87.9% ± 6.35) and E_2 (91.2% ±

2.49) mice respectively. (Figure 25B, white bars). No significant difference in the uterus DC frequency was observed regardless of treatment or time (Figure 25A, black bars). There was a higher frequency of uterus AV+ DCs in the d28 vehicle treatment group (89.4% ± 3.55) than E_2 treatment group (70.9% ± 9.95; Figure 25B, black bars).

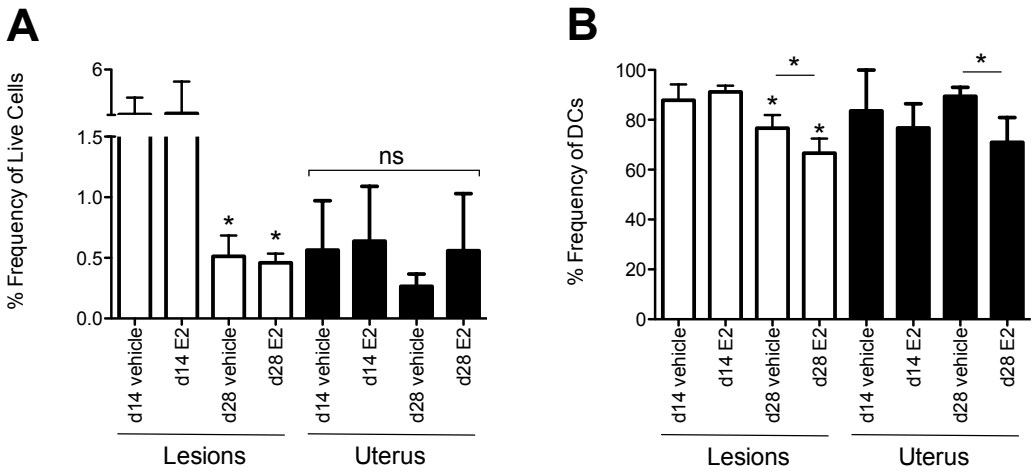

Figure 25: Frequency of dendritic cells and Annexin V+ dendritic cells in the lesions and uterus of C57BL/6 mice

There were two treatments (vehicle and E_2) and two treatment periods of 14 *(n=10)* and 28 *(n=10)* days. **A:** The y-axis shows the frequency of dendritic cells (DCs) as percentage of total live cells. The x-axis shows the different treatment groups and treatment periods. The lesions (white bars) from d28 vehicle and E_2 mice had significantly lower frequency of DCs than d14 vehicle and E_2 mice respectively. In the uterus (black bars) no significant difference in DC frequency was observed. **B:** The y-axis shows the frequency of Annexin V+ (AV+) DCs as percentage of total DCs. The x-axis is the same as A. The lesions from d28 vehicle and E_2 mice had significantly lower frequency of AV+ DCs than d14 vehicle and E_2 mice respectively. There was a higher frequency of uterus AV+ DCs in the d28 vehicle treatment group than E_2 treatment group. Error bars depict standard deviation. Significant: $*p \leq 0.05$, ns: not significant (one-way ANOVA Tukey's Multiple Comparison Post Hoc Test).

Gene and Protein Expression Analysis for Apoptosis

RNA was extracted and real time-PCR (RT-PCR) was performed to check the expression of genes that may be involved in the modulation of apoptosis in the mouse endometriotic lesions. Bcl-2 (B-cell lymphoma 2) family of apoptosis regulator proteins have either an inhibitory effect on programmed cell death (anti-apoptotic) or block the protective effect of inhibitors (pro-apoptotic). Bcl-2 is the founding member of these regulators of apoptosis and is anti-apoptotic. A comparison of lesions from d4 and 7 with d14 and 28 showed that there was significantly higher expression of Bcl-2 mRNA in the two latter time points regardless of E_2 supplementation (Figure 26A). Protein expression analysis using Western Blotting showed that there was no difference in the level of Bcl-2 protein at d14 and 28 lesions regardless of treatment (Figure 26B).

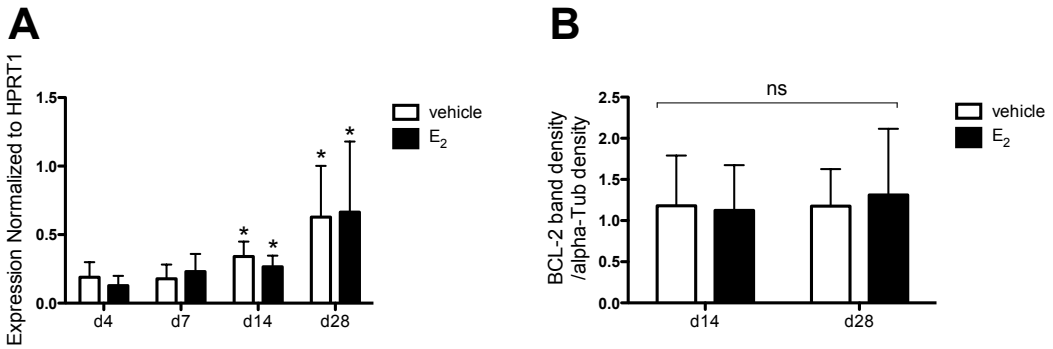

Figure 26: Gene and protein expression analysis of Bcl-2 in the lesions of C57BL/6 mice

There were two treatment groups of vehicle (white bars) and E_2 (black bars). **A:** The y-axis shows fold expression of mRNA as normalized to the internal control HPRT1. The x-axis shows the four treatment periods of 4 *(n=10)*, 7 *(n=10)*, 14 *(n=31)*, and 28 *(n=34)* days. Regardless of treatment, there was a significant increase in Bcl-2 expression between d4 and 7 lesions and d14 and 28 lesions. **B:** The y-axis shows band intensity of Bcl-2 protein as normalized to the gel loading control alpha-tubulin. The x-axis shows treatment periods of 14 *(n≥13)*, and 28 *(n=15)* days. There was no difference in the expression of Bcl-2 protein in d14 and 28 lesions regardless

Figure 26 continued: of treatment. Error bars depict standard deviation. Significant: *$p \leq 0.05$, ns: not significant (one-way ANOVA Tukey's Multiple Comparison Post Hoc Test).

The BH3 interacting-domain death agonist (BID) is a pro-apoptotic member of the Bcl-2 protein family. Regardless of treatment, there was an increase in lesion BID mRNA expression between d4 mice and d7, 14 and 28 mice (Figure 27A). Second mitochondria-derived activator of caspases (SMAC) moderates the caspase inhibition of the inhibitor of apoptosis proteins or IAPs (Vucic, et al., 2002). In the absence of E_2, significantly higher expression of SMAC was observed in the d14 and 28 lesions in comparison to d4 lesions. Following a similar trend, in the presence of E_2, significantly higher SMAC expression was seen at d7, 14 and 28 as compared with d4 lesions. No difference in SMAC expression was observed between the vehicle treated animals and the E_2 treated animals regardless of treatment period (Figure 27B). Baculoviral IAP repeat-containing protein 1a (Birc1a) is a protein that can interact with active caspases and inhibit apoptosis. There was a significant decrease in Birc1a expression when comparing lesions from d4 vehicle treated animals with d7 and 14 vehicle treated animals. Interestingly, at d14 and 28 treatment periods there was a significantly higher expression of Birc1a in the lesion of E_2 treated mice when compared with the vehicle treated animals (Figure 27C).

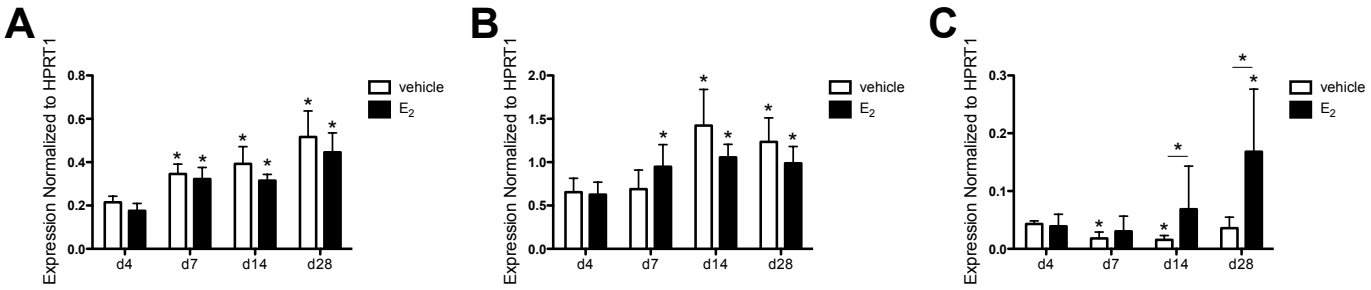

Figure 27: Gene expression analysis of BID, SMAC and Birc1a in the lesions of C57BL/6 mice

There were two treatment groups of vehicle (white bars) and E_2 (black bars). The y-axis shows fold expression of RNA as normalized to the internal control HPRT1. The x-axis shows the four treatment periods of 4 *(n=10)*, 7 *(n=10)*, 14 *(n=31)*, and 28 *(n=34)* days. **A:** Regardless of treatment, there was a significant increase in BID expression between d4 and 7 lesions and d14 and 28 lesions. **B:** There was a higher expression of SMAC at d7, 14 and 28 regardless of treatment in comparison to d4 lesions. **C:** There was a significant decrease in Birc1a expression when comparing lesions from d4 vehicle treated animals with d7 and 14 vehicle treated animals. At d14 and 28 treatment periods there was a significantly higher expression of Birc1a in the lesion of E_2 treated mice when compared with the vehicle treated animals. Error bars depict standard deviation. Significant: $*p \leq 0.05$, ns: not significant (one-way ANOVA Tukey's Multiple Comparison Post Hoc Test).

Tunel Measurement of Apoptosis

Terminal deoxynucleotidyl transferase dUTP nick end labeling (Tunel) was used for detecting DNA fragmentation, major characteristic of cells undergoing apoptosis. Tunel staining of mouse endometriotic lesions showed few dark brown colored (Tunel+) cells in glandular epithelium and stroma (Figure 28A-B). For control, the majority of cells from C57BL/6 mouse testes treated with DNase I were dark brown due to the high DNA fragmentation caused by the enzyme. The testes not treated with DNase I had few Tunel+ cells (Figure 28C-D).

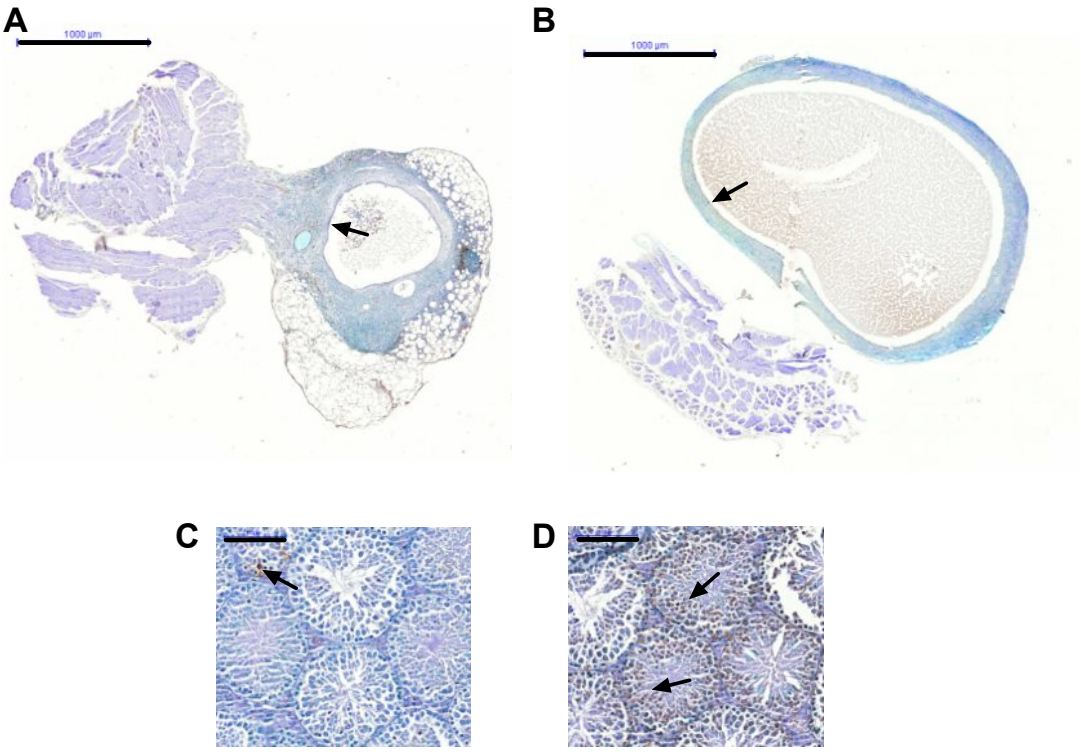

Figure 28: Tunel measurement of apoptosis in lesions from FVB/N mice

The cells containing DNA fragmentation are dark brown stained (Tunel+, black arrows). **A:** Lesion from vehicle treated animal at d28 post transplantation, scale bar 1000 µm. **B:** Lesion from E_2 treated animal at d28 post transplantion, scale bar 1000 µm. **C:** C57BL/6 mouse testes not treated with DNase I, scale bar 100 µm. **D:** C57BL/6 mouse testes treated with 100 µg/mL DNase I, scale bar 100 µm.

The frequency of Tunel positive cells was quantified in percentage of total cells as described in Materials and Methods. In the C57BL/6 strain no significant difference in Tunel+ cells was seen in between the vehicle and E_2 treatments in the treatment time points of 14 and 28 days (Figure 29A). In the FVB/N lesions there was a significant decrease in the percentage Tunel+ cells in between d14 vehicle treated mice (4.05% ± 0.772) and d28 vehicle treated mice (2.38% ± 0.375; Figure 29B). Com-

bined analysis of lesions from the two mouse strains showed that there was no significant difference in Tunel+ cell frequency between C57BL/6 mice (3.55% ± 2.71) and FVB/N mice (3.01% ± 1.44; Figure 29C).

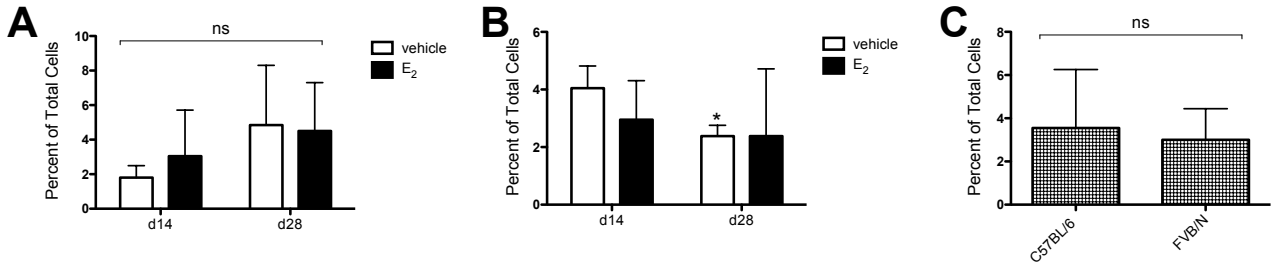

Figure 29: Analysis of Tunel+ cells in the lesions of C57BL/6 and FVB/N mice

There were two treatment groups of vehicle (white bars) and E_2 (black bars). The y-axis shows the frequency of Tunel+ cells as a percentage of total cells. **A:** The x-axis shows the treatment periods of 14 *(n=8)*, and 28 *(n=8)* days. In the C57BL/6 mice no significant difference in Tunel+ cell frequency was observed. **B:** The x-axis shows the two treatment periods of 14 *(n=5)*, and 28 *(n=5)* days. In the FVB/N lesions there was a significant decrease in the Tunel+ cells in between d14 vehicle treated mice and d28 vehicle treated mice. **C:** Combined analysis of lesions from the two mouse strains showed that there was no significant difference in Tunel+ cell frequency between C57BL/6 mice and FVB/N mice. Error bars depict standard deviation. Significant: $*p \leq 0.05$, ns: not significant (one-way ANOVA Tukey's Multiple Comparison Post Hoc Test).

In summary, using flow cytometry Annexin V staining, there were E_2 and time dependent fluctuations in non-leukocytes as well as few subtypes of leukocytes cell frequency. Furthermore, gene expression analysis of lesions revealed possible sex hormone regulation of apoptosis at the RNA level, but this did not translate to a difference in protein level in the case of Bcl2 as determined by western blotting. However, looking at total apoptosis using flow cytometry (AV) and immunohistochemis-

try (Tunel) as readouts, no difference was seen in the lesions from C57BL/6 and FVB/N mouse strains regardless of treatment or time.

3.1.5 Immune Cell Composition of Lesions Is Altered According to Time and Treatment

The number of DAPI- (live) cells recovered from C57BL/6 mouse endometriotic lesions was measured using flow cytometry. The lesions from d4 vehicle treatment group (3,477 ± 2,131) had significantly higher numbers of DAPI- cells than d14 (1,774 ± 1,456) and 28 (1,631 ± 765.9) vehicle treated mice. There was significantly lower number of DAPI- cells present in the lesions of d14 E_2 treated animals (1,802 ± 908.7) than d4 E_2 treated animals (4,858 ± 1,544). The latter group possessed significantly less DAPI- cells than the lesions from d28 E_2 treated animals (11,593 ± 16,125). At day 28, there was significantly higher number of DAPI- cells in the E_2 treated animals as compared with the vehicle treated animals (Figure 30A).

The immune system is suggested to play an important role in the initiation and the progression of endometriosis. White blood cells, or leukocytes, are major participants in the immune response and possibly maintenance of peritoneal tissue homeostasis. In order to determine occurrence of leukocytes in C57BL/6 mouse endometriotic lesions, the frequency of total DAPI- cells that expressed CD45 antigen was measured using flow cytometry. No difference in CD45+ cell frequency was observed regardless of treatment or treatment period (Figure 30B).

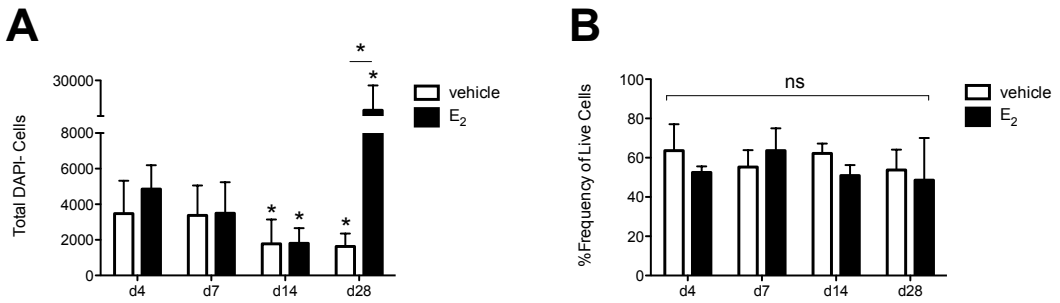

Figure 30: Total number of live cells and frequency of leukocytes in C57BL/6 mouse endometriotic lesions

There were two treatments groups of vehicle (white bars) and E_2 (black bars) plus four treatment periods of 4 *(n=10)*, 7 *(n=10)*, 14 *(n=31)*, and 28 *(n=34)* days. DAPI was used to exclude dead cells as described in Materials and Methods. **A:** The y-axis shows the total number of DAPI- (live) cells recovered from the lesions. The x-axis shows the treatment periods. The lesions from d4 vehicle group had significantly higher numbers of DAPI- cells than d14 and 28 vehicle groups. There was significantly lower number of DAPI- cells present in the lesions of d14 E_2 treated animals than d4 E_2 treated animals. The latter group had significantly less DAPI- cells than the lesions from d28 E_2 treated animals. At day 28, there was significantly higher number of DAPI- cells in the E_2 treated animals as compared with the vehicle treated animals. **B:** The y-axis shows the frequency of leukocytes (CD45+) as percentage of DAPI- cells. The x-axis is the same as A. No difference in CD45+ cell frequency was observed across all time points and treatment groups. Error bars depict standard deviation. Significant: $*p \leq 0.05$, ns: not significant (one-way ANOVA Tukey's Multiple Comparison Post Hoc Test).

Lymphocytes

Lymphocytes, immune cells from lymphoid lineage, that comprise T, B and natural killer (NK) cells play essential roles in determining either accept or reject survival, implantation, and proliferation of endometrial and endometriotic cells in patients with endometriosis (Osuga, et al., 2011). Indeed, in the mouse endometriotic lesions, differences in lymphocyte composition were observed. In the lesions of vehicle treated animals there was a significantly lower NK cell frequency at d4 (1.94% ±

0.515) than d7 (3.11% ± 0.285) and d14 (2.95% ± 0.639). Furthermore, there was a decrease in NK cell frequency at d28 vehicle treatment (1.71% ± 0.496) in comparison with d14 vehicle treatment. There was significantly higher frequency of NK cells in the d14 E_2 treated mice (2.99% ± 0.932) than d28 E_2 treated mice (1.59% ± 0.876; Figure 31A). There was no difference observed in the lesions of vehicle and E_2 treated animals.

B cell frequency remained unchanged in the lesions of vehicle treated animals (Figure 31B). However, upon E_2 treatment, there was significantly higher B cell frequency in at d7 (4.76% ± 1.45) than d4 (1.24% ± 0.212), 14 (2.70% ± 1.06) and 28 (1.67% ± 1.06) treatment periods. In the lesions of vehicle treated animals there was significantly lower frequency of T cells at d4 (2.19% ± 0.774) than d7 (6.46% ± 0.822), 14 (9.62% ± 3.95) and 28 (9.69% ± 4.71; Figure 31C). In the E_2 treated mice there was significantly higher frequency of T cells at d7 (6.56% ± 1.54) and 14 (7.09% ± 4.02) in comparison to d4 (1.27% ± 0.506) treatment period.

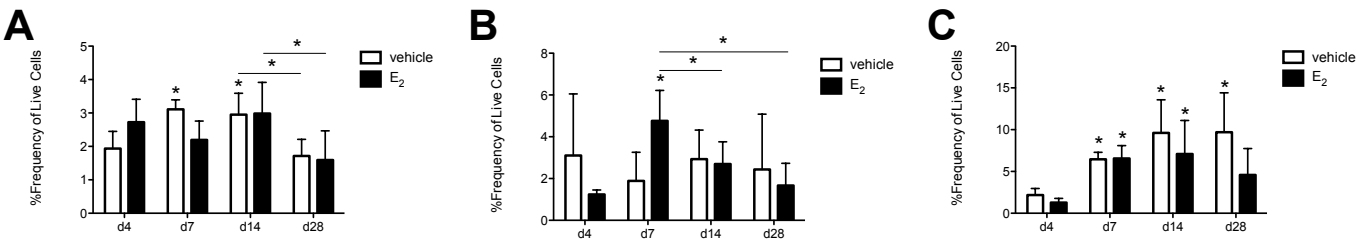

Figure 31: Frequency of NK, B and T cells in the lesions of C57BL/6 mice

There were two treatments groups of vehicle (white bars) and E_2 (black bars) plus four treatment periods of 4 *(n=10)*, 7 *(n=10)*, 14 *(n=31)*, and 28 *(n=34)* days. DAPI was used to exclude dead cells as described in Materials and Methods. **A:** The y-axis shows the frequency of NK cells as percentage of total DAPI- (live) cells. The x-axis shows the different treatment periods. In the vehicle treated animals there was a significantly lower NK cell frequency at d4 than d7 and 14. There was a decrease in NK cell frequency at d28 vehicle group than d14 vehicle group. There was significantly higher frequency of NK cells in the d14 E_2 treated mice than d28 E_2 treated mice. **B:** The y-axis shows the frequency of B cells as percentage of total DAPI- cells. The x-axis is the same as A. Upon E_2 treatment there was significantly higher B cell frequency in at d7 than d4, 14 and 28. **C:** The y-axis shows the frequency of T cells as percentage of total DAPI- cells. The x-axis is the same as A. In the vehicle treated animals there was significantly lower frequency of T cells at d4 than d7, 14 and 28. In the E_2 treated mice there was significantly higher frequency of T cells at d7 and 14 in comparison to d4. Error bars depict standard deviation. Significant: $*p \leq 0.05$, ns: not significant (one-way ANOVA Tukey's Multiple Comparison Post Hoc Test).

The frequency of two subtypes of T cells, helper T cells and cytotoxic T cells, was measured as described in the Materials and Methods. There was lower frequency of helper T cells in the lesions from d4 vehicle (1.25% ± 0.318) treated animals than d7 (3.25% ± 0.590), 14 (5.22% ± 1.33) and 28 (4.47% ± 1.97) vehicle treated animals. Similarly, upon E_2 treatment, there was significantly lower frequency of helper T cells at d4 (0.940% ± 0.255) than d7 (3.14% ± 0.411), 14 (4.13% ± 2.10) and 28 (2.27% ± 1.39; Figure 32A). Accordingly, a higher frequency of helper T cells was observed in d28 vehicle than E_2 treated animals. There was significantly higher fre-

quency of activated (CD69+) helper T cells in d28 vehicle (42.7% ± 10.3) and E_2 (52.7% ± 13.4) treated animals in comparison to d4 vehicle (30.6% ± 6.39) and E_2 (28.7% ± 2.97) as well as d14 vehicle (30.3% ± 7.63) and E_2 (37.8% ± 7.34; Figure 32B) treated animals respectively.

There was significantly lower cytotoxic T cell frequency at d4 vehicle treatment (0.940% ± 0.610) than d7 (3.21% ± 0.240), 14 (6.49% ± 1.18) and 28 (6.52% ± 2.42). Following a similar trend, upon E2 treatment, d4 lesions (0.600% ± 0.0141) exhibited significantly lower frequency of cytotoxic T cell in comparison to d7 (3.42% ± 1.15), 14 (3.98% ± 1.37) and 28 (3.35% ± 2.17) treatment time points. Furthermore, there was a significantly higher frequency of cytotoxic T cells in the lesions of vehicle treated animals at d14 and 28 in comparison to the E2 groups from the same time points (Figure 32C). There was significantly higher percentage of activated cytotoxic T cells in the lesions from vehicle treated animals at d28 (44.8% ± 9.57) than d4 (27.0% ± 13.3). Upon E2 treatment, there was significantly higher frequency of activated cytotoxic T cells at d28 (53.5% ± 15.7) than d7 (25.8% ± 5.77) and 14 (34.4% ± 6.82; Figure 32D).

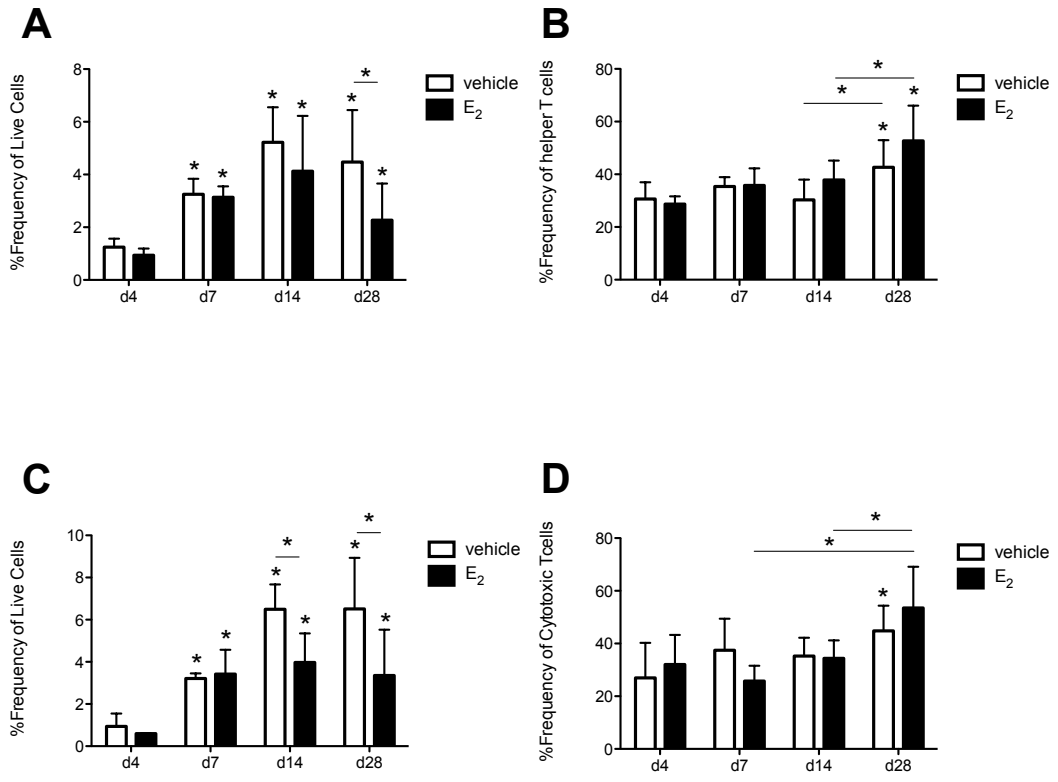

Figure 32: Frequency of helper T cells and cytotoxic T cells in the lesions of C57BL/6 mice

There were two treatments groups of vehicle (white bars) and E_2 (black bars) plus four treatment periods of 4 *(n=10)*, 7 *(n=10)*, 14 *(n=31)*, and 28 *(n=34)* days. DAPI was used to exclude dead cells as described in Materials and Methods. **A:** The y-axis shows the frequency of helper T cells as percentage of total DAPI- (live) cells. The x-axis shows the different treatment periods. There was lower frequency of helper T cells in the lesions from d4 vehicle group than d7, 14, and 28. There was significantly lower frequency of helper T cells in d4 E_2 animals than d7, 14 and 28. A higher frequency of helper T cells was seen in d28 vehicle group than E_2 group. **B:** The y-axis shows the frequency of CD69+ (activated) helper T cells as percentage of total helper T cells. The x-axis is the same as A. There was significantly higher frequency of CD69+ helper T cells in d28 vehicle and E_2 treated animals than d4 vehicle and E_2 as well as d14 vehicle and E_2 respectively. **C:** The y-axis shows the frequency of cytotoxic T cells as percentage of total DAPI- cells. The x-axis is the same as A. There was significantly lower cytotoxic T cell frequency in d4 vehicle animals than d7, 14 and 28. Upon E_2 treatment, d4 lesions exhibited significantly lower frequency of cytotoxic T cell in comparison to d7, 14 and 28 E_2 treatment time points. There was a significantly higher percentage of cytotoxic T cells in the lesions of vehicle treated animals at d14 and 28 in comparison to the E_2 groups from the same time points. **D:** The y-axis shows the frequency of CD69+ cytotoxic T cells as percentage

Figure 32 continued: of total helper T cells. The x-axis is the same as A. There was significantly higher percentage of CD69+ cytotoxic T cells in the lesions from vehicle treated animals at d28 than d4. Upon E_2 treatment, there was significantly higher frequency of CD69+ cytotoxic T cells at d28 than d7 and 14. Error bars depict standard deviation. Significant: $*p \leq 0.05$, ns: not significant (one-way ANOVA Tukey's Multiple Comparison Post Hoc Test).

Monocytes

Monocytes are a type of leukocyte that is primarily involved in the innate immune system. Their function involves differentiation into macrophages and dendritic cells (DCs) to elicit an immune response (Swirski, et al., 2009). Macrophages kill cells, such as retrograde endometrial tissues, and their presence is commonly associated with an inflammatory process. There was significantly higher frequency of macrophages in d4 (26.3% ± 8.46) vehicle group than d14 (11.3% ± 1.67). There was significantly higher frequency of macrophages in the d4 E_2 treated animals (26.0% ± 2.05) than d7 (17.0% ± 1.20), 14 (6.8% ± 0.608) and 28 (7.78% ± 3.97). There was significantly lower frequency of macrophages in E_2 treated animals at d14 and 28 in comparison to the vehicle group from the same time points respectively (Figure 33A). Major histocompatability complex class II (MHCII) and CD206 were used as markers to distinguish activated macrophages (Veltman, et al., 2010). There was on average 34.6% (± 13.5) of macrophages that exhibited the activation markers with no significant difference observed regardless of treatment or time (data not shown).

Dendritic cells are involved in the initiation and modulation of the adaptive immune response. The lesions from d7 vehicle (2.16% ± 0.359) and E_2 (2.02% ± 0.641) mice had significantly lower frequency of DCs than d4 vehicle (6.35% ± 3.42) and E_2

(5.86% ± 1.21) mice respectively (Figure 33B). Mature DCs exhibit MHCII and CD206 (Banchereau and Steinman, 1998). There was on average 74.7% (± 15.5) of DCs that exhibited the maturation markers with no significant difference observed regardless of treatment or time (data not shown).

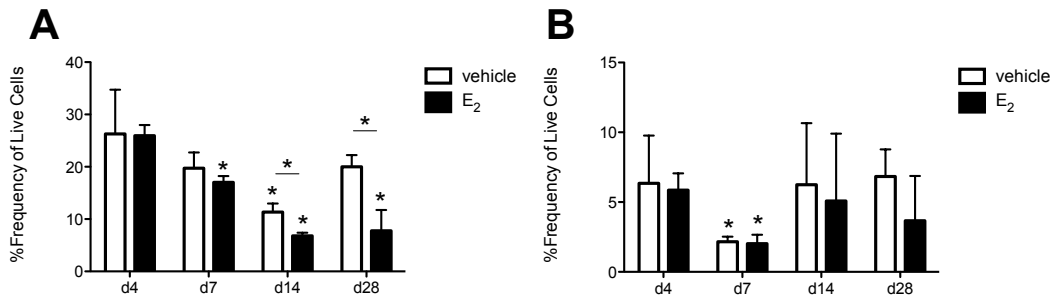

Figure 33: Frequency of macrophages and dendritic cells in the lesions of C57BL/6 mice

There were two treatments groups of vehicle (white bars) and E_2 (black bars) plus four treatment periods of 4 *(n=10)*, 7 *(n=10)*, 14 *(n=31)*, and 28 *(n=34)* days. DAPI was used to exclude dead cells as described in Materials and Methods. **A:** The y-axis shows the frequency of macrophages as percentage of total DAPI- (live) cells. The x-axis shows the different treatment periods. There was significantly higher frequency of macrophages in d4 vehicle group than d14. There was significantly higher frequency of macrophages in the d4 E_2 treated animals than d7, 14 and 28. There was significantly lower frequency of macrophages in E_2 treated animals at d14 and 28 in comparison to the vehicle group from the same time points respectively. **B:** The y-axis shows the frequency of dendritic cells (DCs) as percentage of total DAPI- cells. The x-axis is the same as A. The lesions from d7 vehicle and E_2 mice had significantly lower frequency of DCs than d4 vehicle and E_2 mice respectively. Error bars depict standard deviation. Significant: $*p \leq 0.05$, ns: not significant (one-way ANOVA Tukey's Multiple Comparison Post Hoc Test).

Granulocytes

Although many of the studies on the immunology of endometriosis focus on macrophages, T cells and NK cells, there has been little attention paid to granulocytes. The first two are motile phagocytes that can migrate from the blood into the tissue space

while the latter is nonphagositic and functions by releasing pharmacologically active substances from their granules. Using anti-Gr1 antibody, the frequency of mature granulocytes in mouse endometriotic lesions was measured. Although 20.3% (± 9.77) of the cells recovered from the lesions were granulocytes, no change in the frequency of this cell type was observed regardless of treatment and time (data not shown).

Using flow cytometry, cell frequency of lesions from mice treated with and without E_2 was determined. Looking at total cell numbers, there was significantly higher number of cells recovered from d28 lesions of the E_2 treated animals than all other groups. No difference in the frequency of total leukocytes was observed regardless of time and treatment. Looking closer at different subtypes of leukocytes, fluctuation based on time and treatment was observed. Since no different in total proliferation (Section 3.1.3) and apoptosis (Section 3.1.4) was observed in these experiments, perhaps there is influx and out-flux of cells occurring between the mouse endometriotic lesions and the peritoneal location. This idea was further investigated in the next segment of the project.

3.1.6 Measurement of Host Cells Infiltration Into the Implants Using a Novel Syngeneic Mouse Model

The fluctuation in immune cell composition of mouse endometriotic lesions supports the idea that that there is a close cellular interplay between host peritoneum and ectopic tissue. Initial experiments within the Transgenic and in vivo Pharmacol-

ogy (TASIP) department at Bayer Healthcare confirmed estrogen receptor modulated host cell infiltration between the peritonea and the transplanted uterus punch biopsies. Here, uterus fragments from normal cycling (intact ovaries), luciferase-expressing syngeneic FVB/N mice were transplanted onto the peritonea of normal cycling wild type syngeneic FVB/N mice. Operated animals received daily s.c. application of either vehicle or 1 mg/kg SERD (selective estrogen receptor destabilizer). There were five treatment periods of 14 *(n≥10)*, 21 *(n≥10)*, 28 *(n≥10)*, 35 *(n≥10)*, and 42 *(n≥10)* days. Ex vivo imaging of the animals was performed to determine bioluminescence intensity of lesions over time. In the SERD treatment groups, there was significantly lower bioluminescence at d28 (1556 ± 709.3), 35 (1522 ± 702.5), and 42 (1440 ± 623.9) as compared with d14 (2594 ± 1277) and d21 (2362 ± 504.5) animals. In the vehicle treatment groups, no significant difference among different time points was observed. There was significantly lower bioluminescence in the vehicle treated animals from d28 (2935 ± 923.0), 35 (2470 ± 670.0), and 42 (2402 ± 1293) than the SERD treated mice from the same time points respectively (Figure 34A).

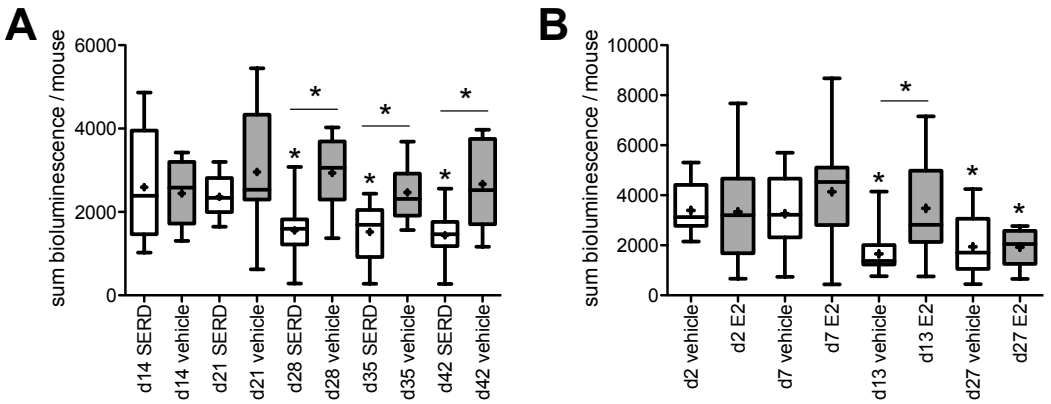

Figure 34: Bioluminescence measurement of endometriotic lesions from FVB/N mice

The y-axis shows the sum bioluminescence per mouse. The x-axis shows the different treatment periods. **A:** Uterus biopsies from normal cycling, syngeneic, luciferase-expressing FVB/N mice were sutured onto the peritonea of normal cycling, syngeneic, wild type FVB/N mice as described in Materials and Methods. The animals were treated with SERD or vehicle for 14, 21, 28, 35, and 42 days. In the SERD treated mice, there was significantly lower bioluminescence at d28, 35, and 42 as compared with d14 and 21. There was significantly lower bioluminescence in the vehicle treated animals from d28, 35, and 42 than the animals treated with SERD from the same time points respectively. **B:** Same setup as A, except all donor and acceptor mice were ovariectomized. The mice were treated with either vehicle or E_2 for two, seven, 13, and 27 days. In the vehicle treatment groups, there was significantly lower bioluminescence at d13 and 27 as compared with d2 and d7. Mice treated with E_2 for 27 days had lesions with significantly lower bioluminescence than ones treated for two, seven, and 13 days. There was significantly lower bioluminescence in the E_2 treated animals from d13 than vehicle treated mice from the same time point. Error bars depict standard deviation. Significant: $*p \leq 0.05$ (one-way ANOVA Tukey's Multiple Comparison Post Hoc Test).

In the current study, the aforementioned experiment was repeated using the same animals as donor and acceptor with the addition that all were ovariectomized as described in the Materials and Methods. The operated animals were treated with vehicle or E_2 for two *(n≥18)*, seven *(n≥18)*, 13 *(n≥18)*, and 27 *(n=10)* days. In the vehicle treatment groups, there was significantly lower bioluminescence at d13 (1657 ±

782.9) and 27 (1944 ± 1196) as compared with d2 (3392 ± 1005) and d7 (3260 ± 1443) animals. Mice treated with E_2 for 27 days (1924 ± 771.4) had lesions with significantly lower bioluminescence than ones treated for two (3336 ± 1969), seven (4136 ± 1824), and 13 (3481 ± 1885) days. Interestingly, there was significantly lower bioluminescence in the E_2 treated animals from d13 than vehicle treated mice from the same time point (Figure 34B).

To summarize, the lesions from the E_2 treated ovx mice and vehicle treated normal cycling mice showed higher luminescence than the lesions from vehicle treated ovx animals and SERD treated normal cycling animals; meaning in the latter groups, less of the originally transplanted tissue was present. This result along with the lack of change in proliferation and apoptosis hints at a dynamic interplay between the ectopic site (peritoneal cavity) and the misplaced uterus tissue.

3.2 Lesion Kinetics in a Non-human Primate Model of Endometriosis

The influx of host cells into the transplanted uterus tissue in the mouse model demonstrated the dynamic nature of the lesions. Furthermore, strong kinetics of lesion parameters, lesion activity that does not necessarily run in parallel to lesion size, and spontaneous lesion progression as well as regression has been observed in the mouse model for endometriosis. Lesion dynamics describe spontaneous lesion progression and regression, the development of new lesions and changes in lesion ap-

pearance over time. Lesion turnover is a consequence of these dynamics, which are likely induced by hormonal and inflammatory fluctuations. Here lesion kinetics was investigated using a menstruating non-human primate model as described in the Materials and Methods.

3.2.1 Baboon Endometrial Lesion Location and Morphology

A total of 542 endometriotic lesions were observed in the baboons investigated. Lesions were commonly found on the peritoneal surfaces involving the pouch of Douglas, bladder and the perimetrium (Figure 35A). Lesions were characterized as red, black, blue, powder burn, blister like, multicolored and white. Morphologically, Gomori trichrome staining of baboon lesions revealed distinct endometrial glands and stroma that was observed in all lesion types (Figure 35B). A comparison of lesions characterized by different colors exhibited visible hemorrhaging in the red lesions and the presence of more connective tissue in the white lesions.

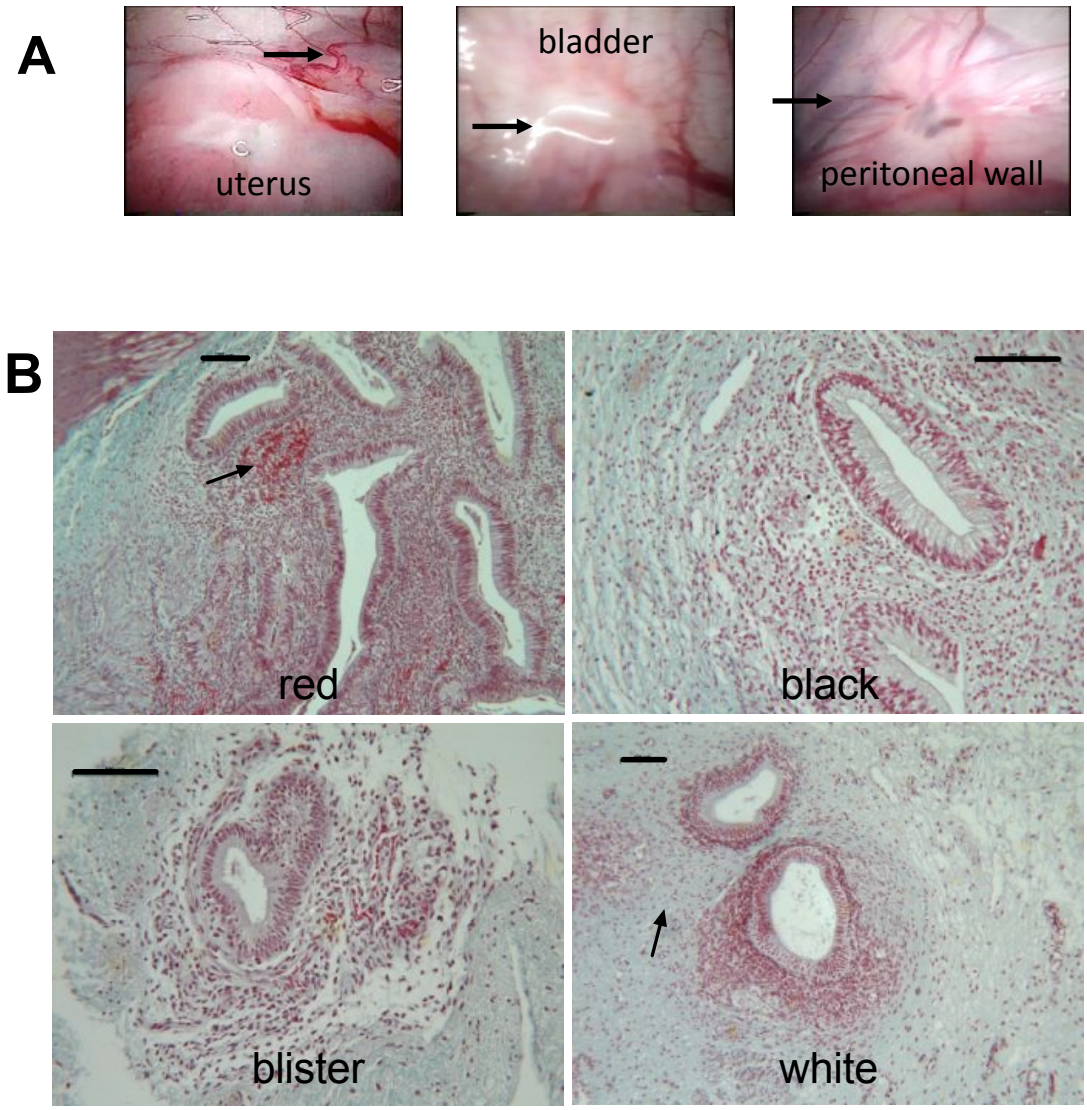

Figure 35: Endometriotic lesion location and morphology in an experimental model of endometriosis in baboons

Nine baboons were experimentally induced with endometriosis by i.p. inoculation with autologous menstrual endometrium, as described in Materials and Methods. **A:** Common locations of baboon endometriotic lesions in the abdomen were the perimetrium, the bladder and the peritoneum at the Pouch of Douglas. **B:** Gomori trichrome staining revealed distinct endometrial glands and stroma. Hemorrhaging was observed in the red lesions (arrow), while more connective tissue was present in the white lesions (arrow). Scale bar: 100 μm

3.2.2 Lesion Development in Baboons Inoculated with Menstrual Tissue

Early Lesion Occurrence and Persistence

At each diagnostic laparoscopy a total of 9 (±5) lesions per animal were detected. This average excludes the 15-month necropsy where 22 (±6) lesions per animal were detected. During the 15 months following induction of endometriosis, 330 new lesions were detected in the nine baboons. There was no significant variation in the number of new lesions observed between laparoscopies and 15-month necropsy (Figure 36A, one-way ANOVA Tukey's Multiple Comparison Post Hoc Test). Interestingly, at 12 months post inoculation 19 of 37 (51%) lesions present were newly detected lesions indicating that new lesions were continuously evolving throughout the disease model. With regard to lesion persistence, there was no significant difference between the number of lesions persisting over time between each time point (Figure 36B). Twenty-four of 59 (41%) lesions initially observed at second inoculation were still present at the 15-month necropsy.

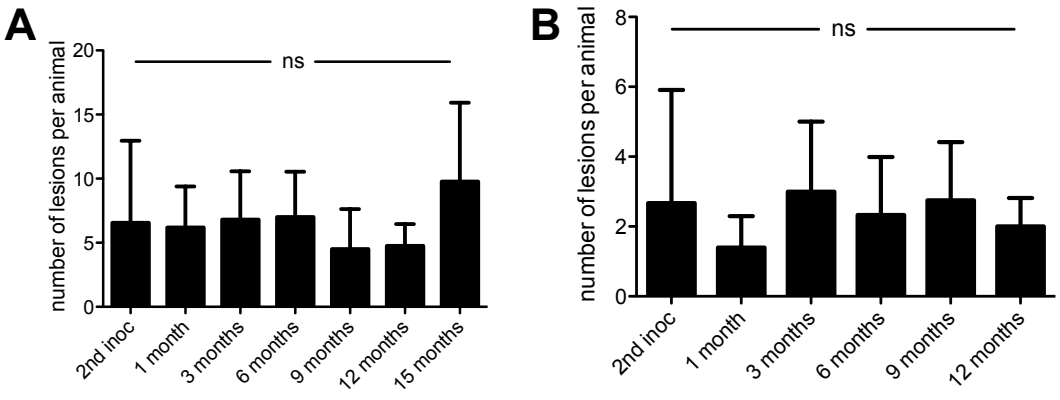

Figure 36: Number of new lesions and their persistence over time in an experimental model of endometriosis in baboons

Nine baboons underwent diagnostic laparoscopies at 1, 3, 6, 9 and 12 months as well as a necropsy at 15 months following two i.p. inoculations with autologous menstrual endometrium. Each lesion was recorded upon initial sighting and the site was specifically assessed at subsequent laparoscopies. **A:** Mean number of new lesions per inoculated animal at each laparoscopy and 15-month necropsy. **B:** The mean number of lesions first seen at each laparoscopy in the inoculated animals that are still present at 15-month necropsy. Columns represent the mean number of lesions per animal (n=9). Error bars depict SD. ns: not significant (one-way ANOVA Tukey's Multiple Comparison Post Hoc Test).

Lesions Characterized by Different Colors

The color and location of the endometriotic lesions observed at each laparoscopy in the inoculated group was recorded. The most frequent colors observed in each baboon were blue (15 ± 8, 138 total), followed by black (15 ± 6, 135 total), white (10 ± 6, 86 total), and red lesions (8 ± 5, 74 total, Figure 37A). Multicolored lesions did not allow a clear classification into certain lesion type but were significantly less than the above mentioned lesion types. Figure 37B summarizes the frequency of lesion types according to color at each surgical intervention. Heterogeneity in color was noted across all time points.

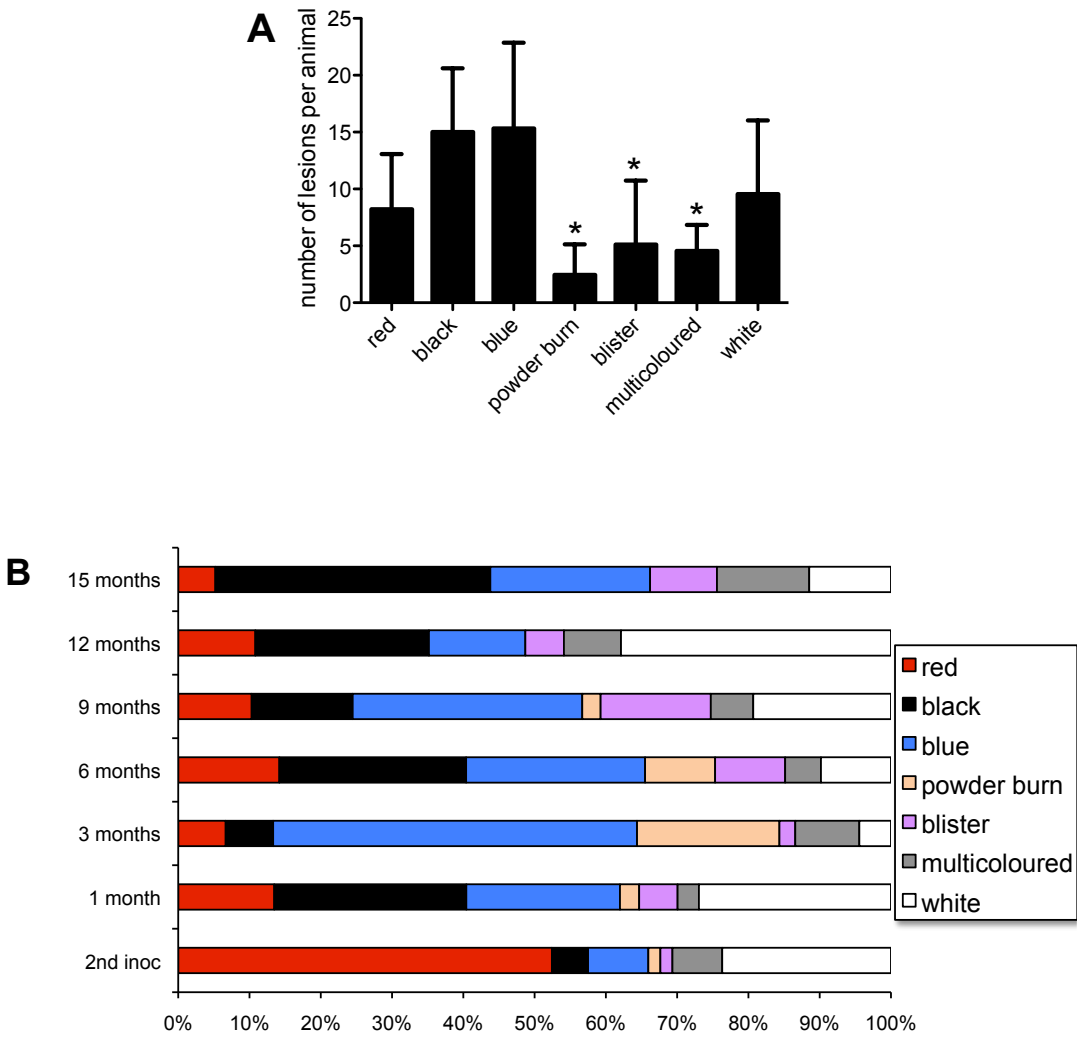

Figure 37: Number of endometriotic lesions characterized by different colors in an experimental model of endometriosis in baboons

Each lesion was recorded upon initial sighting and tracked at each subsequent laparoscopy where colors were recorded. **A:** There were significantly lower numbers of powder burn, blister and multicolored lesions observed per animal in comparison to black and blue lesions (*p value ≤ 0.05, one-way ANOVA Tukey's Multiple Comparison Post Hoc Test). Columns represent the mean number of lesions per animal (n=9). Error bars represent the SD of the mean **B:** Frequency of lesions (in % of total number of lesions per time point) characterized by different colors in the nine baboons at different time points post inoculation.

As each lesion was recorded, the site of the lesion was specifically assessed at subsequent laparoscopies and 15-month necropsy. When the site of the lesion was accessible and no lesion was observed, the lesion was categorized as regressed (not present). When the site of the lesion was not surgically accessible the lesion was categorized as not found / not visible. Figures 38A, C, E, and G show the total number of red, black, blue, and white lesions at each laparoscopy. Figures 38B, D, F, and H describe changes in lesion color over time. The majority (31/59) of lesions found at the second inoculation were red lesions (Figure 38A). Red lesions subsequently transformed into endometriotic foci characterized by several different colors over the 15 month period (Figure 38B). The highest occurrence of black lesions, as determined by laparoscopy, was at 6 months with 24 total. At necropsy, there were 74 black lesions present (Figure 38C). Black lesions most often remained black, or turned blue, white or regressed (Figure 38D). The highest occurrence of blue lesions was observed at 3 months post-inoculation (Figure 38E) and in contrast to the red lesions, blue lesions remained consistently blue (Figure 38F). White lesions were present at each time point, the lowest frequency being at 3 months (Figure 38G). White lesions often disappeared (not present) or became scar tissue at subsequent surgery (Figure 38H). The infrequent lesions, such as powder burn, blister and multicolored, turned into different lesion types at subsequent surgeries or disappeared (data not shown).

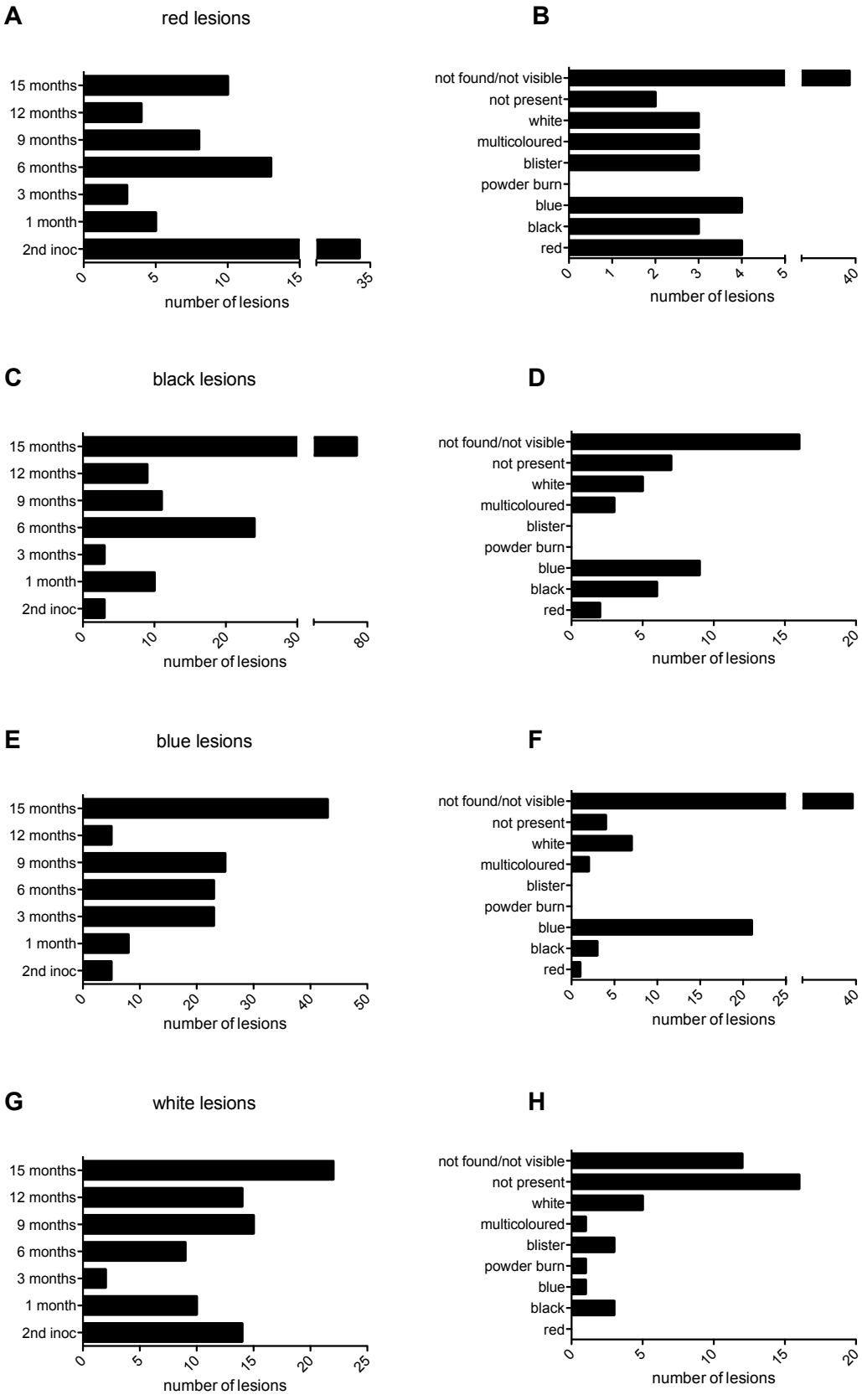
A
red lesions
15 months
12 months
9 months
6 months
3 months
1 month
2nd inoc
0
5
10
15
35
number of lesions
B
not found/not visible
not present
white
multicoloured
blister
powder burn
blue
black
red
0
1
2
3
4
5
40
number of lesions
C
black lesions
15 months
12 months
9 months
6 months
3 months
1 month
2nd inoc
0
10
20
30
80
number of lesions
D
not found/not visible
not present
white
multicoloured
blister
powder burn
blue
black
red
0
5
10
15
20
number of lesions
E
blue lesions
15 months
12 months
9 months
6 months
3 months
1 month
2nd inoc
0
10
20
30
40
50
number of lesions
F
not found/not visible
not present
white
multicoloured
blister
powder burn
blue
black
red
0
5
10
15
20
25
40
number of lesions
G
white lesions
15 months
12 months
9 months
6 months
3 months
1 month
2nd inoc
0
5
10
15
20
25
number of lesions
H
not found/not visible
not present
white
multicoloured
blister
powder burn
blue
black
red
0
5
10
15
20
number of lesions

Figure 38: Turnover of endometriotic lesions characterized by different colors in an experimental model of endometriosis in baboons

At each surgery the locations of previously identified endometriotic lesions were analyzed and the evolution of each lesion tracked. When the site of the lesion was not accessible, the lesion was categorized as not found / not visible. When the site of the lesion was accessible and no lesion was observed, the lesion was categorized as regressed (not present). A, C, E, and G show the number of red, black, blue, and white lesions at each laparoscopy. B, D, F, and H demonstrate the evolution of red, black, blue, and white lesions at the subsequent laparoscopy. The bars correspond to the total number of lesions per time point or lesion type, respectively.

3.2.3 Recurrence of Excised/Ablated Lesions in Baboons Inoculated with Menstrual Tissue

All visible lesions (26 total) from two animals with induced endometriosis were removed 6 months after inoculation. Subsequent laparoscopies were conducted at 9 and 12 months followed by necropsy at 15 months post-inoculation and recurrence of lesions was recorded. In one animal, three out of 16 visible lesions reappeared as early as 3 months later. In the two animals, 18 of 26 (69%) lesions removed at 6 month returned by necropsy (Figure 39A). Excision and ablation were used interchangeably as determined by the surgeon. Fifteen out of 20 (75%) excised lesions returned while three out of six (50%) ablated lesions returned (Figure 39B).

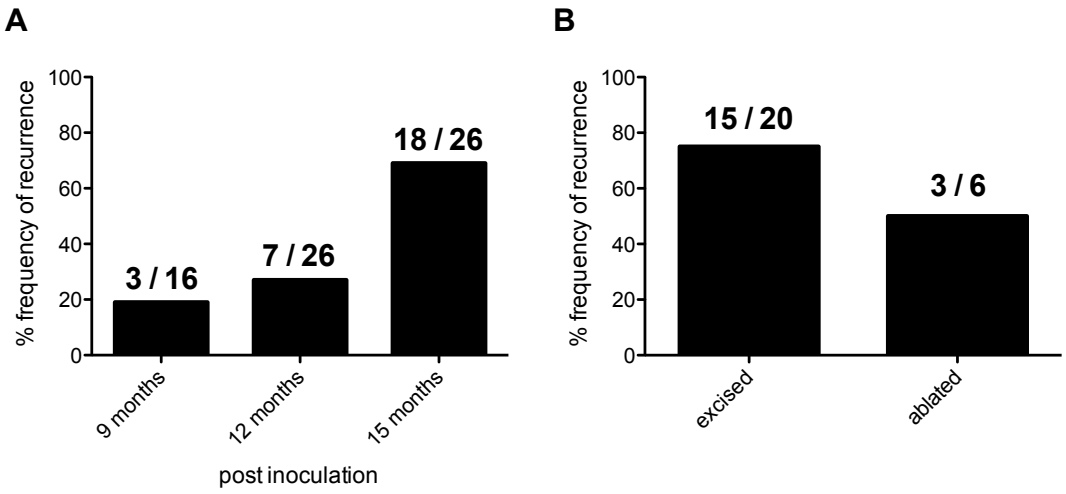

Figure 39: Recurrence of excised/ablated endometriotic lesions in an experimental model of endometriosis in baboons

In two animals that were inoculated with autologous menstrual tissue, lesions were excised or ablated 6 months after the second inoculation. Laparoscopies were performed at 9 and 12 months and a necropsy at 15 months to control for lesion recurrence. **A:** Of the removed lesions at 6 months post-inoculation, three of 16 returned 3 months after excision, seven of 26 returned 6 months after excision, and at 15-month necropsy 18 of 26 (69%) lesions had returned. **B:** Excision and ablation were used interchangeably as determined by the surgeon. 15 of 20 (75%) excised lesions returned by 15-month necropsy while three of six (50%) ablated lesions returned by necropsy.

The excised/ablated lesions included one red, 11 black, six blue, one powder burn, three blisters and four white lesions. The single red lesion recurred as blue at subsequent laparoscopy and remained blue until 15-month necropsy. Of the 11 excised/ablated black lesions, two returned as black, two as blisters, and seven were not found / not visible at subsequent laparoscopy. At 15-month necropsy, four were black, one was blue, three were blisters, and three had regressed (not present). All six of the removed blue lesions were not found / not visible at subsequent laparoscopy while at necropsy one appeared as black, three were blue, one was blister and one had regressed. Figure 40 shows recurrence of the excised/ablated black and

blue lesion at subsequent laparoscopy (40A) and at 15-month necropsy (40B). One removed blister lesion recurred as blue and two were not found / not visible at subsequent laparoscopy. At necropsy, two were blue and one had regressed. Of the four removed white lesions, one recurred as white, one as blister, and two were not found / not visible at subsequent laparoscopy while at necropsy one was a blister and three had regressed (data not shown).

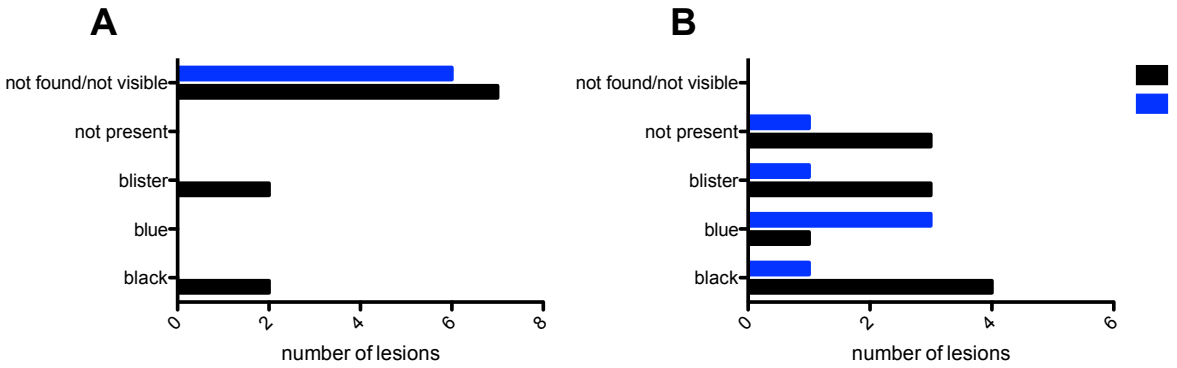

Figure 40: Turnover of reoccurring excised/ablated endometriotic lesions in an experimental model of endometriosis in baboons

Excision/ablation of all visible endometriotic lesions was performed in two baboons 6 months after experimental induction of endometriosis, as described in Materials and Methods. Laparoscopies were conducted at 9 and 12 months and a necropsy at 15 months post-inoculation to determine the incidence of lesion recurrence and macroscopic changes within the peritoneal cavity. When the site of the lesion was not accessible, the lesion was categorized as not found / not visible. When the site of the lesion was accessible and no lesion was observed, the lesion was categorized as regressed (not present). Black and blue bars represent the status of excised/ablated black and blue endometriotic lesions after recurrence. **A:** The reoccurring excised/ablated black and blue lesions at subsequent laparoscopy. Each bar represents the number of each type of lesion manifested after reoccurrence. **B:** The reoccurring excised/ablated black and blue lesions at 15-month necropsy. Each bar represents the number of each type of lesion manifested at necropsy.

3.2.4 Lesion Occurrence in Baboons Not Inoculated with Menstrual Tissue

Five control baboons did not undergo inoculations but were subjected to diagnostic laparoscopies followed by endometrectomy to harvest eutopic tissue at each surgical time point. All five animals developed endometriotic lesions with one animal having as many as 13 lesions (Figure 41A). In this animal, the two earliest lesions appeared at 6-month laparoscopy and were characterized as red and blue. These two lesions were not found / not visible at subsequent laparoscopies and by 15-month necropsy had regressed. A total of 27 peritoneal lesions were observed in the five control animals with the majority being detected at 12-month laparoscopy (*n*=11) and 15-month necropsy (*n*=14) (Figure 41B).

Five out of 11 lesions discovered at 12-month laparoscopy were present at necropsy and had progressed to different colors. They included one red lesion turning to white, two black lesions, one remaining black and one turning to blue, one blue lesion staying blue, and one multicolored lesion that turned to black (data not shown). The location of lesions, as with the induced endometriosis group, was on both visceral and parietal peritoneum. Similarly, a heterogeneous mixture of endometriotic lesion colors was observed with the majority being black and blue colored lesions (Figure 41C).

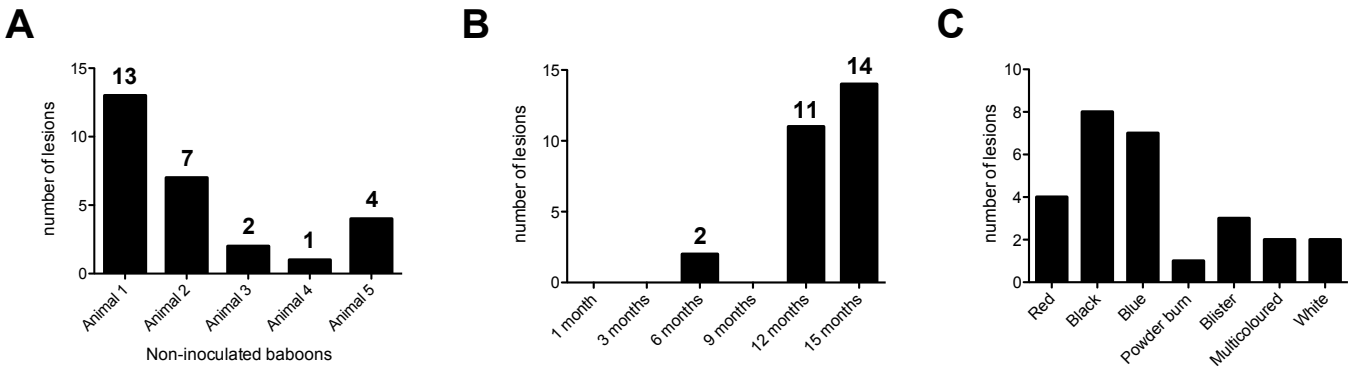

Figure 41: Control baboons not inoculated with menstrual tissue

Five animals did not undergo inoculation, but were subjected to the same schedule of surgeries as the experimental groups to control for the effects of the surgeries themselves. Twenty-seven endometriotic lesions were observed in the five animals. **A:** Each bar represents the total number of endometriotic lesions found per animal. **B:** Each bar represents the number of newly detected lesions at the corresponding time point. **C:** Each bar represents the total number of each lesion type observed.

3.2.5 Gene Expression Analysis of Baboon Lesions

RNA was extracted from paraffin embedded baboon endometriotic lesions as described in the Materials and Methods. Twelve lesions from 3-month time point and 15 from 15-month time point were utilized, which included eight black, seven blue, eight multicolored, and four white lesions.

Gene Expression Analysis of Select Genes

Real time-PCR (RT-PCR) was performed to check the expression of 30 genes that may be involved in the modulation of immune system, endocrine system, proliferation, apoptosis, and tissue composition. Only genes expressed in four or more le-

sions were analyzed based on time (3 vs. 15) and color. RPS17 was used as loading control. Four genes met the criteria for analysis. There was higher expression of Cysteine-rich angiogenic inducer 61 (CYR61), estrogen receptor 1 (ESR1), and TGFβ3 at 3 months than at 15 months. The blue lesions showed a lower expression

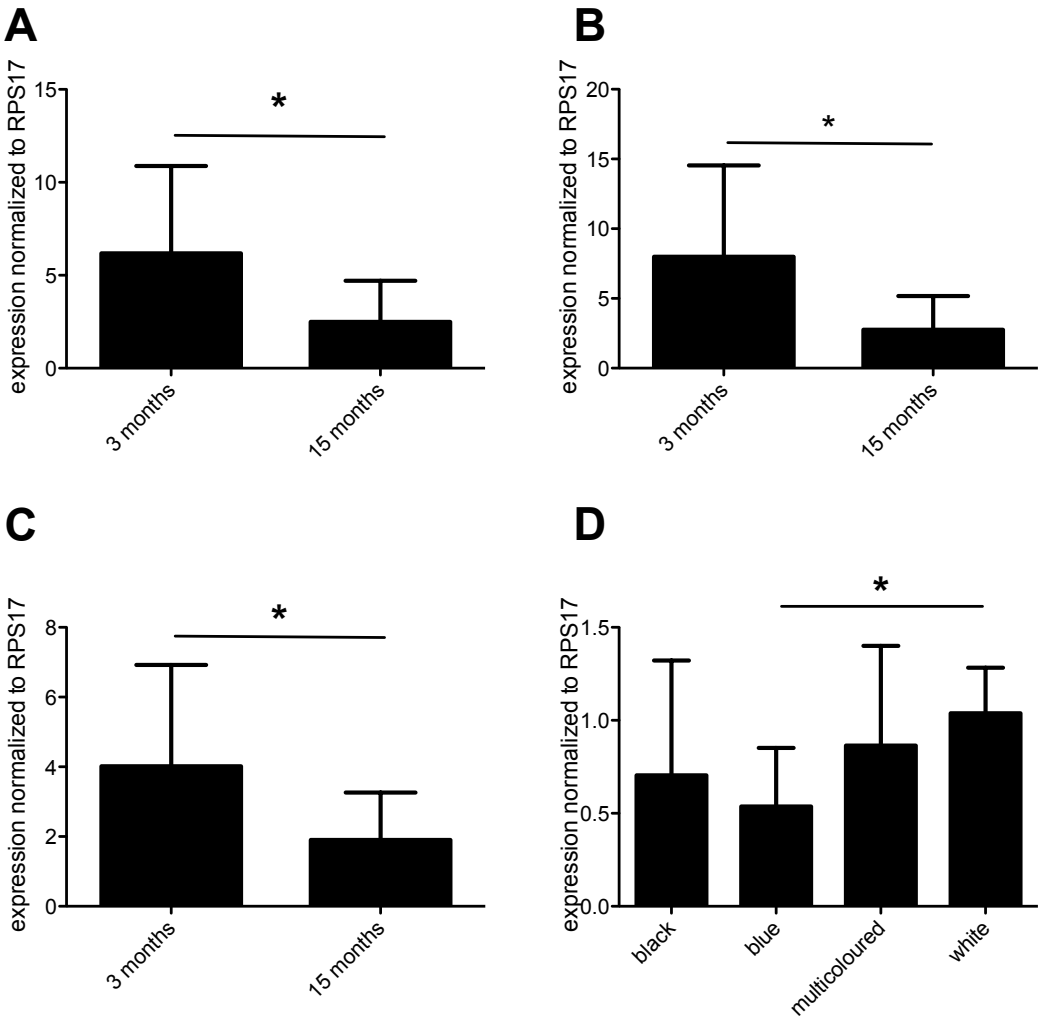

of Insulin-like growth factor 2 (IGF2) than the white lesions (Figure 42).

Figure 42: Gene expression analysis of CYR61, ESR1, TGFβ3, and IGF2 in baboon lesions

Lesions from baboons that were inoculated with autologous menstrual tissue were excised, fixed, and embedded in paraffin. RNA was extracted from 3-month (*n=12*) and 15-month (*n=15*) lesions including black, blue, multicolored, and white lesions. The y-axis shows fold expression of RNA as normalized to the internal control

RPS17. **A:** The x-axis shows the two time points. There was significantly higher CYR61 expression at 3 months than at 15 months. **B:** The x-axis is the same as A. **Figure 42 continued:** There was significantly higher ESRI expression at 3 months than at 15 months. **C:** The x-axis is the same as A. There was significantly higher TGFβ3 expression at 3 months than at 15 months. D: The x-axis shows the different lesion colors analyzed. There was significantly lower IGF2 expression in blue lesions as compared with white lesions. Error bars depict standard deviation. Significant: $*p \leq 0.05$, ns: not significant (one-way ANOVA Tukey's Multiple Comparison Post Hoc Test).

Taqman Array Micro Fluidic Cards

Twelve lesions from 3-month and 12 from 15-month time points were analyzed using Applied Biosystem's Human Immune Array (94 genes) and Human Protein Kinase Array (68 kinase and 26 non-kinase genes). Only genes expressed in four or more lesions were analyzed. For internal control 18S was included on every Micro Fluidic Cards. Using two-tailed T test several genes show regulation between 3-month and 15-month time points (data not shown). Confirmation studies are ongoing in Prof. Fazleabas' lab at Michigan State University College of Human Medicine.

4 Discussion

Investigating the dynamics of endometriosis evokes the need for experimental animal models. In the current study, mouse and baboon models were used to gain further insight into the disease and consequently help in identifying new therapeutic approaches.

4.1 Effects of Estradiol on Experimental Endometriosis

The effect of 17ß-estradiol (E_2) on the establishment, development, and persistence of endometriotic lesions in syngeneic transplantation mouse model, a homologous experimental model for endometriosis modified from Becker et al. (2005), was analyzed using two mouse strains: C57BL/6 and FVB/N. To counteract the variation in biological estrogen levels and estrous cycle between individual mice, the ovaries, major source of estrogen (Bulun, et al., 2005), were removed (ovariectomized, ovx) at least one-week prior to the transplantation surgery. Additionally, each group was supplemented subcutaneously (s.c.) with daily dose of E_2 or vehicle, allowing direct comparison of lesion attributes in the presence and absence of the sex hormone.

Endometrium alone could not be used as transplant due to its soft consistency impairing suturing, therefore whole uterus biopsies, containing endometrium, myometrium, and perimetrium, were sutured onto the peritoneum. This, along with lack of menstruation, and different hormonal levels in mice than humans (Byers, et al., 2012), are known limitations of the model since endometriosis is hypothesized to occur via retrograde menstruation of loose endometrial tissue (Sampson, 1927).

Consistency in the spatial orientation of the transplants was maintained since it may lead to implants with different size and attribute (Korbel, et al., 2010). Therefore, to mimic the human mechanism of pelvic endometrial tissue implantation, the mouse uterus fragments were consistently transplanted with the endometrium, as oppose to perimetrium, adjoining the peritonea.

The transplanted syngeneic tissue adhered to the denuded parietal peritoneum, as determined by hematoxylin and eosin staining, and changed macroscopic appearance from red hemosiderin-rich deposits at four days (d4) to cyst-like appearance that displayed a smooth, white to transparent homogenous surface from d7 onward. Validating these visual changes observed in the mouse lesions over time, analysis of humans and non-human primates showed that endometriosis is a dynamic disorder, which includes spontaneous progression, regression, and changes in lesion appearance over time (Harirchian, et al., 2012).

4.1.1 Estradiol Impacted Size, But Not the Establishment of Mouse Endometriotic Lesions

All transplanted uterus biopsies developed into site-specific endometriotic lesions with histological features similar to human endometriosis, such as anechoic cyst-like dilated glands, glandular epithelium, and stromal structures (Albee, et al., 2008). The metamorphosis of uterus transplants into endometriotic lesions occurred regardless of E_2 administration. This confirmed previous findings in similar transplantation model using ovx syngeneic C57BL/6 mice (Hirata, et al., 2005, Lin, et al.,

2006) and estrogen receptor (ER) knockout mice (Burns, et al., 2012) where E_2 and intact ER signaling were not necessary for the establishment of ectopic implants respectively.

Detailed analysis of two dimensional lesion areas from ovx C57BL/6 and FVB/N mice showed that at days 14 and 28 post transplantation, there was significantly higher lesion area in E_2 treated animals in comparison to vehicle treated animals from the same time points. Interestingly, in vehicle treated mice, there was significantly lower lesion area at d14 and 28 in comparison to d4 while no significant difference between d4, 7, 14, and 28 E_2 treated mice was seen suggesting that the difference between the two treatment groups was due to lesion size reduction in the absence of E_2. Comparatively larger lesion size seen in mice supplemented with E_2 demonstrated estrogen dependency of the model, which is a hallmark of endometriosis and confirms previous studies using similar syngeneic model with ovx C57BL/6 (Lin, et al., 2006) and ovx B6C3F1/J (Cummings and Metcalf, 1995) mouse strains. This E_2 effect was not due to the transplantation of whole uterus punch biopsies since ovx rats transplanted with autologous endometrium also exhibited smaller lesion size in the absence of E_2 (Rajkumar, et al., 1990). The possible mechanisms for the sex hormone modulation of lesion area were analyzed by looking at proliferation, apoptosis, and cell composition of mouse endometriotic lesions.

4.1.2 Total Proliferation Was Unchanged in Mouse Edometriotic Lesions Regardless of E_2 Treatment

Total proliferation in the mouse lesions was analyzed using immunohistochemistry (IHC) Ki-67 staining. C57BL/6 lesions from four, seven, 14, and 28 days showed no significant difference in Ki-67 staining intensity regardless of treatment. Similarly, no significant difference in Ki-67 staining intensity of FVB/N lesions from 14 and 28 days of vehicle or E_2 treatment was observed. Interestingly, the larger lesion area observed in FVB/N mice (Section 4.1.1) did not translate to more proliferation since on average lesions from C57BL/6 mice had significantly higher Ki-67 stain intensity than lesions from FVB/N mice. Conversely, heterologous mouse studies with human endometrial tissue as transplants, using ovx nude and SCID mice, showed significant reduction in Ki-67 stating in the absence of E_2 (Grummer, et al., 2001, Monckedieck, et al., 2009). Nude and SCID mice are immunodeficient, have impaired ability to make lymphocytes, lacking an important signaling pathway for the control of proliferation, and cannot efficiently fight infections, nor reject tumors and transplants, which may explain the difference observed between the two models.

Enhanced proliferation capability of ectopic implants may be a precondition for initiation and persistence of endometriosis. However, proliferation activity of endometriotic lesions is described with contradictory results. Ki-67 histology showed that endometrial tissue at the epithelial and stromal levels from women with endometriosis has significantly higher degree of cell proliferation in comparison with eutopic endometrium of women without endometriosis (Meresman, et al., 2002) while

other groups saw no difference using the same method (Nisolle, et al., 1997, Scotti, et al., 2000). Additionally, increase in IHC staining of proliferating cell nuclear antigen (PCNA) of endometriotic lesions (Li, et al., 1993) and endometrium from women with endometriosis in comparison to patients without endometiosis (Wingfield, et al., 1995) has been observed. Not surprisingly, interpretation of human studies is limited by the lack of proper controls as well as disease stage variations and differing phases of menstrual cycle between patients. Indeed, Ki-67 staining intensity fluctuated in ectopic implants between patients at different stages of the menstrual cycle (Jones, et al., 1995). Since synergistic events such as abnormal proliferation and apoptosis (see next section) may be important mechanisms of growth and persistence for ectopic implants, in the current study additional methods for the measurement of proliferation were used with large number of animals and proper controls in a well-defined hormonal setting.

Bromodeoxyuridine (BrdU) can incorporate into newly synthesized DNA during proliferation and was supplemented in the drinking water. Confirming Ki-67 results, using flow cytometry as readout for BrdU, the mouse endometriotic lesions showed no difference in proliferation frequency between vehicle and E_2 treated groups for total cell proliferation and specific cell subgroups: immune cells (CD45+ leukocytes), non-immune cells (CD45- non-leukocytes), and epithelial cells (CD45-, cytokeratin+). It should be noted that the estradiol induced proliferation in human endometriotic lesions has been attributed to ER2 signaling (Burns, et al., 2012) and

C57BL/6 uterus has lower ER2 mRNA expression than the human uterus (Couse, et al., 1997, Lecce, et al., 2001).

In the mouse uterus, the anticipated hormone induced fluctuations in cell proliferation was observed since E_2 is a known facilitator of cellular proliferation especially in the epithelial compartments of the reproductive organ (Quarmby and Korach, 1984). Comparison of BrdU+ cell frequency from lesions and uterus showed no significant difference in the proliferation of total cells, leukocytes, non-leukocytes, and epithelial cells between the eutopic and ectopic tissues. This result is in contrast to the Lin et al. (2006) study using identical ovx C57BL/6 model suturing uterus biopsies onto the peritoneum, where upon E_2 treatment, total BrdU+ positive cells measured using IHC, increased in lesions between one, two, five, and seven days of treatment while in the uterus no difference between vehicle and E_2 treatment was observed. This discrepancy could be due to difference in the readout, administration method, and incubation period of BrdU since in the current study animals were continuously provided BrdU in their drinking water starting four days prior to necropsy while in the Lin et al. experiment BrdU was given via intraperitoneal (i.p.) injection 2 hours prior to necropsy.

The role of E_2 as stimulator of endometrial cell proliferation, *in vivo* (Deligdisch, 2000) as well as *in vitro* (Pierro, et al., 2001), is well known; yet the molecular mechanism by which it may regulate endometrial growth is not clearly defined. Rider et al. (1998) proposed that E_2 might be essential for the synthesis of receptors

and growth factors, which are needed for cell cycle regulation. Cyclin B1 is a major regulator of the cell cycle machinery. In this study, no difference in cyclin B1 mRNA expression of lesions was observed between the vehicle and E_2 treated animals regardless of treatment period. Higher cyclin B1 mRNA expression in women with endometriosis was observed in ectopic than eutopic endometrium while no difference between ectopic tissue from sex-hormone dependent proliferative phase and secretory phases was observed. At the same time, cyclin B1 expression was correlated with E_2 serum levels (Tang, et al., 2009). It should be noted that the location of lesions and the stage of endometriosis were not distinguished in the aforementioned study making the E_2 results hard to correlate. However, since eutopic expression was not analyzed in the current study, ectopic and eutopic differences in cyclin B1 expression cannot be ruled out in the current mouse model.

Transforming growth factor β1 (TGF-β1) is a cytokine that can regulate cellular proliferation. Pizzo et al. (2002) showed that TGF-β1 protein level from 26 women with endometriosis was elevated in the peritoneal fluid (PF) and serum as compared with control patients: five women affected by non-immunologic infertility, diagnosed by explorative laparoscopy. In the current study, while the serum and PF expressions were not determined, the mouse lesion TGF-β1 mRNA expression showed no difference between the vehicle and E_2 treated mice regardless of the length of treatment. Interestingly, E_2 supplementation failed to counteract the absence of TGF-β1 in a heterologous mouse model of endometriosis using ovx immunedeficient TGF-β1 knockouts, where a significant reduction in size and weight of endometriotic

lesions was observed (Hull, et al., 2012) implicating sex-hormone independent function of TGF-β1 that may not be related to proliferation. Indeed, as a potent cytokine, TGF-β1 can direct immunoinflmmatory responses via modulation of natural killer cells, lymphocytes, and macrophages (Letterio and Roberts, 1998, Wahl, et al., 2006), which have been implicated in the pathogenesis of the chronic pelvic disorder (section 4.1.4). Additional studies using immunocompotenet mice such as C57BL/6 with analysis at the protein level and localization of expression via IHC may help with understanding immunoinflmmatory role of TGF-β1 in experimental endometriosis. In summary, the three methods utilized to measure proliferation, no difference between the vehicle and E_2 treated mouse endometriotic lesions was observed. Taken together, E_2 mediated proliferation did not contribute to the difference in mouse endometriotic lesion area observed in the current syngeneic transplantation model of endometriosis.

4.1.3 Total Apoptosis Was Unchanged in Mouse Edometriotic Lesions Regardless of E_2 Treatment

Ectopic dissemination of endometrial cells may give rise to endometriotic lesions, but retrograde menstruation occurs in the majority of women. For reasons still not fully elucidated, misplaced endometrial cells in some women survive to develop into endometriotic lesions. This may be caused by abnormalities in apoptosis, which plays a critical role in maintaining tissue homeostasis by eliminating excess, dysfunctional, or misplaced cells without inducing an immune or inflammatory response. When assessing a sex steroid-regulated endometrial event, such as apopto-

sis, consistency in hormonal concentration is a major factor for maintaining homogeneity between groups. Therefore, using ovx mice with controlled E_2 concentration and the mouse transplantation model, several parameters were measured to assess E_2 induced modulations of apoptosis in lesions at different time intervals post-transplantation.

Immunohistochemistry and Terminal deoxynucleotidyl transferase dUTP nick end labeling (Tunel) was used to measure total apoptosis in endometriotic implants. This analysis of DNA fragmentation revealed no difference in total Tunel stained cells in the lesions from C57BL/6 and FVB/N mouse strains regardless of E_2 supplementation or time. These results suggest that in the mouse endometriotic lesions, regulation of total apoptosis may not be entirely E_2 dependent. Similarly, analysis of ectopic endometrium in patients with endometriosis showed no menstrual cycle induced changes in the Tunel+ cell frequency between the sex-hormone dependent proliferative phase and the secretory phase (de Paula, et al., 2012). It should be noted that Tunel analysis is limited since DNA fragmentation occurs in either apoptosis or necrosis (Gold, et al., 1994). Morphologically, in contrast to necrotic cells, apoptotic cells exhibit blebbing, cell shrinkage, nuclear chromatin condensation, and compactness of cytoplasmic organelles (Potten, 1987) allowing *in situ* distinction using electron microscopy (Harada, et al., 1996). Furthermore, careful examination via light microscopy allows identification of cell types undergoing apoptosis.

Comprehensive analysis of Tunel using IHC was impractical for the large number of samples present in this study. Therefore, a second method to measure total apoptosis, detection of Annexin V (AV) using flow cytometry, was utilized. The ability to use multiple markers on a single cell in flow cytometry allowed separation of AV+ apoptotic and necrotic cell using DAPI labeling (Willingham, 1999) as well as differentiation between cell types present in the endometriotic lesions (Section 4.1.4). Looking specifically at DAPI- AV+ cells, identical to the Tunel results, no E_2 and time related differences in total AV+ cells was observed. Programmed cell death is highly regulated by a variety of signaling molecules with two major initiation pathways: the intrinsic mitochondrial pathway and the extrinsic death-receptor signaling pathway (Chen and Wang, 2002), both of which have been implicated in development and persistence of the pelvic disorder.

In the intrinsic mitochondrial pathway, B-cell lymphoma 2 (Bcl-2) protein, the founding member of the Bcl-2 family of apoptosis modulators, blocks cell death by inhibiting Cytochrome c release from the mitochondria (Cory and Adams, 2002). In the current study, Bcl-2 mRNA levels in the mouse lesions increased over time regardless of E_2 treatment, but the protein levels remained constant. The difference between Bcl-2 mRNA and protein can be explained by posttranslational modification (Breitschopf, et al., 2000). However, more interesting was the lack of E_2 regulation of Bcl-2. Sex-hormone dependent cyclical expression of Bcl-2 protein using IHC has been reported in eutopic endometrium from women with and without endometriosis using IHC and Western Blotting (Otsuki, et al., 1994, Watanabe, et al., 1997).

Evidently, in ectopic implants, Bcl-2 expression is extremely sensitive to cell type (glandular or luminal epithelial cells and stromal cells), morphology (cyst and non-cyst), and location (ovarian and peritoneal), making the numerous studies with contradictory results hard to interpret (Critchley, et al., 1999, Nasu, et al., 2011, Nezhat, et al., 2002, Nezhat and Kalir, 2002). Accordingly, the lack of Bcl-2 sex-hormone regulation observed in the mouse model may have transpired due to the inclusion, in the mRNA and protein analysis, of whole lesions, including cysts and non-cysts, which were all situated at one location: the mouse peritoneum.

The extrinsic pathway is initiated by death receptors such as Fas/CD95 and has been shown to induce apoptosis in T lymphocytes, macrophages, and epithelial cells (Richardson, et al., 1994, Sayama, et al., 1994). Fas ligand (FasL) showed higher expression in ectopic than eutopic endometrial tissue from women with endometriosis than women without endemetriosis, independent of menstrual cycle stage (Garcia-Velasco, et al., 2002) while Fas expression was independent of estrogen levels and constant throughout the menstrual cycle in eutopic and ectopic endometrium (Harada, et al., 1996). Apoptotic signal by Fas-FasL interaction is a vital pathway for immune maintenance of homeostasis (Li-Weber and Krammer, 2003). Indeed, it has been postulated that increased FasL production by misplaced endometrial tissue may induce apoptosis in Fas expressing immune cells recruited to eliminate them. In the current study, contrary to published eutopic endometrium human results (Yamashita, et al., 1999), mouse endometriotic lesions showed no E_2 induced difference in Fas and FasL mRNA expression (data not shown). Therefore,

since extrinsic and intrinsic pathways are not distinct, and the activation of one usually involves the other (Nachmias, et al., 2004), the possible E_2 modulation of apoptosis was further analyzed by looking at their convergence.

BH3 interacting-domain death agonist (Bid) is a pro-apoptotic protein, which connects the two apoptosis pathways via death-receptor initiated caspase-8 activation, counteracting the anti-apoptotic protection of Bcl-2 at the mitochondrial membrane and inducing Cytochrome C and second mitochondria-derived activator of caspase (Smac) release (Gross, et al., 1999). Although the Bid pathway has not been extensively analyzed in endometriosis, it may be interesting due to its prevalence in lymphocytes and macrophages (Krammer, 2000, Strasser, et al., 1995). However, in the current model, Bid mRNA expression did not vary between the E_2 and vehicle treated mice. No difference in Smac (also known as Diablo) mRNA was seen regardless of treatment and time. Smac mRNA decreased in the uterus of ovx rats supplemented with E_2 as compared with vehicle (Leblanc, et al., 2003) implicating a sex hormone dependent promotion of survival in the reproductive organ. Furthermore, Leblanc et al. showed using Western Blotting and IHC that the protein levels of Smac in the uterus of normal cycling rats was similar at metestrus, diestrus and proestrus but significantly reduced at the sex-hormone dependent estrus and localized mainly in epithelial cells. Although eutopic Smac expression was not analyzed in the current study, inhibition of the pro-apoptotic Smac by E_2 is an interesting observation and additional studies at the protein level are necessary to correlate this finding in mouse lesions.

The role of Smac, as a mitochondrial protein, is to allow Cytochrome c dependent activation of apoptosis by eliminating the inhibition of caspases via the inhibitors of apoptosis proteins (IAPs), which protect cells from apoptosis by inhibiting or degrading effector caspase 3 and 7 (Roy, et al., 1997, Vucic, et al., 2002). Baculoviral inhibitor of apoptosis repeat-containing (Birc) 1a, also known as neuronal apoptosis inhibitory protein (Naip) 1, was one IAP that showed E_2 dependent regulation at the mRNA level in the mouse endometriotic lesions. Birc1a has not been studied in regards to the pelvic disorder and here was the first analysis of its possible E_2 regulation in an experimental model of endometriosis. Two groups have thus far demonstrated E_2 dependent Birc1a expression in the mouse uterus, but as with many apoptosis modulators, Birc1a does undergo posttranslational modification (Wall, et al., 2013, Yin, et al., 2008). Therefore, two different Birc1a antibodies were tested using Western Blotting, unfortunately both were non-specific and yielded multiple bands (data not shown). Protein expression analysis would be necessary to confirm E_2 regulation and validate Birc1a as an important IAP in the survival of ectopic implants.

The decision whether or not cells undergo apoptosis is determined by opposing forces of pro- and anti-apoptotic effectors leading to a highly controlled process of cellular disassembly that occurs in response to internal or external signals. Although in the current study no E_2 dependent difference in total apoptosis was observed, there might be sex-hormone dependent modulation of specific cells in the mouse endometriotic lesions. This idea was further analyzed using flow cytometry.

4.1.4 Alterations of Cell Composition and Apoptosis Frequency in Mouse Lesions According to Time and Treatment

Endometriosis is defined by the presence of viable endometrial glandular and stromal cells outside the uterine cavity. The human endometrium is comprised of luminal and glandular epithelial cells plus endometrial stromal cells consisting of fibroblasts, vascular smooth muscle cells, endothelial cells, and immune cells. CD45+ immune cells (leukocytes) were separated from non-immune (non-leukocytes) cells in the mouse endometriotic lesions using multi-color flow cytometry, where the frequency and the incidence of apoptosis were determined.

Non-Immune Cell Composition Unaffected by E_2 Treatment in Mouse Endometriotic Lesion

Non-immune cells play an essential role in the pathogenesis of endometriosis, as they are involved in the adhesion, structural organization, establishing blood supply, and modulation of the immune system at the ectopic site (Jimenez-Heffernan, et al., 2004, Nair, et al., 2008, Shi, et al., 2011, Witowski, et al., 2009). CD45- non-immune cells consist of epithelial cells, fibroblasts, vascular smooth muscle cells, and endothelial cells.

The frequency of total CD45- cells increased in mouse endometriotic lesions at d28 post transplantation regardless of E_2 treatment. Furthermore, looking at apoptosis, at d14 post transplantation, when the first significant difference in lesion area was observed, higher percentage of CD45- cells were AV+ in the E_2 treated animals than

the vehicle treated animals. Estradiol and ER1 and 2 signaling may be important in endometriosis-like tissue organization inducing fibrosis and smooth muscle metaplasia as well as glandular structures with polarized epithelial cell-lined lumens (van Kaam, et al., 2008). This was demonstrated using ER 1 and 2 knockout mice where lesion size, cyst volume, and using IHC, smooth muscle cells arrangement around the glandular structures was hampered in the absence of the receptors (Burns, et al., 2012). In the current study, the increased apoptosis of non-immune cells in E_2 treated mice was accompanied by the formation of cysts and may be due to lesion cell organization. At d28, the frequency of apoptosis between the two treatment groups was similar, but significantly lower than the d14 E_2 treated lesions, suggesting that 28 days after transplantation the E_2 induced structural organization may have subsided. Indeed, similar to sex hormone dependent remodeling in the uterus, analysis of periods beyond 28 days may be fruitful in determining the possible cyclical E_2 mediated dynamics occurring in mouse endometriotic lesions. However, for the purpose of this study, long-term hormone induced endometriotic lesion dynamics were analyzed, from the morphological perspective, in normal cycling non-human primates and is discussed in section 4.2.

Fluctuation of Immune Cell Composition and Apoptosis Frequency in Mouse Endometriotic Lesions According to E_2 Treatment and Time

The resident immune cells in the glands and stromal compartment of endometriotic lesions may contribute to the increased inflammatory activity, impaired immune surveillance (Christodoulakos, et al., 2007), and hindered clearance of the misplaced

tissue (Kyama, et al., 2003). Furthermore, using IHC increased number of immune cells, including macrophages (Tran, et al., 2009), dendritic cells (Schulke, et al., 2009), natural killer and T cells, have been observed in ectopic in comparison to eutopic endometrium from women with endometriosis (Berbic and Fraser, 2011). Accordingly, it is important to distinguish cell types as well as origin (see next section) in the study of lesions. While endometriosis research has often been conducted on signaling molecules and the cells present in the PF (Koninckx, et al., 1998), in the current study we focused on the immune cells within the mouse endometriotic lesions using multicolor flow cytometry.

It has been postulated that CD45+ immune cells play crucial roles in either rejecting or accepting implants, directly via cytotoxic/phagocytic capabilities or indirectly by secreting various cytokines that control cell proliferation, apoptosis, inflammation, and angiogenesis in the endometrium (Osuga, et al., 2011). They form a substantial proportion of human eutopic endometrium stromal compartment accounting for approximately 7% in proliferative endometrium and more than 30% in early pregnancy (Kayisli, et al., 2004). Interestingly, in the current study the mouse endometriotic lesions had five times higher frequency of immune cells than the mouse uterus (20.5%:4.3%), confirming studies in patients with endometriosis that showed high density of immune cells in ectopic implants (Jones, et al., 1998, Paul Dmowski and Braun, 2004). However, the frequency of immune cells remained constant in both the mouse lesions and uterus regardless of E_2 supplementation or time. Looking at apoptosis, the frequency of CD45+ cells that were AV+ in the lesions de-

creased over time independent of E_2 treatment while it was unchanged in the mouse uterus. This decrease in immune cell apoptosis of already established lesions over time might promote further lesion progression by increasing inflammation at the ectopic site.

In the mouse lesions from the vehicle treated animals, the frequency of natural killer (NK) cells increased between d4, 7, and 14, then decreased at d28. This result correlated with the reduction of lesion area observed between d4 and d28 vehicle treated mice (section 4.1.1). The decrease in NK cell frequency at d28 in comparison to d14 was also seen in the E_2 treated animals, but not the decrease in lesion area. Natural killer cells, as the first-line defense against misplaced tissues, were cytotoxic towards ectopic endometrial cells *ex vivo* using chromium release assay (Oosterlynck, et al., 1991). Using the same readout, impaired cytotoxicity of peripheral NK cells has been reported in patients with endometriosis (Maeda, et al., 2012). Additionally, E_2 can suppress cytotoxic function of peripheral NK cells *in vivo* as determined by the chromium assay (Garzetti, et al., 1993).

It should be noted that a specific subset of NK cells are found only in the uterus. Uterine NK (uNK) cells inherently have lower cytotoxic activity than peripheral NK cells (Moffett-King, 2002). Since in the current study subsets of NK cells were not distinguished, it remains to be determined whether uNK cells from the transplanted uterus biopsies or peripheral NK cells that infiltrated the implants are responsible for the NK cell frequency fluctuation. Interestingly, in the mouse uterus, no change

in the frequency of NK cells was observed while in the AV+ NK cells of the uterus, E_2 induced an increase at d14 and then a decrease at d28 in comparison to vehicle treated mice from the corresponding time points. In the lesions, only time dependent, not sex hormone dependent, decrease in NK cell apoptosis between d14 and d28 groups was observed.

Numerous studies have been conducted on the signaling, frequency, and viability of peritoneal lymphocytes in endometriosis with excellent review articles available (Braun and Dmowski, 1998, Khan, et al., 2008, Lebovic, et al., 2001, Wu and Ho, 2003), but little attention has been paid to the resident lymphocytes of endometriotic lesions. T lymphocytes, as determined by IHC, are one of the major immune cell subpopulations in human endometriotic lesions (Oosterlynck, et al., 1993). Similarly, there was increased staining for lymphocytes in both eutopic and ectopic endometrium of women with endometriosis in comparison to eutopic endometrium of women without endometriosis. In the current study two classical subpopulations of T lymphocytes residing in the mouse endometriotic lesions were analyzed: helper T cells (CD4+) and cytotoxic T cells (CD8+). Furthermore, T cell activation marker CD69 was utilized to determine E_2/time-mediated differences in the activation state of T lymphocytes. Additionally, the frequency of apoptosis was determined using the AV antibody.

CD4+ Helper T cells do not have cytotoxic capabilities, but rather transmit signals from antigen presenting cells (APCs) and CD8+ T cells to propagate additional im-

mune response (Kindt, et al., 2007). Patients with endometriosis showed high frequency of helper T cells in the PF (Hill, et al., 1988), with their activation being suppressed (Gallinelli, et al., 2004) along with impairment in function in comparison with women without endometriosis (Martinez-Roman, et al., 1997). Importantly, research regarding lymphocytes in endometriosis has mainly been conducted on the PF and not endometriotic lesions. Here, for the first time, we look at sex hormone and time-induced lymphocyte changes in the mouse lesions. The frequency of helper T cells increased over time regardless of treatment, but at d28 there was a significant E_2 dependent reduction in comparison to the vehicle treated mice. Additionally, increased activation of helper T cells was observed over time, independent of E_2 treatment. Looking at the frequency of apoptosis, upon E_2 treatment, a decrease in AV+ helper T cells from d28 lesions was seen in comparison to d14, while no difference in apoptosis rate of CD69+ cells was observed.

In the current study, total activated helper T cells were analyzed in the mouse lesions. However, activated CD4+ T cells, as important facilitators of immune function, differentiate into subtypes Th1 and Th2, with cell-mediated immunity being a Th1 phenomenon and humoral immunity being a Th2 phenomenon (Harrington, et al., 2005, Mosmann, et al., 1986). Indeed, it is crucial for the body to maintain tight regulation of Th1/Th2 ratio in the peritoneal environment, to control the cytotoxic and phagocytic activity of the roaming immune cells. Although Th1 cells are reported to be the predominant helper T cell population in the PF of women with endometriosis (Ho, et al., 1997a), upregulation of the minority Th2 cell cytokines, in-

terleukin (IL) 4 and 10, in the PF of women with endometriosis has been reported (Harada, et al., 2001, Ho, et al., 1997b, Hsu, et al., 1997). Cell-mediated immunity, including T lymphocyte-mediated cytotoxicity is activated or suppressed by cytokines produced by Th1 and Th2 cells. Furthermore, IL4 and 10 decreased CD8+ T cell cytotoxicity *in vivo* (Kyama, et al., 2003). Therefore, an increase in their concentrations in the PF may promote initial implantation of endometrial fragments (Podgaec, et al., 2007). Recently, helper T cell interactions in endometriosis have become more complicated with the discovery of two additional subsets: Th17 and regulatory T (Treg) cells, which have been detected in the PF of women with and without endometriosis (Hirata, et al., 2008, Olkowska-Truchanowicz, et al., 2013). Indeed, Th17 was detected in endometriotic cyst fluid, from patients with high PF concentration of estrogen synthetase (aromatase), indirectly associating Th17 cells with high estradiol levels (Velasco, et al., 2010). Treg transcription factor was detected in human endometriotic lesions (Budiu, et al., 2009). It remains to be elucidated the full complex role subsets of CD4+ T cells play in the immune system in general, while additional studies, like the ones conducted here, may facilitate better understanding of their role in the chronic pelvic disorder.

Like NK cells, cytotoxic T cells (CD8+) can lyse and destroy specific target cells (Kindt, et al., 2007). In patients with endometriosis, a decrease in the PF frequency of activated cytotoxic T cells has been shown (Gallinelli, et al., 2004) while the cytotoxicity of T lymphocytes that manage to reach autologous endometrial cells was hampered (Steele, et al., 1984). Classical studies of PF from women with endometri-

osis showed a decrease in CD4+ to CD8+ T cell ratios as compared with women without endometriosis (Oosterlynck, et al., 1994). In the current analysis of the mouse lesions, on average no change in the CD4+ to CD8+ T cell ratio as well as their activation was observed, regardless of time or treatment. Overall, the frequency, activation, and apoptosis profile of cytotoxic T cells was similar to helper T cells in the mouse endometriotic lesions. The role that E_2 plays in relations to T lymphocytes is not limited to expression and cytotoxicity, but also their interaction with APCs may be regulated by the sex hormone (Straub, 2007).

The principal functions of B cells, as major effector cell of the adaptive immune system and the humoral immune response, are to make antibodies against antigens, be APCs, and consequently develop into memory B cells (Abbas, et al., 2012). In the current study E_2 induced a significant decrease in mouse endometriotic lesions' B cell frequency and apoptosis at d28 in comparison to d28 vehicle and d14 E_2 treated groups. Endometriosis is a menstrual cycle dependent disease only manifested between menarche and menopause. Therefore, direct or indirect regulation of B cells by cycling E_2 concentrations may be an important player in allowing or facilitating possible ectopic implant related autoimmune inflammation. Cumulatively, the various immunoinflammatory anomalies described in endometriosis has led some investigators to argue that it may be a chronic autoimmune disorder (Giudice and Kao, 2004, Matarese, et al., 2003, Nothnick, 2001). Similar to endometriosis, the sex hormone's affect on some autoimmune disorders in women are so profound that E_2 promoted disorders only appear during the reproductive years (i.e. lupus erythema-

tosus) while E_2 inhibited disorders manifest post-menopause (i.e. Sjögren's syndrome). Indeed, in some autoimmune disorders, E_2 promoted progression only when autoreactive B cells were present, while it inhibited the disease in their absence (Straub, 2007). Furthermore, E_2 has been shown to inhibit T cell regulation of B cells (Paavonen, et al., 1981). Characterization of endometriosis as an autoimmune disorder remains controversial, but the overwhelming evidence of sex hormone dependence along with lymphocyte interplay makes a compelling argument.

Macrophages, the primary peritoneal mononuclear phagocytes, are said to infiltrate ectopic endometriotic implants. Indeed, as determined by IHC, they are the major immune cell subpopulation found in human endometriotic lesions (Oosterlynck, et al., 1993). Like B cells, they function as APCs while also possessing cytotoxic and phagocytic capabilities. In the peritoneum, these versatile immune cells are also the major source of cytokines involved in regulating inflammation (Topley, et al., 1996). In the current study, the frequency of macrophages decreased over time regardless of treatment in the mouse endometriotic lesions. In 14 and 28-day treatment periods, corresponding to the lesions area increase, E_2 treatment induced additional drop in macrophage frequency in comparison to vehicle treated mice. It should be noted that macrophages reside in endometrial stroma plus glands and the lesions from d14 and d28 of E_2 treated animals possessed smaller stromal compartment than d4 and d7, as determined microscopically by IHC. Additionally, increase in the appearance of cysts like glands that contained large amounts of unspecifically

stained dead cellular residue was observed hinting at possible increase in macrophage death.

Indirect analysis of apoptosis in peritoneal (flow cytometry) and lesion (IHC) macrophages from women with endometriosis showed high expression of anti-apoptotic Bcl-2 protein in contrast to PF and eutopic endometrium of women without endometriosis (McLaren, et al., 1997). In the current study, apoptosis of resident macrophage in mouse endometriotic lesions was measured directly using AV staining. Interestingly, E_2 induced an increase in apoptosis at d14 in comparison to d14 vehicle and d28 E_2 treated animals. Justifiably, estradiol-mediated lesion area increase subsided at d14 in the current mouse model as no significant difference between d14 and d28 E_2 treated mice was observed (section 4.1). Indeed, in the peritoneal environment, interactions between misplaced endometrial cells and macrophages are mediated by growth factors, cytokines, and chemokines that paradoxically lead to their survival (Lebovic, et al., 2001). Furthermore, Gebel et al. (1998), in an *ex vivo* analysis using ELISA, showed lower spontaneous apoptosis in ectopic than eutopic endometrium. Perhaps, inside endometriotic tissue, the cellular interactions differ and endometriotic cells may induce macrophage apoptosis while escaping macrophage-mediated cytotoxicity resulting in lesion persistence and growth.

A Complex Pattern of Cellular Composition and Apoptosis Based on E_2 Treatment and Time in Mouse Endometriotic Lesions Exists

In summary, the mechanisms underlying the onset, progression, and maintenance of endometriotic implants may include an abnormal inflammatory response and persistent immune cell recruitment. Indeed, in the current syngeneic transplantation mouse model of endometriosis, cell composition and apoptosis frequency of endometriotic lesions fluctuated based on time and E_2 treatment (Table 4).

	E_2 Induced Change		Time Induced Change	
Cell Type	**Composition**	**Apoptosis**	**Composition**	**Apoptosis**
Non-immune Cells (CD45-)	0	+	+	-
Immune Cells (CD45+)	0	0	0	-
NK Cells	0	0	+ & -	-
Helper T Cells	-	-	+	0
Cytotoxic T Cells	-	0	+	-
B Lymphocytes	-	-	-	0
Macrophages	-	+ & -	-	0
Dendritic Cells	0	-	+ & -	-
Granulocytes	0	n/m	0	n/m

Table 4: Summary findings of E_2 and time modulated changes in cell composition and apoptosis in mouse endometriotic lesions

Frequency and apoptosis (Annexin V) profile of different cells residing in mouse endometriotic lesions was determined using flow cytometry. The two parameters used were time and E_2 treatment. Legend: 0 means no change, + means increase, - means decrease, + & - means increase and decrease, n/m means not measured

As discussed in section 4.1, lesions with different morphology were observed in the current mouse study. It has been postulated that differing immune cell populations exists depending on type and location of lesions (Donnez et al., 1998). For example, increase in the frequency of immune cells was observed in red human endometriotic lesions as compared to black and white lesions (Bullimore, 2003). Specifically,

red lesions had the largest frequency of macrophages in comparison with black and white lesions (Ishimaru, et al., 2004, Khan, et al., 2004, Zeller, et al., 1987). These findings expose a limitation of the current study since the mouse lesions with different morphologies were not distinguished in the flow cytometry readout.

Over the last decade, the potential role of the immune system in the pathophysiology of endometriosis has increasingly gained attention and intense research efforts have ensued. The immune system seems to play a paradoxical role in endometriosis, while many of its effects might be expected to facilitate control of the disease, by secretion of inflammatory and mitogenic proteins, immune cells in collaboration with ectopic endometrial tissue contribute to a cascade of events that result in the establishment and persistence of lesions (Berbic and Fraser, 2011, Lebovic, et al., 2001). Furthermore, the ever-changing composition and signaling characteristics of endometriotic and peritoneal immune cells, likely due to changes in sex hormone levels, are features that may enhance the symptoms of the chronic pelvic disorder.

4.1.5 Compromised Estrogen Receptor Signaling Decreased Mouse Endometriotic Lesion Inflammation

Novel Syngeneic Transplantation Mouse Model Allowed Noninvasive Monitoring of Lesions

Here I am reporting the use of uterus fragments from mice ubiquitously expressing firefly luciferase in a syngeneic transplantation mouse model, where i.p. injection of the substrate luciferin induced a quantifiable luminescence signal. Syngeneic lu-

ciferase expressing uterus punch biopsies were transplanted into identical nonluminescent (wild-type) recipient mice. This allowed, for the first time, monitoring of implants from syngeneic donors inside syngeneic acceptor mice, using noninvasive luminescence imaging.

The advantages of using luciferase expressing tissue in the syngeneic transplantation mouse model, similar to most homologous transplantation mouse models, was the high take rates, easy recovery of implants, and the opportunity to examine large groups of identical animals with a well-characterized murine genome (Grummer, 2006). Additionally, the introduction of luminescent implants facilitated noninvasive imaging of progression and regression during treatment. Previously, using non-syngeneic donors and acceptors, Becker et al. (2006) showed that transabdominal luminescence compared well with the location of the endometriotic lesions and lesion size correlated with the intensity of luminescence. Furthermore, the firefly luciferase protein, in contrast to other reporter proteins, has a rapid turnover with a short half-life of 3 hours (Thompson, et al., 1991) with exceptionally high signal-to-noise ratio (Kaijzel, et al., 2007) making it ideal for kinetic and dynamic analysis. Additionally, luciferase expression is permanent in cells derived from these mice (syngeneic FVB/N-Tg (B-Actin-Luc)-Xen mice), allowing prolonged noninvasive monitoring of endometriotic implants. Major limitation of this model was the possible blockage of lesions by fat or adhesions, inhibiting exposure to the luciferin substrate and the activation of luminescence. To reduce this possibility, mice were ad-

ministered luciferin prior to anesthesia to allow dispersion in the peritoneal cavity via their natural hyperactivity.

The advantage of using this model in the current study was that changes in implant cell composition could be traced to the luminescent transplants or the nonluminescent host cells, depending on the signal intensity detected at each time point. Initial experiments conducted within the Transgenic and *in vivo* Pharmacology (TASIP) department at Bayer Healthcare used normal cycling mice with two treatment groups: SERD (selective estrogen receptor destabilizer) and vehicle. SERD is a pure estrogen antagonist that causes efficient disruption of ER signaling (Hoffmann, et al., 2004). In the current study, the same strain of mice was ovariectomized to control the estrous cycle and the sex hormone concentration; they were then supplemented with either E_2 or vehicle. The results of both experiments are compared and discussed in the following paragraphs.

Compromised Estrogen Receptor Signaling Led to Decreased Luminescence in Mouse Endometriotic Lesions

Sex hormone dependent interactions among peritoneal and endometriotic immune and non-immune cells are suggested to promote abnormal mitogenic, angiogenic, and inflammatory processes implicated in the pathogenesis of endometriosis (Osuga, et al., 1999, Yoshino, et al., 2003). To this extent, the current luminescence mouse model was used to detect E_2 and time modulated changes in concentrations of peritoneal and endometrial cells in the mouse lesions.

The lesions from mice with compromised E_2 levels (vehicle treated ovx mice) and ones with disrupted ER (SERD treated normal cycling mice), showed a reduction in luminescence over time suggesting that inhibition of E_2 signaling leads to reduction in the concentration of originally transplanted cells in the mouse endometriotic lesions. Furthermore, in normal cycling mice, only at days 28, 35, and 42 post-transplantation and not days 14 and 21, SERD did induce a significant reduction in lesion luminescence in comparison to vehicle treated animals from corresponding time points. In contrast, the ovx mice showed significant vehicle induced luminescence reduction at day 14 post-transplantation in comparison to d14 E_2 treated animals while at d28 both vehicle and E_2 treated lesions showed reduced luminescence in comparison to earlier time points of the same treatment regiments respectively. The ovx experiment did not include d35 and d42 time points. Importantly, it cannot be ruled out that SERD and E_2 may interact with additional receptor proteins other than ER 1 and 2. Therefore, SERD's affect as an ER inhibitor may not fully equal the ovariectomy induced E_2 level reduction in mice. Nevertheless, the comparison of the two studies implicates ER signaling influencing concentration of cells within mouse endometriotic lesions.

To correlate luminescence findings obtained by *in vivo* imaging with the two-dimensional lesion area, mice were sacrificed at the end of the experiment (days 14 and 28 in the ovx study) and lesion area was measured macroscopically (section 4.1.1). Analysis of ovx mouse lesion area and luminescence over time, in the pres-

ence or absence of ER signaling, hinted at sex hormone receptor dependence in the maintenance of lesion area. Indeed, in the vehicle treated mice at d14 and 28 with compromised ER signaling, there was a significant decrease in lesion area in conjunction to a significant decrease in luminescence. There are three plausible explanations for this reduction in luminescence via disruption of the ER pathway: 1) more cells from the original transplant underwent apoptosis due to increased apoptotic signaling or competent cytotoxic immune cells, 2) cells from the host have integrated into the transplants, diluting the luminescence signal, or 3) the phagocytic cells from the host have started to engulf misplaced tissue, again diluting the signal.

No difference in total apoptosis was observed in the lesions from ovx mouse regardless of time or treatment (section 4.1.3). Interestingly however, there was E_2 and time related fluctuations in the apoptosis profile of cells present in the mouse endometriotic lesions (section 4.1.4). Specifically, compromised ER signaling decreased apoptosis frequency of non-immune cells in mouse lesions at d14 while it increased apoptosis in T and B lymphocytes at d28. Additionally, in the absence of the sex hormone signal, fluctuation of macrophage apoptosis over time and increased dendritic cell (DC) apoptosis at d28 was observed. Review of cell composition analysis in lesions showed that reduced ER signaling primarily increased immune cell frequency while it had no affect on non-immune cell frequency. This change in cell composition happened while no difference in proliferation of immune cells and non-immune cells including epithelial cells was observed (section 4.1.3). Although it may seem counter intuitive, these results suggest that the increased le-

sion ability, in the absence of intact E_2 induced ER signaling, to promote apoptosis of immune cells may explain the decrease in lesion area and luminescence seen in the vehicle treated animals.

As discussed in the previous section, the immune system seems to play a paradoxical role in endometriosis, while apoptosis of immune cells is expected to help survival of endometriotic implants, the sex hormone dependent survival of immune cells in the current model, via collaboration with ectopic endometrial tissue, may promote lesion inflammation and exasperate endometriotic symptoms. Therefore, the dilution of luminescence signal in the absence of E_2 may be due to increase in apoptosis of lesion's resident immune cells, which in the absence of proliferation (section 4.1.2) and infiltration, leads to decreased inflammation, explaining the reduced lesion area seen in the vehicle treated animals. Furthermore, I propose that in the syngeneic transplantation mouse model utilized in the current study, apoptosis in resident lesion immune cells plus reduction in inflammation, and not infiltration of non-luminescent peritoneal cells, was responsible for the reduction of luminescence and consequently the lesion area in the vehicle treated animals.

4.2 Lesion Kinetics in Non-human Primate Model of Endometriosis

The severity of the symptoms of endometriosis has not always correlated with the anatomic severity of the disease (Abbott, et al., 2003, Crosignani, et al., 1996, Garry,

et al., 2000). This lack of correlation may be due, in part, to variations in the activity of the endometriotic lesions present at different episodes of the disease. Indeed, careful macroscopic analysis of the mouse endometriotic lesions over time showed dynamic changes in lesion morphology. Additionally, studies in humans and non-human primates showed that endometriosis is a dynamic disorder, which includes spontaneous lesion progression and regression, the development of new lesions, and changes in lesion appearance over time. Lesion turnover is a consequence of these dynamics and was analyzed retrospectively by studying videos and surgical notes from a more relevant non-human primate experiment conducted at Michigan State University in Professor Fazleabas' laboratory.

4.2.1 Lesion Turnover in Baboons Inoculated with Menstrual Tissue

Experimental endometriosis was induced by mimicking retrograde menstruation using the well-established baboon model of endometriosis (Braundmeier and Fazleabas, 2009). The experiments were performed in a controlled setting where all animals were normally cycling and negative for endometriosis and adhesions prior to inoculation. Upon induction of endometriosis, the lesion color, location, and turn-over were assessed at precise and consistent time points. This enabled, for the first time, kinetic analysis of how quickly lesions can turnover (not just that they change color). Additionally, once lesions were found, they were followed at subsequent lap-aroscopies to determine their progression.

A high number of lesions persisted for up to 15 months post-inoculation. At each laparoscopy on average 9 (±5) lesions per animal was observed. These data compared favorably with a human study that focused on the number of superficial endometrial implants in women with endometriosis, in which an average of 10 implants per patient (43 total) was observed (Muzii, et al., 2000). Similar to the human disease, endometriotic lesions in the baboon were found in the peritoneum, specifically in the pouch of Douglas, bladder and the perimetrium (Hastings and Fazleabas, 2006). Interestingly, in contrast to the human disease, no ovarian cysts (endometrioma) or deeply infiltrating rectovaginal lesions were detected. This absence could be related to the early termination point of the baboon experiment (15 months), whereas women can suffer with endometriosis for 8–12 years even before diagnosis (Hadfield, et al., 1996). Conversely, this could be explained by pathophysiological differences in the aetiology of endometriosis: it has been proposed that the development of the three endometrial implants; peritoneal, ovarian cysts and deep infiltrating lesions, can be caused by different mechanisms (Brosens, 2004, Garry, 2004). The baboon model primarily reflects peritoneal disease.

The lesions were tracked at each laparoscopy and the colors and locations were recorded at precise time points. Many lesions, first seen during initial laparoscopies, continued to be visible until 15-month necropsy. This could be due to the persistence of the same lesion, however the appearance of a new lesion at the same location cannot be excluded. The majority of the lesions found at the time of the second inoculation were red lesions. These early red lesions frequently transformed into

lesions of different colors. Indeed, thereafter there was a heterogeneous mixture of lesions characterized by different colors, consistent with the dynamic character of the pathology. Most of the lesions observed in this model were black and blue. Black lesions most often remained black, or turned blue, white or regressed. Blue lesions had a slower turnover cycle and often remained blue at subsequent laparoscopies. Powder burn, blister and multicolored lesions are postulated to have the shortest turnover cycle or to represent an intermediate appearance, as these lesions were present in significantly lower numbers than others. White lesions were evident at the later laparoscopies and often disappeared or became scar tissue, indicating that they may occur at late stages of the lesion life cycle.

These results confirm in a more precise manner a previous finding where a high number of red lesions were observed immediately after inoculation and, over time, decreased in parallel with an increase in white lesions (D'Hooghe, et al., 1995). In the current study, detailed monitoring of each lesion type also allowed for continuous observation of powder burn lesions and blisters that seem to be highly active due to their fast turnover. These previously neglected lesion types require further attention, as they are potentially hyperactive endometriotic tissues, which often get overlooked during routine diagnostic laparoscopies.

Changes in lesion morphology over time have been observed in women with endometriosis. Jansen and Russell (1986) documented changes in lesion color between non-pigmented lesions and pigmented lesions at 6 to 24 months after initial laparo-

scopies in patients with endometriosis. There is evidence that lesions characterized by different colors possess different biochemical activity (Vernon, et al., 1986). Immunohistochemical staining for PCNA demonstrated that red lesions possess a higher proliferation index compared to black lesions and continue to proliferate, more so than white lesions (Fujishita, et al., 1999). Additionally the number of endothelial cells and the number of blood vessels were higher in red lesions when compared to black and white lesions. Kuroda and colleagues (2009) confirmed increased vessel density in red lesions versus black and white lesions using narrow-band imaging system. Furthermore, our previous studies in the baboon model revealed higher levels of the angiogenic factors, vascular endothelial growth factor A and CYR61, in red lesions (Gashaw, et al., 2006). Moreover, in patients with endometriosis the increased vascularization and morphologic appearance of red lesions suggest that red lesions may be recently implanted refluxed endometrial cells (Nisolle and Donnez, 1997). Hence, increased cell proliferation and angiogenesis could be critical processes in the formation of new ectopic implants, which may explain why red lesions are observed in the early stages of the lesion life cycle.

In the revised ASRM classification of endometriosis (ASRM, 1997) peritoneal and ovarian implants are categorized into three subgroups: red (including red, red-pink and clear lesions), white (including white, white-brown, yellow-brown and peritoneal defects) and black (including black and blue lesions). Accordingly, blue and black lesions belong to one entity. However, in our model we clearly differentiated between blue and black lesions and their turnover is evidently different, as blue le-

sions remain blue for several months. Blue lesions appear to be derived from black lesions or the change in color may simply reflect the amount of hemosiderin contained within the lesions.

4.2.2 Recurrence of Excised/Ablated Lesions in Baboons Inoculated with Menstrual Tissue

For the first time, lesion excision/ablation recurrence was analyzed in the baboon model for endometriosis. In two animals with experimentally induced endometriosis all of the lesions (26 total) were excised/ablated at 6 months. Animals were subsequently subjected to laparoscopies at 9 and 12 months followed by necropsy at 15 months. The majority (18/26) of lesions recurred by the 15-month necropsy. However it has been shown that pelvic inflammation related to manipulation and microtrauma to the pelvic organs can occur during laparoscopy in baboons (D'Hooghe, et al., 1999). It remains unclear whether this lesion recurrence was caused by partial removal of the lesion or implantation of new eutopic endometrium from subsequent retrograde menstruation preferentially at these sites of surgical microtrauma. Additionally it has been hypothesized that the mesothelial lining of the peritoneum acts as a defensive barrier, which may prevent the adhesion of ectopic tissues (Groothuis, et al., 1999, Groothuis, et al., 1998, van der Linden, et al., 1994). Therefore, disrupting the peritoneal integrity through excision and ablation together with retrograde menstruation may positively promote the development of disease.

These findings, although preliminary in nature and only including two animals, indicate that surgical management may not be the best approach for permanently eliminating endometriotic lesions. Indeed, women with endometriosis who undergo local excision of lesions experience short-term relief of symptoms. Shakiba et al., (2008) demonstrated that of 109 women who underwent lesion excision, as many as 55% had to have a repeat operation within 7 years. Furthermore, Candiani et al., (1991) reported that in a sample size of 42 patients with endometriosis who underwent lesion excision, 75% had to have repeat surgeries within 2 years owing to the return of pain. It must be noted that the number of lesions does not necessarily correlate with the severity of pain, although in the Candiani et al., (1991) study, the removal of lesions did lead to short-term relief of pain. Lesion excision/ablation may have short-term benefits (i.e. prior to an IVF cycle in subfertile women), but for long-term relief of symptoms perhaps medical therapy is more effective than surgical therapy. The baboon model primarily reflects the peritoneal disease and due to the limitations of the experimental model, we were unable to evaluate fertility before and after lesion excision/ablation.

4.2.3 Lesion Occurrence in Baboons Not Inoculated With Menstrual Tissue

The rate of spontaneous endometriosis for baboons in captivity, as reported in the literature, is 1-25% (D'Hooghe, et al., 1991, D'Hooghe, et al., 1996c, Dehoux, et al., 2011, Dick, et al., 2003). In our study spontaneous endometriosis resulting from

consecutive surgeries was demonstrated using animals with no previous surgeries. Indeed, the control group underwent the same schedule of surgeries as the experimental group allowing precise assessment of the effects of consecutive surgical procedures. All five animals developed endometriotic lesions, albeit at a much lower rate and at a later time point than the inoculated animals. A total of 27 lesions were observed in the control group; the earliest lesion development was observed at the 6-month laparoscopy. This incidence of non-induced endometriosis may be attributed, in part, to the repeat endometrectomies these animals underwent at the time of diagnostic laparoscopies. D'Hooghe et al., (1991) have shown that history of previous hysterotomy greatly increased the rate of spontaneous endometriosis in baboons. However, the more likely cause could be repeat laparoscopies. It has been demonstrated that the incidence of spontaneous endometriosis in baboons increased over time owing to repeat laparoscopies (D'Hooghe, et al., 1996d). Therefore, as with lesion excision/ablation, the inflammation induced by repeated surgeries could leave these animals more susceptible to endometriosis.

Currently, the gold standard for diagnosis of pelvic disease is surgical assessment, via laparoscopy. Additionally, surgical approaches to relieve endometriosis-related pain are frequently used as first-line therapy or after brief and failed medical therapies. However, laparoscopic removal of lesions leads to short-lived relief of symptoms (Jacobson, et al., 2009, Yeung, et al., 2009). Therefore, a focused emphasis on non-surgical diagnosis and therapies to prevent or control endometriosis is critical.

Understanding the kinetics of lesion development in an appropriate non-human primate model could be an initial step towards this goal.

5 Conclusions and Outlook

In the present thesis, two experimental animal models for endometriosis were used to gain further insight into dynamics of endometriotic implants and consequently assist in developing new therapeutic approaches.

The effect of 17ß-estradiol (E_2) on mouse endometriotic lesions was analyzed using a syngeneic transplantation mouse model of endometriosis and two strains of ovariectomized mice. Interestingly, at days 14 and 28 post transplantation, higher lesion area in E_2 treated animals was observed in comparison to vehicle. This change in area was not due to changes in proliferation. Detailed cell composition and apoptosis analysis revealed sex hormone dependent regulation of immune and non-immune cells within the lesions. Additionally, using a novel syngeneic transplantation luminescence mouse model demonstrated decrease in the concentration of cells from the originally transplanted tissue in the vehicle treated animals. Consequently, we proposed that apoptosis in resident lesion immune cells plus reduction in inflammation, and not proliferation or infiltration of host peritoneal cells, was responsible for the decrease in lesion area seen in vehicle treated animals. Additional studies on the role of E_2 and estrogen receptor signaling plus its modulation of immune cell facilitated inflammation may help further the understanding of lesion growth in mice and consequently facilitate drug discovery efforts for endometriosis.

Macroscopic appearance and kinetic of endometriotic lesions was analyzed retrospectively in a non-human primate model of endometriosis with the goal of providing a better understanding of lesion dynamics. The lesions changed their morphology from red to white over time. Different lesion types underwent metamorphosis at different rates. Thus, classification of lesions based on morphological appearance may help in determining the prognosis of the disease and in the examination of the effects of the lesions on symptoms. This understanding may provide new opportunities for targeted therapies to prevent or control endometriosis. Surgical excision/ablation of endometriotic lesions resulted in a high incidence of recurrence. Spontaneous endometriosis developed in control baboons in the absence of deposited autologous menstrual endometrium suggesting that repetitive surgical procedures alone can induce the spontaneous evolution of the chronic disease.

6 Summary

Endometriosis is a chronic, endocrine dependent, gynecological disorder affecting 10% of women of reproductive age. It is characterized by the presence of endometrial glands and stroma outside the uterus transforming into enometriotic lesions, predominantly in the pelvic peritoneum. The symptoms include chronic pelvic pain, dyspareunia, dysmenorrhoea as well as sub- and infertility. Currently there is no cure for endometriosis. In the present study, two experimental animal models for endometriosis were used to gain further insight into dynamics of endometriotic implants and consequently assist in developing new therapeutic approaches.

The effect of 17ß-estradiol (E_2) on mouse endometriotic lesions was analyzed using a syngeneic transplantation mouse model of endometriosis and two strains of ovariectomized mice. Interestingly, at days 14 and 28 post transplantation, higher lesion area in E_2 treated animals was observed in comparison to vehicle. This change in area was not due to changes in proliferation. Detailed cell composition and apoptosis analysis revealed sex hormone dependent regulation of immune and non-immune cells within the lesions. Additionally, using a novel syngeneic transplantation luminescence mouse model demonstrated decrease in the concentration of cells from the originally transplanted tissue in the vehicle treated animals. Consequently, we proposed that apoptosis in resident lesion immune cells plus reduction in inflammation, and not proliferation or infiltration of host peritoneal cells, was responsible for the decrease in lesion area seen in vehicle treated animals. Additional studies on the role of E_2 and estrogen receptor signaling plus its modulation of immune

cell facilitated inflammation may help further the understanding of lesion growth in mice and consequently facilitate drug discovery efforts for endometriosis.

Macroscopic appearance and kinetic of endometriotic lesions was analyzed retrospectively in a non-human primate model of endometriosis with the goal of providing a better understanding of lesion dynamics. The lesions changed their morphology from red to white over time. Different lesion types underwent metamorphosis at different rates. Thus, classification of lesions based on morphological appearance may help in determining the prognosis of the disease and in the examination of the effects of the lesions on symptoms. This understanding may provide new opportunities for targeted therapies to prevent or control endometriosis. Surgical excision/ablation of endometriotic lesions resulted in a high incidence of recurrence. Spontaneous endometriosis developed in control baboons in the absence of deposited autologous menstrual endometrium suggesting that repetitive surgical procedures alone can induce the spontaneous evolution of the chronic disease.

Zusammenfassung

German translation in progress!

7 References

Abbas, A. K., Lichtman, A. H. and Pillai, S. (2012) Cellular and molecular immunology. 7th edn, Elsevier/Saunders, Philadelphia.

Abbott, J. A., Hawe, J., Clayton, R. D. and Garry, R. The effects and effectiveness of laparoscopic excision of endometriosis: a prospective study with 2-5 year follow-up. Hum Reprod 2003;18: 1922-1927.

Agic, A., Djalali, S., Wolfler, M. M., Halis, G., Diedrich, K. and Hornung, D. Combination of CCR1 mRNA, MCP1, and CA125 measurements in peripheral blood as a diagnostic test for endometriosis. Reprod Sci 2008;15: 906-911.

Aitken, R. J., Baker, M. A., Doncel, G. F., Matzuk, M. M., Mauck, C. K. and Harper, M. J. As the world grows: contraception in the 21st century. J Clin Invest 2008;118: 1330-1343.

Akoum, A., Lemay, A., McColl, S., Turcot-Lemay, L. and Maheux, R. Elevated concentration and biologic activity of monocyte chemotactic protein-1 in the peritoneal fluid of patients with endometriosis. Fertil Steril 1996;66: 17-23.

Albee, R. B., Jr., Sinervo, K. and Fisher, D. T. Laparoscopic excision of lesions suggestive of endometriosis or otherwise atypical in appearance: relationship between visual findings and final histologic diagnosis. J Minim Invasive Gynecol 2008;15: 32-37.

American Fertility Society. Revised American Fertility Society classification of endometriosis: 1985. Fertil Steril 1985;43: 351-352.

American Society for Reproductive Medicine. Revised American Society for Reproductive Medicine classification of endometriosis: 1996. Fertil Steril 1997;67: 817-821.

Bacci, M., Capobianco, A., Monno, A., Cottone, L., Di Puppo, F., Camisa, B., Mariani, M., Brignole, C., Ponzoni, M., Ferrari, S. et al. Macrophages are alternatively activated in patients with endometriosis and required for growth and vascularization of lesions in a mouse model of disease. Am J Pathol 2009;175: 547-556.

Ball, E., Koh, C., Janik, G. and Davis, C. Gynaecological laparoscopy: 'see and treat' should be the gold standard. Curr Opin Obstet Gynecol 2008;20: 325-330.

Banchereau, J. and Steinman, R. M. Dendritic cells and the control of immunity. Nature 1998;392: 245-252.

Barbieri, R. L. Etiology and epidemiology of endometriosis. Am J Obstet Gynecol 1990;162: 565-567.

Barrier, B. F. Immunology of endometriosis. Clin Obstet Gynecol 2010;53: 397-402.

Becker, C. M., Sampson, D. A., Rupnick, M. A., Rohan, R. M., Efstathiou, J. A., Short, S. M., Taylor, G. A., Folkman, J. and D'Amato, R. J. Endostatin inhibits the growth of endometriotic lesions but does not affect fertility. Fertil Steril 2005;84 Suppl 2: 1144-1155.

Becker, C. M., Wright, R. D., Satchi-Fainaro, R., Funakoshi, T., Folkman, J., Kung, A. L. and D'Amato, R. J. A novel noninvasive model of endometriosis for monitoring the efficacy of antiangiogenic therapy. Am J Pathol 2006;168: 2074-2084.

Bedaiwy, M. A. and Falcone, T. Peritoneal fluid environment in endometriosis. Clinicopathological implications. Minerva Ginecol 2003;55: 333-345.

Beliard, A., Noel, A. and Foidart, J. M. Reduction of apoptosis and proliferation in endometriosis. Fertil Steril 2004;82: 80-85.

Bengtsson, A. K., Ryan, E. J., Giordano, D., Magaletti, D. M. and Clark, E. A. 17beta-estradiol (E2) modulates cytokine and chemokine expression in human monocyte-derived dendritic cells. Blood 2004;104: 1404-1410.

Berbic, M. and Fraser, I. S. Regulatory T cells and other leukocytes in the pathogenesis of endometriosis. J Reprod Immunol 2011;88: 149-155.

Bernuit, D., Ebert, A.D., Halis, G., Strothmann, A., Gerlinger, C., Geppert, K., Faustmann, T. Female perspectives on endometriosis: findings from the uterine bleeding and pain women's research study. J Endometr 2011; 3(2): 73–85

Braun, D. P. and Dmowski, W. P. Endometriosis: abnormal endometrium and dysfunctional immune response. Curr Opin Obstet Gynecol 1998;10: 365-369.

Braundmeier, A. G. and Fazleabas, A. T. The non-human primate model of endometriosis: research and implications for fecundity. Mol Hum Reprod 2009;15: 577-586.

Breitschopf, K., Haendeler, J., Malchow, P., Zeiher, A. M. and Dimmeler, S. Posttranslational modification of Bcl-2 facilitates its proteasome-dependent degradation: molecular characterization of the involved signaling pathway. Mol Cell Biol 2000;20: 1886-1896.

Brenner, R. M., Nayak, N. R., Slayden, O. D., Critchley, H. O. and Kelly, R. W. Premenstrual and menstrual changes in the macaque and human endometrium: relevance to endometriosis. Ann N Y Acad Sci 2002;955: 60-74; discussion 86-68, 396-406.

Brosens, I. Endometriosis rediscovered? Hum Reprod 2004;19: 1679-1680; author reply 1680-1671.

Bruner, K. L., Matrisian, L. M., Rodgers, W. H., Gorstein, F. and Osteen, K. G. Suppression of matrix metalloproteinases inhibits establishment of ectopic lesions by human endometrium in nude mice. J Clin Invest 1997;99: 2851-2857.

Bubner, B., Gase, K. and Baldwin, I. T. Two-fold differences are the detection limit for determining transgene copy numbers in plants by real-time PCR. BMC Biotechnol 2004;4: 14.

Budiu, R. A., Diaconu, I., Chrissluis, R., Dricu, A., Edwards, R. P. and Vlad, A. M. A conditional mouse model for human MUC1-positive endometriosis shows the presence of anti-MUC1 antibodies and Foxp3+ regulatory T cells. Dis Model Mech 2009;2: 593-603.

Bullimore, D. W. Endometriosis is sustained by tumour necrosis factor-alpha. Med Hypotheses 2003;60: 84-88.

Bulun, S. E. Endometriosis. N Engl J Med 2009;360: 268-279.

Bulun, S. E., Lin, Z., Imir, G., Amin, S., Demura, M., Yilmaz, B., Martin, R., Utsunomiya, H., Thung, S., Gurates, B. et al. Regulation of aromatase expression in estrogen-responsive breast and uterine disease: from bench to treatment. Pharmacol Rev 2005;57: 359-383.

Burns, K. A., Rodriguez, K. F., Hewitt, S. C., Janardhan, K. S., Young, S. L. and Korach, K. S. Role of estrogen receptor signaling required for endometriosis-like lesion establishment in a mouse model. Endocrinology 2012;153: 3960-3971.

Byers, S. L., Wiles, M. V., Dunn, S. L. and Taft, R. A. Mouse estrous cycle identification tool and images. PLoS One 2012;7: e35538.

Candiani, G. B., Fedele, L., Vercellini, P., Bianchi, S. and Di Nola, G. Repetitive conservative surgery for recurrence of endometriosis. Obstet Gynecol 1991;77: 421-424.

Chae, H. J., Kang, J. S., Byun, J. O., Han, K. S., Kim, D. U., Oh, S. M., Kim, H. M., Chae, S. W. and Kim, H. R. Molecular mechanism of staurosporine-induced apoptosis in osteoblasts. Pharmacol Res 2000;42: 373-381.

Chen, M. and Wang, J. Initiator caspases in apoptosis signaling pathways. Apoptosis 2002;7: 313-319.

Christodoulakos, G., Augoulea, A., Lambrinoudaki, I., Sioulas, V. and Creatsas, G. Pathogenesis of endometriosis: the role of defective 'immunosurveillance'. Eur J Contracept Reprod Health Care 2007;12: 194-202.

Cory, S. and Adams, J. M. The Bcl2 family: regulators of the cellular life-or-death switch. Nat Rev Cancer 2002;2: 647-656.

Coukos, G., Benencia, F., Buckanovich, R. J. and Conejo-Garcia, J. R. The role of dendritic cell precursors in tumour vasculogenesis. Br J Cancer 2005;92: 1182-1187.

Couse, J. F., Lindzey, J., Grandien, K., Gustafsson, J. A. and Korach, K. S. Tissue distribution and quantitative analysis of estrogen receptor-alpha (ERalpha) and estrogen receptor-beta (ERbeta) messenger ribonucleic acid in the wild-type and ERalpha-knockout mouse. Endocrinology 1997;138: 4613-4621.

Cramer, D. W. and Missmer, S. A. The epidemiology of endometriosis. Ann N Y Acad Sci 2002;955: 11-22; discussion 34-16, 396-406.

Critchley, H. O., Tong, S., Cameron, S. T., Drudy, T. A., Kelly, R. W. and Baird, D. T. Regulation of bcl-2 gene family members in human endometrium by antiprogestin administration in vivo. J Reprod Fertil 1999;115: 389-395.

Crosignani, P. G., Vercellini, P., Biffignandi, F., Costantini, W., Cortesi, I. and Imparato, E. Laparoscopy versus laparotomy in conservative surgical treatment for severe endometriosis. Fertil Steril 1996;66: 706-711.

Cummings, A. M. and Metcalf, J. L. Induction of endometriosis in mice: a new model sensitive to estrogen. Reprod Toxicol 1995;9: 233-238.

de Paula, L.B., Braga, N.P., Mendonça, M., Moro, L., Geber, S., Apoptosis of ectopic endometrial cells is impaired in women with endometriosis. J Endometr 2012; 4(1): 17-20

D'Hooghe, T. M., Bambra, C. S., Cornillie, F. J., Isahakia, M. and Koninckx, P. R. Prevalence and laparoscopic appearance of spontaneous endometriosis in the baboon (Papio anubis, Papio cynocephalus). Biol Reprod 1991;45: 411-416.

D'Hooghe, T. M., Bambra, C. S., De Jonge, I., Lauweryns, J. M. and Koninckx, P. R. The prevalence of spontaneous endometriosis in the baboon (Papio anubis, Papio cynocephalus) increases with the duration of captivity. Acta Obstet Gynecol Scand 1996c;75: 98-101.

D'Hooghe, T. M., Bambra, C. S., Isahakia, M. and Koninckx, P. R. Evolution of spontaneous endometriosis in the baboon (Papio anubis, Papio cynocephalus) over a 12-month period. Fertil Steril 1992;58: 409-412.

D'Hooghe, T. M., Bambra, C. S., Raeymaekers, B. M., De Jonge, I., Lauweryns, J. M. and Koninckx, P. R. Intrapelvic injection of menstrual endometrium causes endometriosis in baboons (Papio cynocephalus and Papio anubis). Am J Obstet Gynecol 1995;173: 125-134.

D'Hooghe, T. M., Bambra, C. S., Raeymaekers, B. M. and Hill, J. A. Pelvic inflammation induced by diagnostic laparoscopy in baboons. Fertil Steril 1999;72: 1134-1141.

D'Hooghe, T. M., Bambra, C. S., Raeymaekers, B. M. and Koninckx, P. R. Serial laparoscopies over 30 months show that endometriosis in captive baboons (Papio anubis, Papio cynocephalus) is a progressive disease. Fertil Steril 1996a;65: 645-649.

D'Hooghe, T. M., Bambra, C. S., Raeymaekers, B. M. and Koninckx, P. R. Development of spontaneous endometriosis in baboons. Obstet Gynecol 1996d;88: 462-466.

D'Hooghe, T. M., Bambra, C. S., Raeymaekers, B. M. and Koninckx, P. R. Increased prevalence and recurrence of retrograde menstruation in baboons with spontaneous endometriosis. Hum Reprod 1996b;11: 2022-2025.

Davis, L., Kennedy, S. S., Moore, J. and Prentice, A. Modern combined oral contraceptives for pain associated with endometriosis. Cochrane Database Syst Rev 2007;CD001019.

Dehoux, J. P., Defrere, S., Squifflet, J., Donnez, O., Polet, R., Mestdagt, M., Foidart, J. M., Van Langendonckt, A. and Donnez, J. Is the baboon model appropriate for endometriosis studies? Fertil Steril 2011;96: 728-733 e723.

Deligdisch, L. Hormonal pathology of the endometrium. Mod Pathol 2000;13: 285-294.

Delvoux, B., Groothuis, P., D'Hooghe, T., Kyama, C., Dunselman, G. and Romano, A. Increased production of 17beta-estradiol in endometriosis lesions is the result of impaired metabolism. J Clin Endocrinol Metab 2009;94: 876-883.

Deveraux, Q. L., Stennicke, H. R., Salvesen, G. S. and Reed, J. C. Endogenous inhibitors of caspases. J Clin Immunol 1999;19: 388-398.

Dick, E. J., Jr., Hubbard, G. B., Martin, L. J. and Leland, M. M. Record review of baboons with histologically confirmed endometriosis in a large established colony. J Med Primatol 2003;32: 39-47.

Ding, A. H., Nathan, C. F. and Stuehr, D. J. Release of reactive nitrogen intermediates and reactive oxygen intermediates from mouse peritoneal macrophages. Comparison of activating cytokines and evidence for independent production. J Immunol 1988;141: 2407-2412.

Dmowski, W. P., Steele, R. W. and Baker, G. F. Deficient cellular immunity in endometriosis. Am J Obstet Gynecol 1981;141: 377-383.

Donnez, J., Smoes, P., Gillerot, S., Casanas-Roux, F. and Nisolle, M. Vascular endothelial growth factor (VEGF) in endometriosis. Hum Reprod 1998;13: 1686-1690.

Eskenazi, B. and Warner, M. L. Epidemiology of endometriosis. Obstet Gynecol Clin North Am 1997;24: 235-258.

Fainaru, O., Adini, A., Benny, O., Adini, I., Short, S., Bazinet, L., Nakai, K., Pravda, E., Hornstein, M. D., D'Amato, R. J. et al. Dendritic cells support angiogenesis and promote lesion growth in a murine model of endometriosis. FASEB J 2008;22: 522-529.

Falcone, T. and Hurd, W. W. (2007) Clinical reproductive medicine and surgery, Mosby/Elsevier, Philadelphia.

Fang, Z., Yang, S., Lydon, J. P., DeMayo, F., Tamura, M., Gurates, B. and Bulun, S. E. Intact progesterone receptors are essential to counteract the proliferative effect of estradiol in a genetically engineered mouse model of endometriosis. Fertil Steril 2004;82: 673-678.

Fanton, J. W. and Hubbard, G. B. Spontaneous endometriosis in a cynomolgus monkey (Macaca fascicularis). Lab Anim Sci 1983;33: 597-599.

Farquhar, C. Endometriosis. BMJ 2007;334: 249-253.

Fay, M. P. and Proschan, M. A. Wilcoxon-Mann-Whitney or t-test? On assumptions for hypothesis tests and multiple interpretations of decision rules. Stat Surv 2010;4: 1-39.

Fazleabas, A. T., Brudney, A., Gurates, B., Chai, D. and Bulun, S. A modified baboon model for endometriosis. Ann N Y Acad Sci 2002;955: 308-317; discussion 340-302, 396-406.

Ferenczy, A., Bertrand, G. and Gelfand, M. M. Proliferation kinetics of human endometrium during the normal menstrual cycle. Am J Obstet Gynecol 1979;133: 859-867.

Fridman, J. S. and Lowe, S. W. Control of apoptosis by p53. Oncogene 2003;22: 9030-9040.

Fujishita, A., Hasuo, A., Khan, K. N., Masuzaki, H., Nakashima, H. and Ishimaru, T. Immunohistochemical study of angiogenic factors in endometrium and endometriosis. Gynecol Obstet Invest 1999;48 Suppl 1: 36-44.

Fukui, A., Fujii, S., Yamaguchi, E., Kimura, H., Sato, S. and Saito, Y. Natural killer cell subpopulations and cytotoxicity for infertile patients undergoing in vitro fertilization. Am J Reprod Immunol 1999;41: 413-422.

Gallinelli, A., Chiossi, G., Giannella, L., Marsella, T., Genazzani, A. D. and Volpe, A. Different concentrations of interleukins in the peritoneal fluid of women with endometriosis: relationships with lymphocyte subsets. Gynecol Endocrinol 2004;18: 144-151.

Garcia-Velasco, J. A., Arici, A., Zreik, T., Naftolin, F. and Mor, G. Macrophage derived growth factors modulate Fas ligand expression in cultured endometrial stromal cells: a role in endometriosis. Mol Hum Reprod 1999;5: 642-650.

Garcia-Velasco, J. A., Mulayim, N., Kayisli, U. A. and Arici, A. Elevated soluble Fas ligand levels may suggest a role for apoptosis in women with endometriosis. Fertil Steril 2002;78: 855-859.

Gardner, G. H., Greene, R. R. and Ranney, B. The histogenesis of endometriosis; recent contributions. Obstet Gynecol 1953;1: 615-637.

Garry, R. Is insulin resistance an essential component of PCOS?: The endometriosis syndromes: a clinical classification in the presence of aetiological confusion and therapeutic anarchy. Hum Reprod 2004;19: 760-768.

Garry, R., Clayton, R. and Hawe, J. The effect of endometriosis and its radical laparoscopic excision on quality of life indicators. BJOG 2000;107: 44-54.

Garzetti, G. G., Ciavattini, A., Provinciali, M., Fabris, N., Cignitti, M. and Romanini, C. Natural killer cell activity in endometriosis: correlation between serum estradiol levels and cytotoxicity. Obstet Gynecol 1993;81: 665-668.

Gashaw, I., Hastings, J. M., Jackson, K. S., Winterhager, E. and Fazleabas, A. T. Induced endometriosis in the baboon (Papio anubis) increases the expression of the proangiogenic factor CYR61 (CCN1) in eutopic and ectopic endometria. Biol Reprod 2006;74: 1060-1066.

Gavrieli, Y., Sherman, Y. and Ben-Sasson, S. A. Identification of programmed cell death in situ via specific labeling of nuclear DNA fragmentation. J Cell Biol 1992;119: 493-501.

Gazvani, M. R., Christmas, S., Quenby, S., Kirwan, J., Johnson, P. M. and Kingsland, C. R. Peritoneal fluid concentrations of interleukin-8 in women with endometriosis: relationship to stage of disease. Hum Reprod 1998;13: 1957-1961.

Gebel, H. M., Braun, D. P., Tambur, A., Frame, D., Rana, N. and Dmowski, W. P. Spontaneous apoptosis of endometrial tissue is impaired in women with endometriosis. Fertil Steril 1998;69: 1042-1047.

Giudice, L. C. Clinical practice. Endometriosis. N Engl J Med 2010;362: 2389-2398.

Giudice, L. C. and Kao, L. C. Endometriosis. Lancet 2004;364: 1789-1799.

Gold, R., Schmied, M., Giegerich, G., Breitschopf, H., Hartung, H. P., Toyka, K. V. and Lassmann, H. Differentiation between cellular apoptosis and necrosis by the combined use of in situ tailing and nick translation techniques. Lab Invest 1994;71: 219-225.

Greenberg, J. S., Bruess, C. E. and Conklin, S. C. (2007) Exploring the dimensions of human sexuality. 3rd edn, Jones and Bartlett Publishers, Sudbury, Mass.

Greer, L. F., 3rd and Szalay, A. A. Imaging of light emission from the expression of luciferases in living cells and organisms: a review. Luminescence 2002;17: 43-74.

Griesinger, G., Felberbaum, R. and Diedrich, K. GnRH-antagonists in reproductive medicine. Arch Gynecol Obstet 2005;273: 71-78.

Groothuis, P. G., Koks, C. A., de Goeij, A. F., Dunselman, G. A., Arends, J. W. and Evers, J. L. Adhesion of human endometrium to the epithelial lining and extracellular matrix of amnion in vitro: an electron microscopic study. Hum Reprod 1998;13: 2275-2281.

Groothuis, P. G., Koks, C. A., de Goeij, A. F., Dunselman, G. A., Arends, J. W. and Evers, J. L. Adhesion of human endometrial fragments to peritoneum in vitro. Fertil Steril 1999;71: 1119-1124.

Groothuis, P. G., Nap, A. W., Winterhager, E. and Grummer, R. Vascular development in endometriosis. Angiogenesis 2005;8: 147-156.

Gross, A., Yin, X. M., Wang, K., Wei, M. C., Jockel, J., Milliman, C., Erdjument-Bromage, H., Tempst, P. and Korsmeyer, S. J. Caspase cleaved BID targets mitochondria and is required for cytochrome c release, while BCL-XL prevents this release but not tumor necrosis factor-R1/Fas death. J Biol Chem 1999;274: 1156-1163.

Grummer, R. Animal models in endometriosis research. Hum Reprod Update 2006;12: 641-649.

Grummer, R., Schwarzer, F., Bainczyk, K., Hess-Stumpp, H., Regidor, P. A., Schindler, A. E. and Winterhager, E. Peritoneal endometriosis: validation of an in-vivo model. Hum Reprod 2001;16: 1736-1743.

Hadfield, R., Mardon, H., Barlow, D. and Kennedy, S. Delay in the diagnosis of endometriosis: a survey of women from the USA and the UK. Hum Reprod 1996;11: 878-880.

Hall, S. E., Mao, A., Nicolaidou, V., Finelli, M., Wise, E. L., Nedjai, B., Kanjanapangka, J., Harirchian, P., Chen, D., Selchau, V. et al. Elucidation of binding sites of dual antagonists in the human chemokine receptors CCR2 and CCR5. Mol Pharmacol 2009;75: 1325-1336.

Halme, J., Hammond, M. G., Hulka, J. F., Raj, S. G. and Talbert, L. M. Retrograde menstruation in healthy women and in patients with endometriosis. Obstet Gynecol 1984;64: 151-154.

Harada, M., Suganuma, N., Furuhashi, M., Nagasaka, T., Nakashima, N., Kikkawa, F., Tomoda, Y. and Furui, K. Detection of apoptosis in human endometriotic tissues. Mol Hum Reprod 1996;2: 307-315.

Harada, T., Iwabe, T. and Terakawa, N. Role of cytokines in endometriosis. Fertil Steril 2001;76: 1-10.

Harirchian, P., Gashaw, I., Lipskind, S. T., Braundmeier, A. G., Hastings, J. M., Olson, M. R. and Fazleabas, A. T. Lesion kinetics in a non-human primate model of endometriosis. Hum Reprod 2012;27: 2341-2351.

Harrington, L. E., Hatton, R. D., Mangan, P. R., Turner, H., Murphy, T. L., Murphy, K. M. and Weaver, C. T. Interleukin 17-producing CD4+ effector T cells develop via a lineage distinct from the T helper type 1 and 2 lineages. Nat Immunol 2005;6: 1123-1132.

Hastings, J. M. and Fazleabas, A. T. A baboon model for endometriosis: implications for fertility. Reprod Biol Endocrinol 2006;4 Suppl 1: S7.

Helvacioglu, A., Aksel, S. and Peterson, R. D. Endometriosis and autologous lymphocyte activation by endometrial cells. Are lymphocytes or endometrial cell defects responsible? J Reprod Med 1997;42: 71-75.

Hever, A., Roth, R. B., Hevezi, P., Marin, M. E., Acosta, J. A., Acosta, H., Rojas, J., Herrera, R., Grigoriadis, D., White, E. et al. Human endometriosis is associated with plasma cells and overexpression of B lymphocyte stimulator. Proc Natl Acad Sci U S A 2007;104: 12451-12456.

Higuchi, R., Fockler, C., Dollinger, G. and Watson, R. Kinetic PCR analysis: real-time monitoring of DNA amplification reactions. Biotechnology (N Y) 1993;11: 1026-1030.

Hill, J. A., Faris, H. M., Schiff, I. and Anderson, D. J. Characterization of leukocyte subpopulations in the peritoneal fluid of women with endometriosis. Fertil Steril 1988;50: 216-222.

Hirata, T., Osuga, Y., Hamasaki, K., Yoshino, O., Ito, M., Hasegawa, A., Takemura, Y., Hirota, Y., Nose, E., Morimoto, C. et al. Interleukin (IL)-17A stimulates IL-8 secretion, cyclooxygensase-2 expression, and cell proliferation of endometriotic stromal cells. Endocrinology 2008;149: 1260-1267.

Hirata, T., Osuga, Y., Yoshino, O., Hirota, Y., Harada, M., Takemura, Y., Morimoto, C., Koga, K., Yano, T., Tsutsumi, O. et al. Development of an experimental model of endometriosis using mice that ubiquitously express green fluorescent protein. Hum Reprod 2005;20: 2092-2096.

Ho, H. N., Wu, M. Y., Chao, K. H., Chen, C. D., Chen, S. U. and Yang, Y. S. Peritoneal interleukin-10 increases with decrease in activated CD4+ T lymphocytes in women with endometriosis. Hum Reprod 1997;12: 2528-2533.

Ho, H. N., Wu, M. Y. and Yang, Y. S. Peritoneal cellular immunity and endometriosis. Am J Reprod Immunol 1997;38: 400-412.

Hoffmann, J., Bohlmann, R., Heinrich, N., Hofmeister, H., Kroll, J., Kunzer, H., Lichtner, R. B., Nishino, Y., Parczyk, K., Sauer, G. et al. Characterization of new estrogen receptor destabilizing compounds: effects on estrogen-sensitive and tamoxifen-resistant breast cancer. J Natl Cancer Inst 2004;96: 210-218.

Hopwood, D. and Levison, D. A. Atrophy and apoptosis in the cyclical human endometrium. J Pathol 1976;119: 159-166.

Hsu, C. C., Yang, B. C., Wu, M. H. and Huang, K. E. Enhanced interleukin-4 expression in patients with endometriosis. Fertil Steril 1997;67: 1059-1064.

Hughes, G. C. and Clark, E. A. Regulation of dendritic cells by female sex steroids: relevance to immunity and autoimmunity. Autoimmunity 2007;40: 470-481.

Hull, M. L., Johan, M. Z., Hodge, W. L., Robertson, S. A. and Ingman, W. V. Host-derived TGFB1 deficiency suppresses lesion development in a mouse model of endometriosis. Am J Pathol 2012;180: 880-887.

Ishimaru, T., Khan, K. N., Fujishita, A., Kitajima, M. and Masuzaki, H. Hepatocyte growth factor may be involved in cellular changes to the peritoneal mesothelium adjacent to pelvic endometriosis. Fertil Steril 2004;81 Suppl 1: 810-818.

Izawa, M., Harada, T., Taniguchi, F., Ohama, Y., Takenaka, Y. and Terakawa, N. An epigenetic disorder may cause aberrant expression of aromatase gene in endometriotic stromal cells. Fertil Steril 2008;89: 1390-1396.

Jackman, M., Lindon, C., Nigg, E. A. and Pines, J. Active cyclin B1-Cdk1 first appears on centrosomes in prophase. Nat Cell Biol 2003;5: 143-148.

Jacobson, T. Z., Duffy, J. M., Barlow, D., Koninckx, P. R. and Garry, R. Laparoscopic surgery for pelvic pain associated with endometriosis. Cochrane Database Syst Rev 2009;CD001300.

Jansen, R. P. and Russell, P. Nonpigmented endometriosis: clinical, laparoscopic, and pathologic definition. Am J Obstet Gynecol 1986;155: 1154-1159.

Javert, C. T. Pathogenesis of endometriosis based on endometrial homeoplasia, direct extension, exfoliation and implantation, lymphatic and hematogenous metastasis, including five case reports of endometrial tissue in pelvic lymph nodes. Cancer 1949;2: 399-410.

Jiang, Q. Y. and Wu, R. J. Growth mechanisms of endometriotic cells in implanted places: a review. Gynecol Endocrinol 2012;28: 562-567.

Jimenez-Heffernan, J. A., Aguilera, A., Aroeira, L. S., Lara-Pezzi, E., Bajo, M. A., del Peso, G., Ramirez, M., Gamallo, C., Sanchez-Tomero, J. A., Alvarez, V. et al. Immunohistochemical characterization of fibroblast subpopulations in normal peritoneal tissue and in peritoneal dialysis-induced fibrosis. Virchows Arch 2004;444: 247-256.

Jin, P., Hardy, S. and Morgan, D. O. Nuclear localization of cyclin B1 controls mitotic entry after DNA damage. J Cell Biol 1998;141: 875-885.

Jones, C. J., Denton, J. and Fazleabas, A. T. Morphological and glycosylation changes associated with the endometrium and ectopic lesions in a baboon model of endometriosis. Hum Reprod 2006;21: 3068-3080.

Jones, R. K., Bulmer, J. N. and Searle, R. F. Immunohistochemical characterization of proliferation, oestrogen receptor and progesterone receptor expression in endometriosis: comparison of eutopic and ectopic endometrium with normal cycling endometrium. Hum Reprod 1995;10: 3272-3279.

Jones, R. K., Bulmer, J. N. and Searle, R. F. Phenotypic and functional studies of leukocytes in human endometrium and endometriosis. Hum Reprod Update 1998;4: 702-709.

Jones, R. K., Searle, R. F. and Bulmer, J. N. Apoptosis and bcl-2 expression in normal human endometrium, endometriosis and adenomyosis. Hum Reprod 1998;13: 3496-3502.

Kaijzel, E. L., van der Pluijm, G. and Lowik, C. W. Whole-body optical imaging in animal models to assess cancer development and progression. Clin Cancer Res 2007;13: 3490-3497.

Kayisli, U. A., Guzeloglu-Kayisli, O. and Arici, A. Endocrine-immune interactions in human endometrium. Ann N Y Acad Sci 2004;1034: 50-63.

Khan, K. N., Kitajima, M., Hiraki, K., Fujishita, A., Sekine, I., Ishimaru, T. and Masuzaki, H. Immunopathogenesis of pelvic endometriosis: role of hepatocyte growth factor, macrophages and ovarian steroids. Am J Reprod Immunol 2008;60: 383-404.

Khan, K. N., Masuzaki, H., Fujishita, A., Kitajima, M., Sekine, I. and Ishimaru, T. Differential macrophage infiltration in early and advanced endometriosis and adjacent peritoneum. Fertil Steril 2004;81: 652-661.

Kindt, T. J., Goldsby, R. A., Osborne, B. A. and Kuby, J. (2007) Kuby immunology. 6th edn, W.H. Freeman, New York.

Kishimoto, T. (1998) Leucocyte typing VI : white cell differentiation antigens : proceedings of the sixth international workshop and conference held in Kobe, Japan, 10-14 November 1996, Garland Pub., New York.

Kokawa, K., Shikone, T. and Nakano, R. Apoptosis in the human uterine endometrium during the menstrual cycle. J Clin Endocrinol Metab 1996;81: 4144-4147.

Koninckx, P. R., Kennedy, S. H. and Barlow, D. H. Endometriotic disease: the role of peritoneal fluid. Hum Reprod Update 1998;4: 741-751.

Koninckx, P. R., Meuleman, C., Demeyere, S., Lesaffre, E. and Cornillie, F. J. Suggestive evidence that pelvic endometriosis is a progressive disease, whereas deeply infiltrating endometriosis is associated with pelvic pain. Fertil Steril 1991;55: 759-765.

Koninckx, P. R., Meuleman, C., Oosterlynck, D. and Cornillie, F. J. Diagnosis of deep endometriosis by clinical examination during menstruation and plasma CA-125 concentration. Fertil Steril 1996;65: 280-287.

Korbel, C., Menger, M. D. and Laschke, M. W. Size and spatial orientation of uterine tissue transplants on the peritoneum crucially determine the growth and cyst formation of endometriosis-like lesions in mice. Hum Reprod 2010;25: 2551-2558.

Krammer, P. H. CD95's deadly mission in the immune system. Nature 2000;407: 789-795.

Kuroda, K., Kitade, M., Kikuchi, I., Kumakiri, J., Matsuoka, S., Jinushi, M., Shirai, Y., Kuroda, M. and Takeda, S. Vascular density of peritoneal endometriosis using narrow-band imaging system and vascular analysis software. J Minim Invasive Gynecol 2009;16: 618-621.

Kusakabe, K., Morishima, S., Nakamuta, N., Li, Z. L. and Otsuki, Y. Effect of danazol on NK cells and cytokines in the mouse uterus. J Reprod Dev 2007;53: 87-94.

Kyama, C. M., Debrock, S., Mwenda, J. M. and D'Hooghe, T. M. Potential involvement of the immune system in the development of endometriosis. Reprod Biol Endocrinol 2003;1: 123.

Leblanc, V., Dery, M. C., Shooner, C. and Asselin, E. Opposite regulation of XIAP and Smac/DIABLO in the rat endometrium in response to 17beta-estradiol at estrus. Reprod Biol Endocrinol 2003;1: 59.

Lebovic, D. I., Mueller, M. D. and Taylor, R. N. Immunobiology of endometriosis. Fertil Steril 2001;75: 1-10.

Lecce, G., Meduri, G., Ancelin, M., Bergeron, C. and Perrot-Applanat, M. Presence of estrogen receptor beta in the human endometrium through the cycle: expression in glandular, stromal, and vascular cells. J Clin Endocrinol Metab 2001;86: 1379-1386.

Letterio, J. J. and Roberts, A. B. Regulation of immune responses by TGF-beta. Annu Rev Immunol 1998;16: 137-161.

Li, S. F., Nakayama, K., Masuzawa, H. and Fujii, S. The number of proliferating cell nuclear antigen positive cells in endometriotic lesions differs from that in the endometrium. Analysis of PCNA positive cells during the menstrual cycle and in postmenopause. Virchows Arch A Pathol Anat Histopathol 1993;423: 257-263.

Li-Weber, M. and Krammer, P. H. Function and regulation of the CD95 (APO-1/Fas) ligand in the immune system. Semin Immunol 2003;15: 145-157.

Lin, Y. J., Lai, M. D., Lei, H. Y. and Wing, L. Y. Neutrophils and macrophages promote angiogenesis in the early stage of endometriosis in a mouse model. Endocrinology 2006;147: 1278-1286.

Maeda, N., Izumiya, C., Taniguchi, K., Matsushima, S. and Fukaya, T. Role of NK cells and HLA-G in endometriosis. Front Biosci (Schol Ed) 2012;4: 1568-1581.

Martin, L. A. and Dowsett, M. BCL-2: A New Therapeutic Target in Estrogen Receptor-Positive Breast Cancer? Cancer Cell 2013;24: 7-9.

Martinez-Roman, S., Balasch, J., Creus, M., Fabregues, F., Carmona, F., Vilella, R. and Vanrell, J. A. Immunological factors in endometriosis-associated reproductive failure: studies in fertile and infertile women with and without endometriosis. Hum Reprod 1997;12: 1794-1799.

Massague, J., Blain, S. W. and Lo, R. S. TGFbeta signaling in growth control, cancer, and heritable disorders. Cell 2000;103: 295-309.

Matarese, G., De Placido, G., Nikas, Y. and Alviggi, C. Pathogenesis of endometriosis: natural immunity dysfunction or autoimmune disease? Trends Mol Med 2003;9: 223-228.

Matsuzaki, S., Murakami, T., Uehara, S., Canis, M., Sasano, H. and Okamura, K. Expression of estrogen receptor alpha and beta in peritoneal and ovarian endometriosis. Fertil Steril 2001;75: 1198-1205.

McLaren, J., Prentice, A., Charnock-Jones, D. S., Sharkey, A. M. and Smith, S. K. Immunolocalization of the apoptosis regulating proteins Bcl-2 and Bax in human endometrium and isolated peritoneal fluid macrophages in endometriosis. Hum Reprod 1997;12: 146-152.

Meresman, G. F., Auge, L., Baranao, R. I., Lombardi, E., Tesone, M. and Sueldo, C. Oral contraceptives suppress cell proliferation and enhance apoptosis of eutopic endometrial tissue from patients with endometriosis. Fertil Steril 2002;77: 1141-1147.

Meresman, G. F., Vighi, S., Buquet, R. A., Contreras-Ortiz, O., Tesone, M. and Rumi, L. S. Apoptosis and expression of Bcl-2 and Bax in eutopic endometrium from women with endometriosis. Fertil Steril 2000;74: 760-766.

Merrill, J. A. Spontaneous endometriosis in the Kenya baboon (Papio doguera). Am J Obstet Gynecol 1968;101: 569-570.

Milewski, L., Dziunycz, P., Barcz, E., Radomski, D., Roszkowski, P. I., Korczak-Kowalska, G., Kaminski, P. and Malejczyk, J. Increased levels of human neutrophil peptides 1, 2, and 3 in peritoneal fluid of patients with endometriosis: association with neutrophils, T cells and IL-8. J Reprod Immunol 2011;91: 64-70.

Miltenburger, H. G., Sachse, G. and Schliermann, M. S-phase cell detection with a monoclonal antibody. Dev Biol Stand 1987;66: 91-99.

Moffett-King, A. Natural killer cells and pregnancy. Nat Rev Immunol 2002;2: 656-663.

Monckedieck, V., Sannecke, C., Husen, B., Kumbartski, M., Kimmig, R., Totsch, M., Winterhager, E. and Grummer, R. Progestins inhibit expression of MMPs and of angiogenic factors in human ectopic endometrial lesions in a mouse model. Mol Hum Reprod 2009;15: 633-643.

Mosmann, T. R., Cherwinski, H., Bond, M. W., Giedlin, M. A. and Coffman, R. L. Two types of murine helper T cell clone. I. Definition according to profiles of lymphokine activities and secreted proteins. J Immunol 1986;136: 2348-2357.

Murk, W., Atabekoglu, C. S., Cakmak, H., Heper, A., Ensari, A., Kayisli, U. A. and Arici, A. Extracellularly signal-regulated kinase activity in the human endometrium: possible roles in the pathogenesis of endometriosis. J Clin Endocrinol Metab 2008;93: 3532-3540.

Muzii, L., Marana, R., Brunetti, L., Orlando, G., Michelotto, B. and Benedetti Panici, P. Atypical endometriosis revisited: clinical and biochemical evaluation of the different forms of superficial implants. Fertil Steril 2000;74: 739-742.

Nachmias, B., Ashhab, Y. and Ben-Yehuda, D. The inhibitor of apoptosis protein family (IAPs): an emerging therapeutic target in cancer. Semin Cancer Biol 2004;14: 231-243.

Nair, A. S., Nair, H. B., Lucidi, R. S., Kirchner, A. J., Schenken, R. S., Tekmal, R. R. and Witz, C. A. Modeling the early endometriotic lesion: mesothelium-endometrial cell co-culture increases endometrial invasion and alters mesothelial and endometrial gene transcription. Fertil Steril 2008;90: 1487-1495.

Nasu, K., Nishida, M., Kawano, Y., Tsuno, A., Abe, W., Yuge, A., Takai, N. and Narahara, H. Aberrant expression of apoptosis-related molecules in endometriosis: a possible mechanism underlying the pathogenesis of endometriosis. Reprod Sci 2011;18: 206-218.

Nezhat, F., Cohen, C., Rahaman, J., Gretz, H., Cole, P. and Kalir, T. Comparative immunohistochemical studies of bcl-2 and p53 proteins in benign and malignant ovarian endometriotic cysts. Cancer 2002;94: 2935-2940.

Nezhat, F. R. and Kalir, T. Comparative immunohistochemical studies of endometriosis lesions and endometriotic cysts. Fertil Steril 2002;78: 820-824.

Nisolle, M., Casanas-Roux, F. and Donnez, J. Immunohistochemical analysis of proliferative activity and steroid receptor expression in peritoneal and ovarian endometriosis. Fertil Steril 1997;68: 912-919.

Nisolle, M. and Donnez, J. Peritoneal endometriosis, ovarian endometriosis, and adenomyotic nodules of the rectovaginal septum are three different entities. Fertil Steril 1997;68: 585-596.

Noble, L. S., Simpson, E. R., Johns, A. and Bulun, S. E. Aromatase expression in endometriosis. J Clin Endocrinol Metab 1996;81: 174-179.

Nothnick, W. B. Treating endometriosis as an autoimmune disease. Fertil Steril 2001;76: 223-231.

Ohata, Y., Harada, T., Miyakoda, H., Taniguchi, F., Iwabe, T. and Terakawa, N. Serum interleukin-8 levels are elevated in patients with ovarian endometrioma. Fertil Steril 2008;90: 994-999.

Oldham, R. K. Natural killer cells: artifact to reality: an odyssey in biology. Cancer Metastasis Rev 1983;2: 323-336.

Olive, D. L. and Pritts, E. A. Treatment of endometriosis. N Engl J Med 2001;345: 266-275.

Olkowska-Truchanowicz, J., Bocian, K., Maksym, R. B., Bialoszewska, A., Wlodarczyk, D., Baranowski, W., Zabek, J., Korczak-Kowalska, G. and Malejczyk, J. CD4(+) CD25(+) FOXP3(+) regulatory T cells in peripheral blood and peritoneal fluid of patients with endometriosis. Hum Reprod 2013;28: 119-124.

Oosterlynck, D. J., Cornillie, F. J., Waer, M. and Koninckx, P. R. Immunohistochemical characterization of leucocyte subpopulations in endometriotic lesions. Arch Gynecol Obstet 1993;253: 197-206.

Oosterlynck, D. J., Cornillie, F. J., Waer, M., Vandeputte, M. and Koninckx, P. R. Women with endometriosis show a defect in natural killer activity resulting in a decreased cytotoxicity to autologous endometrium. Fertil Steril 1991;56: 45-51.

Oosterlynck, D. J., Meuleman, C., Lacquet, F. A., Waer, M. and Koninckx, P. R. Flow cytometry analysis of lymphocyte subpopulations in peritoneal fluid of women with endometriosis. Am J Reprod Immunol 1994;31: 25-31.

Oosterlynck, D. J., Meuleman, C., Waer, M., Vandeputte, M. and Koninckx, P. R. The natural killer activity of peritoneal fluid lymphocytes is decreased in women with endometriosis. Fertil Steril 1992;58: 290-295.

Ormerod, M. G. (2000) Flow cytometry : a practical approach. 3rd edn, Oxford University Press, Oxford England ; New York.

Osuga, Y. Novel therapeutic strategies for endometriosis: a pathophysiological perspective. Gynecol Obstet Invest 2008;66 Suppl 1: 3-9.

Osuga, Y., Koga, K., Hirota, Y., Hirata, T., Yoshino, O. and Taketani, Y. Lymphocytes in endometriosis. Am J Reprod Immunol 2011;65: 1-10.

Osuga, Y., Tsutsumi, O., Okagaki, R., Takai, Y., Fujimoto, A., Suenaga, A., Maruyama, M., Momoeda, M., Yano, T. and Taketani, Y. Hepatocyte growth factor concentrations are elevated in peritoneal fluid of women with endometriosis. Hum Reprod 1999;14: 1611-1613.

Otsuki, Y., Misaki, O., Sugimoto, O., Ito, Y., Tsujimoto, Y. and Akao, Y. Cyclic bcl-2 gene expression in human uterine endometrium during menstrual cycle. Lancet 1994;344: 28-29.

Paavonen, T., Andersson, L. C. and Adlercreutz, H. Sex hormone regulation of in vitro immune response. Estradiol enhances human B cell maturation via inhibition of suppressor T cells in pokeweed mitogen-stimulated cultures. J Exp Med 1981;154: 1935-1945.

Paul Dmowski, W. and Braun, D. P. Immunology of endometriosis. Best Pract Res Clin Obstet Gynaecol 2004;18: 245-263.

Pierro, E., Minici, F., Alesiani, O., Miceli, F., Proto, C., Screpanti, I., Mancuso, S. and Lanzone, A. Stromal-epithelial interactions modulate estrogen responsiveness in normal human endometrium. Biol Reprod 2001;64: 831-838.

Pizzo, A., Salmeri, F. M., Ardita, F. V., Sofo, V., Tripepi, M. and Marsico, S. Behaviour of cytokine levels in serum and peritoneal fluid of women with endometriosis. Gynecol Obstet Invest 2002;54: 82-87.

Podgaec, S., Abrao, M. S., Dias, J. A., Jr., Rizzo, L. V., de Oliveira, R. M. and Baracat, E. C. Endometriosis: an inflammatory disease with a Th2 immune response component. Hum Reprod 2007;22: 1373-1379.

Potten, C. S. (1987) Perspectives on mammalian cell death, Oxford University Press, Oxford ; New York.

Punnonen, R., Klemi, P. J. and Nikkanen, V. Postmenopausal endometriosis. Eur J Obstet Gynecol Reprod Biol 1980;11: 195-200.

Quarmby, V. E. and Korach, K. S. The influence of 17 beta-estradiol on patterns of cell division in the uterus. Endocrinology 1984;114: 694-702.

Rajkumar, K., Schott, P. W. and Simpson, C. W. The rat as an animal model for endometriosis to examine recurrence of ectopic endometrial tissue after regression. Fertil Steril 1990;53: 921-925.

Ramos-Vara, J. A. Technical aspects of immunohistochemistry. Vet Pathol 2005;42: 405-426.

Raynal, P. and Pollard, H. B. Annexins: the problem of assessing the biological role for a gene family of multifunctional calcium- and phospholipid-binding proteins. Biochim Biophys Acta 1994;1197: 63-93.

Redwine, D. B. Age-related evolution in color appearance of endometriosis. Fertil Steril 1987;48: 1062-1063.

Rice, V. M. Conventional medical therapies for endometriosis. Ann N Y Acad Sci 2002;955: 343-352; discussion 389-393, 396-406.

Richardson, B. C., Lalwani, N. D., Johnson, K. J. and Marks, R. M. Fas ligation triggers apoptosis in macrophages but not endothelial cells. Eur J Immunol 1994;24: 2640-2645.

Rider, V., Kimler, B. F. and Justice, W. M. Progesterone-growth factor interactions in uterine stromal cells. Biol Reprod 1998;59: 464-469.

Rodgers, A. K. and Falcone, T. Treatment strategies for endometriosis. Expert Opin Pharmacother 2008;9: 243-255.

Roy, N., Deveraux, Q. L., Takahashi, R., Salvesen, G. S. and Reed, J. C. The c-IAP-1 and c-IAP-2 proteins are direct inhibitors of specific caspases. EMBO J 1997;16: 6914-6925.

Ryan, I. P. and Taylor, R. N. Endometriosis and infertility: new concepts. Obstet Gynecol Surv 1997;52: 365-371.

Salamonsen, L. A. and Woolley, D. E. Menstruation: induction by matrix metalloproteinases and inflammatory cells. J Reprod Immunol 1999;44: 1-27.

Sampson, J. A. Metastatic or Embolic Endometriosis, due to the Menstrual Dissemination of Endometrial Tissue into the Venous Circulation. Am J Pathol 1927;3: 93-110 143.

Sayama, K., Yonehara, S., Watanabe, Y. and Miki, Y. Expression of Fas antigen on keratinocytes in vivo and induction of apoptosis in cultured keratinocytes. J Invest Dermatol 1994;103: 330-334.

Schenken, R. S. and Asch, R. H. Surgical induction of endometriosis in the rabbit: effects on fertility and concentrations of peritoneal fluid prostaglandins. Fertil Steril 1980;34: 581-587.

Scholzen, T. and Gerdes, J. The Ki-67 protein: from the known and the unknown. J Cell Physiol 2000;182: 311-322.

Schulke, L., Berbic, M., Manconi, F., Tokushige, N., Markham, R. and Fraser, I. S. Dendritic cell populations in the eutopic and ectopic endometrium of women with endometriosis. Hum Reprod 2009;24: 1695-1703.

Scotti, S., Regidor, P. A., Schindler, A. E. and Winterhager, E. Reduced proliferation and cell adhesion in endometriosis. Mol Hum Reprod 2000;6: 610-617.

Shakiba, K., Bena, J. F., McGill, K. M., Minger, J. and Falcone, T. Surgical treatment of endometriosis: a 7-year follow-up on the requirement for further surgery. Obstet Gynecol 2008;111: 1285-1292.

Shi, J. H., Yang, Y. J., Dong, Z., Lang, J. H. and Leng, J. H. Morphological analysis on adhesion and invasion involved in endometriosis with tissue culture. Chin Med J (Engl) 2011;124: 148-151.

Sica, A., Schioppa, T., Mantovani, A. and Allavena, P. Tumour-associated macrophages are a distinct M2 polarised population promoting tumour progression: potential targets of anti-cancer therapy. Eur J Cancer 2006;42: 717-727.

Startseva, N. V. [Clinical immunological aspects of genital endometriosis]. Akush Ginekol (Mosk) 1980;23-26.

Steele, R. W., Dmowski, W. P. and Marmer, D. J. Immunologic aspects of human endometriosis. Am J Reprod Immunol 1984;6: 33-36.

Steller, H. Mechanisms and genes of cellular suicide. Science 1995;267: 1445-1449.

Stich, T. M. Determination of protein covalently bound to agarose supports using bicinchoninic acid. Anal Biochem 1990;191: 343-346.

Story, L. and Kennedy, S. Animal studies in endometriosis: a review. ILAR J 2004;45: 132-138.

Strasser, A., Harris, A. W., Huang, D. C., Krammer, P. H. and Cory, S. Bcl-2 and Fas/APO-1 regulate distinct pathways to lymphocyte apoptosis. EMBO J 1995;14: 6136-6147.

Straub, R. H. The complex role of estrogens in inflammation. Endocr Rev 2007;28: 521-574.

Strowitzki, T., Marr, J., Gerlinger, C., Faustmann, T. and Seitz, C. Dienogest is as effective as leuprolide acetate in treating the painful symptoms of endometriosis: a 24-week, randomized, multicentre, open-label trial. Hum Reprod 2010;25: 633-641.

Suginami, H. A reappraisal of the coelomic metaplasia theory by reviewing endometriosis occurring in unusual sites and instances. Am J Obstet Gynecol 1991;165: 214-218.

Sutton, C. J., Pooley, A. S., Ewen, S. P. and Haines, P. Follow-up report on a randomized controlled trial of laser laparoscopy in the treatment of pelvic pain associated with minimal to moderate endometriosis. Fertil Steril 1997;68: 1070-1074.

Swirski, F. K., Nahrendorf, M., Etzrodt, M., Wildgruber, M., Cortez-Retamozo, V., Panizzi, P., Figueiredo, J. L., Kohler, R. H., Chudnovskiy, A., Waterman, P. et al. Identification of splenic reservoir monocytes and their deployment to inflammatory sites. Science 2009;325: 612-616.

Tang, L., Wang, T. T., Wu, Y. T., Zhou, C. Y. and Huang, H. F. High expression levels of cyclin B1 and Polo-like kinase 1 in ectopic endometrial cells associated with abnormal cell cycle regulation of endometriosis. Fertil Steril 2009;91: 979-987.

Tariverdian, N., Siedentopf, F., Rucke, M., Blois, S. M., Klapp, B. F., Kentenich, H. and Arck, P. C. Intraperitoneal immune cell status in infertile women with and without endometriosis. J Reprod Immunol 2009;80: 80-90.

Taylor, R. N., Lebovic, D. I. and Mueller, M. D. Angiogenic factors in endometriosis. Ann N Y Acad Sci 2002;955: 89-100; discussion 118, 396-406.

Taylor, R. N., Ryan, I. P., Moore, E. S., Hornung, D., Shifren, J. L. and Tseng, J. F. Angiogenesis and macrophage activation in endometriosis. Ann N Y Acad Sci 1997;828: 194-207.

Te Linde, R. W. and Scott, R. B. Experimental endometriosis. Am J Obstet Gynecol 1950;60: 1147-1173.

Telimaa, S., Puolakka, J., Ronnberg, L. and Kauppila, A. Placebo-controlled comparison of danazol and high-dose medroxyprogesterone acetate in the treatment of endometriosis. Gynecol Endocrinol 1987;1: 13-23.

Thompson, J. F., Hayes, L. S. and Lloyd, D. B. Modulation of firefly luciferase stability and impact on studies of gene regulation. Gene 1991;103: 171-177.

Topley, N., Mackenzie, R. K. and Williams, J. D. Macrophages and mesothelial cells in bacterial peritonitis. Immunobiology 1996;195: 563-573.

Towbin, H., Staehelin, T. and Gordon, J. Electrophoretic transfer of proteins from polyacrylamide gels to nitrocellulose sheets: procedure and some applications. Proc Natl Acad Sci U S A 1979;76: 4350-4354.

Tran, L. V., Tokushige, N., Berbic, M., Markham, R. and Fraser, I. S. Macrophages and nerve fibres in peritoneal endometriosis. Hum Reprod 2009;24: 835-841.

Ulukus, M., Ulukus, E. C., Tavmergen Goker, E. N., Tavmergen, E., Zheng, W. and Arici, A. Expression of interleukin-8 and monocyte chemotactic protein 1 in women with endometriosis. Fertil Steril 2009;91: 687-693.

van der Linden, P. J., de Goeij, A. F., Dunselman, G. A., van der Linden, E. P., Ramaekers, F. C. and Evers, J. L. Expression of integrins and E-cadherin in cells from menstrual effluent, endometrium, peritoneal fluid, peritoneum, and endometriosis. Fertil Steril 1994;61: 85-90.

van Kaam, K. J., Schouten, J. P., Nap, A. W., Dunselman, G. A. and Groothuis, P. G. Fibromuscular differentiation in deeply infiltrating endometriosis is a reaction of resident fibroblasts to the presence of ectopic endometrium. Hum Reprod 2008;23: 2692-2700.

Van Langendonckt, A., Casanas-Roux, F. and Donnez, J. Iron overload in the peritoneal cavity of women with pelvic endometriosis. Fertil Steril 2002;78: 712-718.

Velasco, I., Acien, P., Campos, A., Acien, M. I. and Ruiz-Macia, E. Interleukin-6 and other soluble factors in peritoneal fluid and endometriomas and their relation to pain and aromatase expression. J Reprod Immunol 2010;84: 199-205.

Velasco, I., Quereda, F., Bermejo, R., Campos, A. and Acien, P. Intraperitoneal recombinant interleukin-2 activates leukocytes in rat endometriosis. J Reprod Immunol 2007;74: 124-132.

Veltman, J. D., Lambers, M. E., van Nimwegen, M., Hendriks, R. W., Hoogsteden, H. C., Hegmans, J. P. and Aerts, J. G. Zoledronic acid impairs myeloid differentiation to tumour-associated macrophages in mesothelioma. Br J Cancer 2010;103: 629-641.

Vermes, I., Haanen, C., Steffens-Nakken, H. and Reutelingsperger, C. A novel assay for apoptosis. Flow cytometric detection of phosphatidylserine expression on early apoptotic cells using fluorescein labelled Annexin V. J Immunol Methods 1995;184: 39-51.

Vernon, M. W., Beard, J. S., Graves, K. and Wilson, E. A. Classification of endometriotic implants by morphologic appearance and capacity to synthesize prostaglandin F. Fertil Steril 1986;46: 801-806.

Vernon, M. W. and Wilson, E. A. Studies on the surgical induction of endometriosis in the rat. Fertil Steril 1985;44: 684-694.

Vinatier, D., Dufour, P. and Oosterlynck, D. Immunological aspects of endometriosis. Hum Reprod Update 1996;2: 371-384.

Vucic, D., Deshayes, K., Ackerly, H., Pisabarro, M. T., Kadkhodayan, S., Fairbrother, W. J. and Dixit, V. M. SMAC negatively regulates the anti-apoptotic activity of melanoma inhibitor of apoptosis (ML-IAP). J Biol Chem 2002;277: 12275-12279.

Wahl, S. M., Wen, J. and Moutsopoulos, N. TGF-beta: a mobile purveyor of immune privilege. Immunol Rev 2006;213: 213-227.

Wall, E. H., Hewitt, S. C., Liu, L., del Rio, R., Case, L. K., Lin, C. Y., Korach, K. S. and Teuscher, C. Genetic control of estrogen-regulated transcriptional and cellular responses in mouse uterus. FASEB J 2013;27: 1874-1886.

Watanabe, H., Kanzaki, H., Narukawa, S., Inoue, T., Katsuragawa, H., Kaneko, Y. and Mori, T. Bcl-2 and Fas expression in eutopic and ectopic human endometrium during the menstrual cycle in relation to endometrial cell apoptosis. Am J Obstet Gynecol 1997;176: 360-368.

Weed, J. C. and Arquembourg, P. C. Endometriosis: can it produce an autoimmune response resulting in infertility? Clin Obstet Gynecol 1980;23: 885-893.

Willingham, M. C. Cytochemical methods for the detection of apoptosis. J Histochem Cytochem 1999;47: 1101-1110.

Wingfield, M., Macpherson, A., Healy, D. L. and Rogers, P. A. Cell proliferation is increased in the endometrium of women with endometriosis. Fertil Steril 1995;64: 340-346.

Witowski, J., Tayama, H., Ksiazek, K., Wanic-Kossowska, M., Bender, T. O. and Jorres, A. Human peritoneal fibroblasts are a potent source of neutrophil-targeting cytokines: a key role of IL-1beta stimulation. Lab Invest 2009;89: 414-424.

Witz, C. A., Montoya-Rodriguez, I. A., Miller, D. M., Schneider, B. G. and Schenken, R. S. Mesothelium expression of integrins in vivo and in vitro. J Soc Gynecol Investig 1998;5: 87-93.

Wu, M. Y. and Ho, H. N. The role of cytokines in endometriosis. Am J Reprod Immunol 2003;49: 285-296.

Wyllie, A. H., Kerr, J. F. and Currie, A. R. Cell death: the significance of apoptosis. Int Rev Cytol 1980;68: 251-306.

Yamashita, H., Otsuki, Y., Matsumoto, K., Ueki, K. and Ueki, M. Fas ligand, Fas antigen and Bcl-2 expression in human endometrium during the menstrual cycle. Mol Hum Reprod 1999;5: 358-364.

Yeung, P. P., Jr., Shwayder, J. and Pasic, R. P. Laparoscopic management of endometriosis: comprehensive review of best evidence. J Minim Invasive Gynecol 2009;16: 269-281.

Yin, X. M. Signal transduction mediated by Bid, a pro-death Bcl-2 family proteins, connects the death receptor and mitochondria apoptosis pathways. Cell Res 2000;10: 161-167.

Yin, Y., Huang, W. W., Lin, C., Chen, H., MacKenzie, A. and Ma, L. Estrogen suppresses uterine epithelial apoptosis by inducing birc1 expression. Mol Endocrinol 2008;22: 113-125.

Yoshino, O., Osuga, Y., Koga, K., Hirota, Y., Tsutsumi, O., Yano, T., Morita, Y., Momoeda, M., Fujiwara, T., Kugu, K. et al. Concentrations of interferon-gamma-induced protein-10 (IP-10), an antiangiogenic substance, are decreased in peritoneal fluid of women with advanced endometriosis. Am J Reprod Immunol 2003;50: 60-65.

Zeller, J. M., Henig, I., Radwanska, E. and Dmowski, W. P. Enhancement of human monocyte and peritoneal macrophage chemiluminescence activities in women with endometriosis. Am J Reprod Immunol Microbiol 1987;13: 78-82.

Ziegler, S. F., Ramsdell, F. and Alderson, M. R. The activation antigen CD69. Stem Cells 1994;12: 456-465.

8 Appendix

8.1 List of Publications

Parts of this thesis were already published or presented.

Publication

Harirchian, P., Gashaw, I., Lipskind, S. T., Braundmeier, A. G., Hastings, J. M., Olson, M. R. and Fazleabas, A. T. Lesion kinetics in a non-human primate model of endometriosis. *Hum Reprod* 2012;**27**: 2341-2351.

Oral Presentations

Harirchian P, Gashaw I, Lipskind ST, Braundmeier AG, Hastings JM, Olson MR, Fazleabas AT. Lesion Kinetics in a Non-human Primate Model of Endometriosis. Prevention of Recurrence Session at the World Congress on Endometriosis. September 2011; Montpelier, France

Harirchian P, Kirchhoff D, Koch M, Zollner TM, Gashaw I. Estrogen effects lesion composition and persistence in a syngeneic transplantation endometriosis mouse model. Benign Gynecological Disorders Session at the World Congress of Gynecological Endocrinology. March 2010; Florence, Italy

Poster Presentations

Harirchian P, Kirchhoff D, Koch M, Zollner TM, Gashaw I. Estrogen effects lesion persistence in a syngeneic transplantation endometriosis mouse model. Bayer HealthCare Young Scientist Poster Session. October 2010; Berlin, Germany

Harirchian P, Kirchhoff D, Koch M, Zollner TM, Gashaw I. Analyzing the effects of 17β-estradiol alone or in combination with progesterone in a syngeneic transplantation endometriosis mouse model. Bayer Schering Pharma Young Scientist Poster Session. September 2009; Berlin, Germany

8.2 Abbreviations

6-FAM	6-Carboxyfluorescein
AEC	3-amino-9-ethylcarbazole
APC	allophycocyanin
APCs	antigen presenting cells
ART	assisted reproductive technology
AV	Annexin V
BCA	Bicinchoninic Acid
Bcl-2	B-cell lymphoma 2
Bid	BH3 interacting-domain death agonist
Birc1a	Baculoviral IAP repeat-containing protein 1a
BPB	Bromophenol Blue
BSA	Bovine Serum Albumin
cDNA	complementary deoxyribonucleic acid
CLP	common lymphoid progenitor
CMP	common myeloid progenitor
COC	combined oral contraceptive
Cy7	Cyanine 7
DAB	3,3'-Diaminobenzidine
DAPI	4',6-diamidino-2-phenylindole
DC	dendritic cell
DEPC	diethylenepyrocabonate
DMEM	Dulbecco's modified eagle medium
DTT	Dithiothreitol
E_2	17-β estradiol
EGTA	ethylene glycol tetraacetic acid
ELISA	enzyme-linked immunosorbent assay
EP	epithelium
ER	estrogen receptor
F	fat
FCS	Fetal Calf Serum
FITC	fluorescein isothiocyanate
GL	gland
GnRH	gonadotropin releasing hormone
HE	hematoxylin and eosin stain
HEPES	4-(2-hydroxyethyl)-1-piperazineethanesulfonic acid
HRP	Horseradish Peroxidase
hrs	hours
HSC	hematopoietic stem cell
i.p.	intraperitoneally
ICAM	intercellular adhesion molecule

IHC	Immunohistochemistry
IL	interleukin
KDa	kilo Dalton
MCP-1	monocyte chemotactic protein-1
Milli-Q water	Milli-Q Water Purification System from Millipore
min	minutes
MT	muscle tissue
NK cell	natural killer cell
NSAID	non-steroidal anti-inflammatory drugs
OP	operation
ovx	ovariectomy
P_4	progestrone
PBS	Phosphor Buffered Salin
PBST	PBS/0.1% Tween-20
PCNA	proliferating cell nuclear antigen
PCR	Polymerase Chain Reaction
PE	phycoerythrin
PerCP	Peridinin-Chlorophyll-Protein
PF	peritoneal fluid
PS	phosphatidylserine
RNA	ribonucleic acid
rpm	revolutions per minute
RT	room temperature
RT-PCR	real time PCR
S	suture
s.c.	subcutaneosly
SD	standard deviation
SDS	Sodium Dodecyl Sulphate
SDS-PAGE	SDS-polyacrylamide gel electrophoresis
sec	seconds
SERD	selective estrogen receptor down-regulator
Smac	Second mitochondria-derived activator of caspases
ST	stroma
TdT	Terminal deoxynucleotidyl transferase
TGF-β1	Transforming growth factor-β1
TUNEL	Terminal deoxynucleotidyl transferase dUTP nick end labeling
UNG	Uracil-DNA glycosylase
uNK cells	uterine natural killer cells

8.3 Acknowledgements

This work was performed between June 2008 and August 2011 at Bayer Healthcare, Global Drug Discovery, Transgenic and *in vivo* Pharmacology (TASIP), Berlin, Germany and is being presented with their permission.

I am especially grateful to Dr. Isabella Gashaw for supervising my thesis. As the lab head and my direct mentor she was always there for my questions, open for discussions and supported me with scientific knowledge and very helpful advises. A thank you goes to Dr. Dennis Kirchhoff for his assistance with cell flow cytometry and being a great officemate. He along with Dr. Marcus Koch were always available for fruitful discussions with regards to immunology and inflammation. Acknowledgment and thank you goes to Prof. Dr. Khusru Asadullah for allowing me to perform my studies in his research group in Germany.

I am very grateful to my colleagues in TASIP for teaching me everything I know about *in vivo* experiments and their assistance in performing the mouse surgeries and necropsies. Also thank you goes to Prof. Dr. Asgi T. Fazleabas at Michigan State University for allowing me to visit his lab and perform the baboon lesion analysis.

I would like to express my gratitude to Priv. Doz. Dr. Thomas M. Zollner for everything he has done for me in making it possible to perform my PhD studies in his department. Also thank you for being a member and referee of my thesis examination board.

Moreover I would like to thank Prof. Dr. Rupert Mutzel for his willingness to coach me in his function as university professor from FU Berlin and for kindly being the head of my PhD thesis examination board.

Last, but not least, I would like to thank my family for making me who I am and for their never-ending support.